JUSTUS-LIEBIG-UNIVERSITÄT GIESSEN
Institut für Allgemeine Botanik und Pflanzenphysiologie
Senckenbergstr. 17
35390 Gießen

Diplomarbeit

Structural and ecophysiological shoot features of the leafless cucurbit *Acanthosicyos horridus*, a keystone endemic of the Namib desert.

by

Felix Hebeler

December 2000

Betreuung/Supervision:

Prof. Dr. AJE van Bel,
Institut für Allgemeine Botanik und Pflanzenphysiologie
Justus-Liebig-Universität Giessen, Germany
Prof. Dr. CEJ Botha,
Department of Botany, Rhodes University, Grahamstown,
Republic of South Africa

ABSTRACT

Endemic to the Namib desert, the melon *Acanthosicyos horridus* exhibits a range of xeromorphic adaptations including rudimentary leaves and stipulae reduced to photosynthetically active thorns, stomata arranged in longitudinal rows, sunken within the tissue matrix and covered by wax layers, trichomes, a thick cuticle and a high degree of sclerenchymatisation (Gibson 1998).

The ecophysiological concept and the resulting structural and functional relationships were the main aim of this thesis. It's belonging to the Cucurbitaceae family together with its adaptations to the desert habitat proved to arise a number of interesting anatomical and physiological questions.

Stem anatomy, gas exchange and water economy was studied in field and laboratory experiments.

As with the leaves *A. horridus* has also lost its specialised loading phloem, the structure and function of the phloem loading complex was a main interest.

The outer ring of vascular bundles in *A. horridus* differs anatomically from the inner vascular bundles. A single layer of parenchyma cells surrounding the external phloem of these outer vascular bundles show frequent symplastic connections (plasmodesmata) to companion cells. These companion cells are of the intermediary type and much larger than their corresponding sieve elements. The outer vascular bundles are assumed to function as assimilate loading sites. Raffinoseoligosaccharides were found to be the main transport sugars, consistent with the hypothesis of symplastic phloem loading by polymer trapping (Haritatos & Turgeon 1995) in *A. horridus*. The inner vascular bundles correspond to the usual cucurbit type and appear to function as transport vessels.

Ecophysiologically, *A. horridus* seems to have traded in effective photosynthesis under favourable conditions for low but steady assimilation throughout the year to support its large biomass. Assimilation rates are among the lowest recorded but substantially increase after watering and then lie within the range recorded for other aphyllous desert species. Growth rates are average during drought and shoot growth can cease completely while plants bear fruit, but rates can rise up to 0,8 cm/h when groundwater is plentiful.

Measured plant water potentials were high even under drought conditions, supporting the hypothesis of groundwater availability to the plant.

ACKNOWLEDGEMENTS

Much of the practical work for this thesis was done at the Department of Botany and the Electron Microscope Unit of Rhodes University, Grahamstown, RSA.
Field experiments were conducted at the Gobabeb Training and Research Centre, Namibia.
Planning, pre-experiments and the write-up was done at the Institut für Allgemeine Botanik und Pflanzenphysiologie and the scanning electron microscopy was done at the Strahlenzentrum of the Justus-Liebig-Universität Giessen.

Above all, I would like to express my sincere gratitude to my two supervisors:
Prof van Bel, for accepting my project and supporting it during every stage by word and deed, be it through counsel or technical support, with great patience, understanding and knowledge.
Prof Botha, for giving me the opportunity to work under his supervision, and for not only opening all his doors to me to provide all facilities and technical equipment needed, as well as fund-raising, but for being a true host and for introducing me to the local (5 o'clock) customs, including silly sports like cricket and rugby.
Thank you for your guidance, ever willing assistance and endurance.

I would also like to sincerely thank the Deutscher Akademischer Austauschdienst DAAD in Bonn for their scholarship, without which this project would not have been possible, and the South African Foundation for Research and Development FRD for the research grant that allowed me to conduct my research without any financial worries.

At Rhodes University I would like to thank Mr. Brad Ripley for his inspiration and motivation and his willingness to help me with my troubles. And for his colour TV.
I would like to extend my gratitude to everybody at the Rhodes Botany Dept. for making my stay a great experience, especially to Irma Knevel for being a friend who speaks her mind, Rachel Judd for being a soul-mate and Alison Buswell for her tolerance. Thanks to Louise Donaldson for not letting me ship-wreck on the cliffs of administration and SA customs, and to the staff for all their help.

At the Justus-Liebig-Universität I would like to express my thanks to Petra Stutz for wrestling with German customs, the courier and finally the insurance company in my absence with endurance, patience and understanding. Thank you to Ard Schrier for his constant online-support across the world. Special thanks to Katrin Ehlers for sharing her EM experience with me and for trying to show me what professional work means.
I am also obliged to Dietmar Haffer for his interest and endurance in bringing my plants to life against their will.

I owe Mary K. Seely, Joh Henschel and all the staff at the Gobabeb Training and Research Centre, namely Chris and Ed Bark and Lesley Parensey, and the DRFN Office in Windhoek a great deal of this thesis. Thank you for your prompt assistance when I needed help, for your trust, and for giving me access to facilities and data.

I can not thank my parents enough for giving me this great opportunity.
Thank you for your understanding, your moral and financial support and for guiding me to were I am now.

I dedicate this thesis to my grandmother, who did not see me depart.

Table of Contents

LIST OF FIGURES

LIST OF FIGURES (CONTINUED)

LIST OF TABLES

DEFINITION OF SYMBOLS

Symbol	Unit	Definition
A (A_{max})	µmol mol^{-1}	(maximum) Assimilation of CO_2 per unit leaf area
c_i	µmol mol^{-1}	Intercellular carbon dioxide concentration
E	mmol m^{-2} s^{-1}	Transpiration rate
G_s	mol $m^{-2}s^{-1}$	Stomatal conductance
PAR	µmol $m^{-2}s$	Photosynthetically active radiation
R_s	m^2s mol^{-1}	Stomatal resistance
R_{sstc}	m^2s mol^{-1}	Resistance of superstomatal chambers
WUE	µmol $mmol^{-1}$	Water use efficiency (A/E)

DEFINITION OF ABBREVIATIONS

5,(6)-CF	5,(6)-Carboxyfluorescein
5,6-CFDA	5,6-Carboxyfluoresceindiacetate
AP	Assimilation parenchyma
CC	Companion cell
CMV	Cucurbit mosaic virus
CO_2	Carbon dioxide
DMSO	Dimethylsulfoxide
EFP	Extrafascicular phloem
FAA	Formyl acetic alcohol
GA_3	Gibberellic acid
HPLC	High-Pressure-Liquid-Chromatography
IRGA	Infra-red gas analyser
IC	Intermediary cell
IVB	Inner vascular bundles
OVB	Outer vascular bundles
PAS	Photosynthetically active surface
PS	Photosynthesis
RH	Relative humidity
SE	Sieve element
SEM	Scanning electron microscopy
SS	Sclerenchyma Sheath
SE/CC	Sieve Element/Companion Cell Complex
T_{min}	minimum temperature
T_{max}	maximum temperature
TEM	Transmission electron microscopy

1 INTRODUCTION

1.1 The !Nara - Morphology, Distribution, Ecosystem

Acanthosicyos horridus is an unique member of the *Cucurbitaceae* family, adapted to survive in the extreme arid climate of the Namib desert.

The plant *A. horridus*, or !nara (! is the symbol for a certain click-sound in the nama language), as it is called by the Nama people, is endemic to the Namib sand desert. Its distribution is limited to the narrow strip of the coastal Namib sand desert, about 40-60km wide, stretching from the south of the Orange river in the Republic of South Africa 1000km along the coast of Namibia to north of the Kunene in Angola, an area of about 60.000 km^2 in size.

The !naras distribution within this area is again limited to the banks of ephemeral rivers and areas within the dunes, were the water table is high enough or aquifers can be tapped by the plant's extended root system: some roots measure up to 40cm in diameter, and grow more than 30m deep to reach groundwater (Kutschera et al. 1997).

The Namib is said to be the oldest of all deserts with more than 80 million years of continuous semiarid to hyper-arid conditions (Seely 1987) and an average amount of precipitation of less than 100mm per annum.

In this climate, single plants of *A. horridus* get over a hundred years old and can cover up to 300 m^2. Fossils indicate that *A. horridus* is up to 40 million years old (Sandelowsky 1977).

A. horridus presents a plant species around which a special, highly adapted micro-ecosystem has formed, with insects such as bugs (Heteroptera) and beetles (Tenebrioids) (Roer 1975) - some obligate to *A. horridus* - or small mammals and reptiles (Mitchell et al. 1987), that use the plant for shelter or as a nutrient source. The plant population is estimated to be between some hundreds and a few thousands. Over the past few years, a steady decrease in number and fruit-size has been reported (Shilomboleni 1998).

Ecologically, the plant has become adapted to successfully withstand long periods without rain and survive in an extreme desert climate.

The plant is non-succulent but shows a number of xerophytic adaptations: the leaves are reduced to photosynthetically active thorns that repel herbivores, photosynthesis is executed by the stem, and even the petals of the male and female flowers are green.

The plant is associated with VA mycorrhiza (Klopatek *et al.*1992) to maximise retrieval of the sparse nutrients in the desert soils (Abrams *et al.* 1997).

The closest relative is the only other member of the species *Acanthosicyos naudinianus*, (*Cucumis/Citrullus naudinianus*), an annual found from the Namib to the Kalahari and from Angola to the Cape Province.

Figure 1: !Nara plant. Note the yellow and dry sections close to the ground (due to extreme heat and damage through herbivores). Separated patches of a second plant can be seen on a hummock in the background

Figure 2: Detail of female !nara plant. Female inflorescence shortly after flowering. There are no leaves, the stipulae are reduced to photosynthetically active thorns. The stems are ribbed in a longitudinal direction.

Figure 3: !Nara melon. The melons dry quickly after they are ripe and take on a yellowish colour.

1.2 The Namib - Climate, Vegetation, Geology

The word Namib is derived from the nama word for “endless expanse”.
Covering southern Africa's Atlantic coast, from the mouth of the Orange River in the Cape Province of South Africa to Mossamedes in Angola across the length of Namibia, the Namib stretches on for more than 700 km.
As the Atacama, the coastal desert of South America, with which it not only has the frequent fog occurrences in common, its width, too, is only a fraction of its length with no more than 80km, averaging about 50km. Its inland expanse is limited by the climatic influence of the cold Benguela ocean current and the geographical barrier of the Great Western Escarpment in the North and centre, that is raising the more humid highlands 1000-1600m above the desert.
In the south, the Namib gradually transists into the Karoo and merges with the central Kalahari desert.

Formed in the early Pleistocene and often regarded as one of the oldest deserts in the world the Namib is classified as an arid or even “hyper-arid” (Walter & Breckle 1986) desert with annual rainfall of less than 50mm. In some parts, however, due to frequent fog events, total precipitation is somewhat higher. Up to 160mm of fog water have been collected in cylindrical fog screens in some stations (Seely & Henschel 1998), but fog precipitation undergoes seasonal variations in frequency and amount of water, and it is not clear what amount of fog water is available for the desert fauna and flora (Seely *et al.* 1998, Robinson & Seely 1980). Although, unlike in the Atacama, until today no plants have been found in the Namib that use fog water exclusively, a number of plants (*Trianthema hereroensis*, *Stipagrostis* spec.) and insects harvest and utilise fog water (Louw & Seely 1982).

For a desert climate, temperatures are mild, ranging between an absolute maximum of 45 °C and an absolute minimum of 5°C during “summer” (December –March; mean max. 20°C, mean min. 15°C) at the coast (Swakopmund).
Inland, more continental conditions prevail. Coastal humidity is at 100 percent for 19 hours per day in summer and for 11 hours in winter. At the inner edge of the desert, the air is much drier, fog is virtually unknown, and the humidity seldom exceeds 50 percent. This is nevertheless fairly high for a desert region.

Higher temperatures with extremely dry air only prevail during east-wind, when dry wind from the Kalahari is blown down the Great Escarpment. Sand storms are rare. Rain events are rare and occur local, but ephemeral rivers can transport large amounts of water from the highlands to the coast. However, they rarely reach the coast, and due to increasing water withholding and usage in the highlands, floods tend to be weaker in recent years.
Potential evaporation in the coastal area ranges from 1200 to 1500mm p.a. and increases towards the centre of the Kalahari pan.

The Namib can be categorised in three sections: Most of the desert consists of a broad platform of eroded sandstone, gradually rising from the coastline to an elevation of 900 meters at the foot of the escarpment. Most of the central parts of the Namib consist of gravel plains.
Along the coast, sand dunes prevail and form the infamous Skeleton Coast, Namibia's harsh Northern coastline.
South of Walvis Bay and the Tropic of the Capricorn to the Orange river, the vast sand sea of the southern Namib extends, with dunes as high as 250m.
In the southern and central portions, mountains rise about the smooth platform only as isolated individuals and short chains. Most of the mountains are rugged, steep sloped, and almost soil less.

The vegetation of the southern Namib dune sea in general only consists of annual grasses, only in depressions an along vleis or ephemeral rivers and aquifers the !nara *Acanthosicyos horridus* can be found, sometimes associated with *Stipagrostis sabulicola* or *Zygophyllum spec*..
The gravel plains of the central can be covered by seas of annual grasses (mainly of the genus *Stipagrostis*) in years with good rains, but otherwise is barren with only some trees (genus Acacia) and chaenophytes like the pencil-bush *Arthraerua leubnitziae* or lichens and annuals in depressions and washes (Craven & Marais 1986).

In the zone of frequent fog near the coast low succulent bushes grow sporadically and vegetation can form around rocks, were fog water condenses. Along the eastern border, a thin to moderate cover of annual grasses appears in most years,

supporting for a time a variety of antelopes, zebra, ostrich, and their attendant predators. Fauna and flora along the ephemeral rivers is diverse with different *Acacia* species and *Tamarix usneoides* giving shade and thus supporting a number of less specialised plants. Potable water is found only as sub-flow beneath streambeds chiefly of the larger streams that rise in the rainier plateau east of the escarpment. In some cases, dissolved salts render the water unpleasant. In other cases, such as the Kuiseb and the Koichab, which supply Walvis Bay and Lüderitz, the quality is good to excellent.

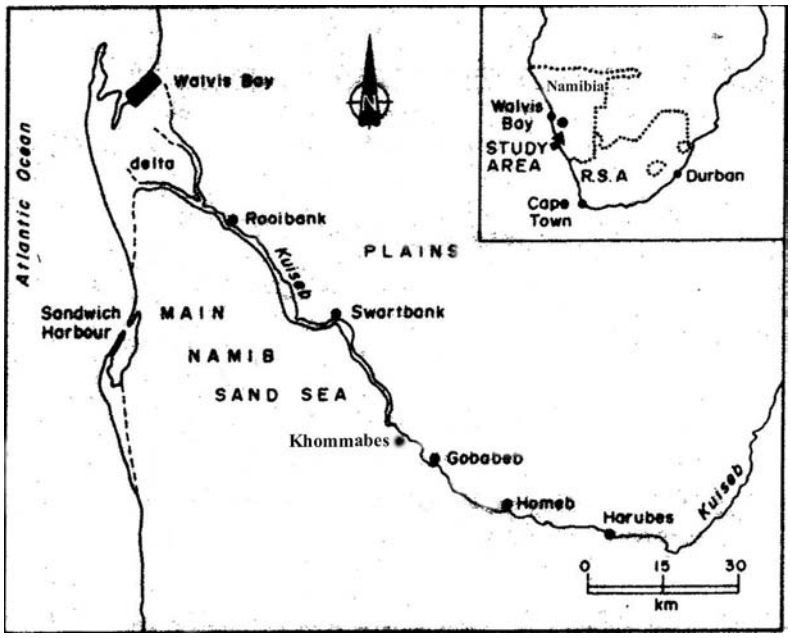

Figure 4: Map of the central Namib. The Kuiseb river separates the Namib sand sea in the south from the gravel plains in the north. Experiments were conducted on plants near the Gobabeb station and in the Khommabes valley.

Figure 5: The Kuiseb river separates the dune system of the southern Namib from the gravel plains of the central Namib. Situated in this contact zone of three extreme eco-habitats is the Gobabeb Training and Research Centre.

1.3 History of Usage and Research of the !Nara plant

For the ethnic of the Topnaar, dwelling along the Kuiseb river, the fruits of the !nara (*A. horridus*) used to be the main food source for a long time (Dentlinger 1977, Pfeifer 1979).

Figure 6: Topnaar woman climbing a !nara hummock.

!Nara fields – for example interdune areas with sufficient groundwater to support large numbers of plants – belong to families or settlements and !nara fruits used to be harvested and processed in traditional ways. The flesh pulp of the melons is boiled (raw melons are extremely high in oxalic acid concentration) and dried in the sand until it has leathery or rubber-like appearance. Seeds are eaten raw or

roasted and are sold to South Africa via Walvis Bay as almond substitute, giving a small income to the families. The skin of the fruits is fed to goats and donkeys.
Different parts of the plant, mainly the roots, are used for medical purposes (van den Eynden *et al.* 1992).

The Topnaar presence in the coastal area around Walvis Bay and more inland is documented from 1670 on, but the !nara has been a food-source for Khoi-khoi or bushman for at least 8000 years (Sandelowsky 1977), as archaeological findings in Mirabib indicate.

Early botanist, settlers and missionaries have described the !nara plant and its association with the Topnaar community: They are mentioned in the reports of the Dutch-Indian Company landing at Sandwichharbour 1670.
J.F. Alexander described them 1838 and Welwitsch found bushes of the !nara (named *A. horridus* Welwitschia after him) in Angola 1859 (Moritz 1992). All of these early reports concentrate on the botany of the plant and the relation the Topnaars have with the plant.
In the beginning of the last century, some !nara plants were introduced to Europe and the USA (Beer 1954, US Dept. Agriculture 1922).
More recent publications focus on the fruits and seeds of the plant (Klopatek & Stock 1994, Joubert & Cooper 1953), on possible medical and biochemical usage (Hylands & Magot 1986, Schwartz & Burke 1958) and agricultural exploitation (Arnold *et al.*1985, Sandelowsky 1990, Storad 1991).

1.3.1 The NARA Project (Natural Resources for the #Anoin people)

The NARA project (Natural Resources for the #Anoin People; # is the symbol for another nama click sound) was initiated because of the ecological importance and the innate scientific value of the !nara, and also because of the !nara's economic and social-cultural value for the Topnaar people. The DRFN and associated scientists together with the Topnaar community work on different aspects of the nara plant, ranging from botanical and physiological to agricultural and economic issues. Studies examine possible reasons for reported decrease in fruit size and number, pollination and seed dispersion of the !nara, influence of wind and water erosion, the ecological role of the !nara, associated herbivores and possible

treatments, as well as traditional harvesting and processing methods and future economic values of !nara products; these studies also examine the possibilities of a more intensive usage as a crop and as a protection against erosion.
The present thesis will provide an anatomical and ecophysiological background for further studies.

1.4 The Cucurbitaceae Family

With many of their members being important crop cultivars like *Cucumis*, *Cucurbita*, *Citrullus* and others, the Cucurbitaceae have been objects of intense research and study from the early stages of botanical research on.
Genetic engineering and gene mapping, yield maximization and pest and disease control of cucurbits have rapidly proceeded.
However, a number of basic anatomical and physiological features are still not fully understood.
According to Esau (1965) and Metcalfe & Chalk (1972), the Cucurbitaceae are described as being herbaceous, seldom woody species with rapid vegetative growth. Tendrils are common features, as well as glandular hairs or trichomes, often with cystoliths around the basis of these hairs.
Stomata are of the Helleborus type and can occur on either side of the leaf. They are frequently raised above the general level, especially in stems, which appears to be a feature designed for the tropical climate most of the cucurbit species originate from (Metcalfe & Chalk 1972). However, there are a number of xerophytes in the cucurbit family, some of which exhibit succulence and/or crassulacean acid metabolism.
Vascular bundles are predominantly bicollateral and frequently arranged in two rings, a few species have exclusively collateral bundles.
Phloem occurs in the vascular bundles as well as in extrafascicular strands. Vascular bundles of the minor veins are surrounded by a bundle sheath.
A ring of sclerenchyma – which is closed in herbaceous species – can be found in the outer part of the cortex, a ring of fibrous cells in the pericycle of young stems.
Only in some species vascular bundles have been found outside of this sclerenchyma ring or sheath, but extrafascicular phloem/sieve tubes occur throughout the stem and in the cortex of most species (ectocyclic sieve tubes: Kempers *et al.* 1993).

For the Cucurbitaceae, Worsdell (1964, in Metcalfe & Chalk 1972) proposed the bicollateral vascular bundles to be “a compound structure consisting of the more or less intimate association or attachment of two distinct vascular bundles, of which the innermost has lost the xylem” and the extrafascicular phloem to be rudimentary vascular bundles.

Whether this interpretation is correct or not, as a matter of fact the function of this adaxial (internal) phloem in cucurbits still is obscure (Schaffer *et al.* 1996), since clearly the abaxial phloem is the site of phloem loading and it was shown that aphids for example preferably feed on the abaxial phloem (Botha & Evert 1978).

Experiments with fluorescent dyes showed that the adaxial phloem in the minor veins is not connected to the transport phloem, but rather to the extrafascicular phloem in the stem (Schmitz *et al.* 1987). Function and physiology of the extrafascicular phloem are still fully obscure at this present time.

1.5 Ecophysiology of Desert Plants

Arid to hyper-arid regions account for 19% of the earth’s land mass, another 15% are categorized as semi-arid (Goudie 1993). Even in these regions where annual precipitation can 50mm or less, plant live is abundant.

Were plants do not avoid drought as therophytes or cryptophytes and only grow after rains, special anatomical and physiological adaptations are necessary to survive and reproduce despite the harshness of deserts.

Early approaches to understand the ecology of desert plants assumed that water conservation was the key issue in the ecophysiology of xerophytes. Since the 1970s, views developed that not merely saving water, but maximizing photosynthetic rates and regulating the energy balance are the functions of many structural and physiological adaptations (Gibson 1998).

Among the physiological adaptations are alterations of the C_3 carbon-fixing pathway that result in CO_2 concentration, namely C_4 and the crassulacean acid metabolism (CAM). In CAM plants, CO_2 is fixed and stored at night when temperature and transpiration is low, and thus the light reaction during the day can be executed with closed stomata. However, the energy cost for carbon pathway is higher than for C_3 plants and Lange *et al.* (1975) showed that under desert conditions with high night-time temperatures, C_3 and C_4 plants can be more effective in carbon fixation and water saving than CAM plants.

Ehleringer & Monson (1993) found that C_4 plants have no significant advantage over C_3 plants in cold deserts.

Also there are some features repeatedly found in many xerophytes, such as microphylly, a high rate of sclerenchymatisation, succulence, an extend roots system etc., strategies of desert plants vary with the desert climate they are adapted to and the ecological niche they fill.

Plants of deserts like the Atacama or the Namib, where regular fog events occur, for example often develop mechanisms to utilise fog precipitation (Louw & Seely 1982, Larcher 1994b).

Roots systems can be shallow and widespread like in many cacti (Larcher 1994b), to maximize the water uptake after the rare rainfall events, or plants might develop tap roots to reach permanent or periodical aquifers.

A feature often seen in desert shrubs is the shedding of leaves during drought to reduce the transpirational surface (Gibson 1983). Leaves are regrown with the onset of rain.

A. horridus is a plant that can support an extremely large biomass (personal observation) for long time spans while its occurrence is limited to an area with less than 50mm average rainfall per annum. The ecological strategy of *A. horridus* is still not understood and promises to be an interesting object of study.

2 MATERIAL AND METHODS

2.1 Plant Material

2.1.1 Plant cultivation for laboratory experiments

Seeds of *Acanthosicyos horridus* were sterilised (5min in 30% bleach) and soaked in tab water overnight. To break dormancy, seeds were kept in an oven at 35-40°C for 3 days.

Seeds were then put in trays with vermiculite or a mixture of 50% sand, 35% vermiculite and 15% compost and kept moist.

Alternatively dormancy was broken with gibberellic acid (GA_3) as follows:

Seeds were pre-treated for 2 hours in a 0,1% GA_3 solution, (GA_3 crystals stirred in demineralised water at 20 °C) and then wrapped in filter paper drenched in GA3 solution to allow for oxygen reaction until the filter paper was dried.

The seeds were then put in a pot (clay pot size 6) with sand (or succulent mix / sand 1:1)

A. horridus seeds readily germinated after heat or GA_3 treatment, in contradiction to the experiences of Small & Botha (1986).

Seedlings were selected and transferred from the trays into plastic pots with a 50% sand, 35% vermiculite, 15% compost mixture after the cotyledons were extended and the first shoot started growing.

Plants were then grown in glasshouse or growing tunnel with additional heaters (1800W thermostated blow heater, Philips Johannesburg, RSA, to keep the temperature above 16°C) and lights (4 Tungsten fluorescence tubes for a 14hour light period- 6.00h-20.00h).

Later on, and at least 2 weeks before any experiments were conducted, plants were transferred into growth chambers (Model S10H, Conviron Controlled Environments Ltd., Winnipeg, Manitoba, Canada. Figure 7), with temperature and humidity settings simulating field conditions (T_{min} [5.00h] 16°C, 80% relative humidity (RH); T_{max} [14.30h] 32,5°C, 35% RH).

Figure 7: Conviron growth cabinet Model S10H with 8 additional halogen lights installed inside the growth chamber.

2.1.2 Plant site selection and sampling in the field

Plant experiments in the field were all conducted in or near the Gobabeb Training and Research Centre in the Namib desert, Namibia.

The two major sites of field research were the !nara plants near the Kuiseb river bed and along the interdune valley close to the Gobabeb research station and plants in the Khommabes valley, approximately 10km east of Gobabeb and 5km south of the Kuiseb river. The Khommabes valley aquifer is discussed to be discontinued with the river groundwater (Teller & Lancaster 1985, Ward 1984).

Plants, especially near settlements, close to the river and around Gobabeb, were heavily grazed by donkeys and goats, shoot tips were eaten by a great number of melenoid beetles and fruits were eaten or damaged by all the above plus jackals, gerbils and probably ostriches and oryx.

Only healthy looking plants, that is plants showing little damage by herbivores, having above ground plant matter of approx. 70cm in height or more and bearing

growing and/or flowering and/or fruiting shoots were selected for gas exchange, phloem sap/starch content or growing rate experiments.

2.2 Anatomy and Ultrastructure

2.2.1 Light microscopy

Whole shoots were collected in the field, placed in water and taken to the Gobabeb research station laboratory. At the Rhodes Botany Department, greenhouse plants were taken to the laboratory and shoots were cut immediately before the experiments.

Fresh tissue was hand-cut at a sufficient distance (10cm or more) from the original cut and stained using safranin (0,5% [g/v] in 50% ethyl alcohol), Crystal Violet (0,25% [g/v] in aqua dest.), Toluidine Blue (0.5% [g/v] in aqua dest.) or Jodid (2g KI, 1g I_2, in 100ml aqua dest.) and observed using a Zeiss Microscope and photographed using a Zeiss MC-63 camera and Agfa Colour ISO 100 film.

Alternatively, longitudinal and transverse segments of about 10mm and 5mm length, respectively, were cut in formyl acetic alcohol (FAA, 3%) and the segments transferred into vials with FAA, sealed, and transported back to Rhodes University. There the segments were sequentially dehydrated in an ethanol (25%, 50%, 75%, 100%) and butynol (2x 100%) series. The segments were infiltrated and embedded in Paraplast wax (Capital Enterprises, New Germany, RSA) and cut into 10-15µm thick sections using a Leitz Wetzlar Minot microtome (Wetzlar, Germany).

Sections were mounted on slides with Haupts adhesive, dried at 45°C in an FSIE Incubator (Labcon (PTY) Ltd., Krugersdorp, RSA) and stained using safranin and Fast Green FCF (0.5% in equal parts of methyl cellosolve, ethyl alcohol abs. and clove oil).

Slides were fixed permanently using Canada Balsam and dried at 45°C for 2 weeks.

Fixed sections were observed using Zeiss Standard Junior 18 microscope and photographed using an Olympus DP-10 digital camera (Figure 8).

Figure 8: Zeiss Standard Junior microscope equipped with fluorescence lamp and filter set and an Olympus DP-10 digital camera.

2.2.2 Fluorescence microscopy

For xylem transport experiments, 10 shoots of approx. 15cm length were cut close to the stem, immediately re-cut under water and placed in 1,5 ml Eppendorf vial with 1µM solution of 5,6-carboxyfluorescein (5,6-CF) (Molecular Probes Europe BV, Leiden, The Netherlands). Shoots were left to transpire for 1,5 hours, transferred to vials with water for 20min and then freehand-sections were taken 3 to 10 cm above the cut.

For phloem loading experiments, 12 shoots were selected on three different plants. On 8 selected shoots, the cuticle was slightly abraded and drops of 5µM 5,6-CFDA (5,6-Carboxyfluoresceindiacetate) in 0,2% DMSO (Dimethylsulphuroxide) applied (Knoblauch & van Bel 1998 and literature cited therein).

Alternatively, for the remaining 4 shoots, 5,6-CFDA in 0,2% DMSO was injected into the hyper- and sub-stomatal cavities with a 100µl micro-syringe.

Plants were left to photosynthesise for 30-90min and the previously selected shoots were then cut and free-hand sections were taken to investigate whether loading of the dye had occurred.

For staining with aniline blue and calcofluor white (fluorescent brightener 28, Sigma No. F-3543, Sigma, Atlasville, RSA), freehand sections were cut and incubated in a 1µM aniline-blue, 1µM calcofluor solution for 1min. (stock: 1mg/ml calcofluor in DMSO).

Sections were observed using a Zeiss Standard Junior 18 microscope equipped with an additional 50Watt UV lamp, a fluorescence filter set and Neofluar objectives (Table 1).

A Zeiss Standard Filter Set (DAPI) was used for all fluorescence dyes (BP: 450-490nm, FT: 510nm, LP: 520nm). For sections stained with aniline-blue/calcofluor an additional Chroma 'Blue/Violet' filter set was used (No. 11003 - BP: 425nm, FT: 475nm, LP: 460nm, Chroma).

Micrographs were taken using a Olympus DP-10 digital camera.

Table 1: Objectives on the different microscopes used.

Zeiss Microscope	Zeiss Standard Junior LM	Zeiss Junior Fluorescence
40x	Plan 40x/1.0 Oil	Ph3 Neofluar 100x/1.3 Oil
25x	Plan 25x/	Plan Neofluar 63x/1.25 Oil
16x	Plan 16x	Plan Neofluar 25x/0.8 Imm.
10x	Plan 10x	Ph2 Neofluar 16x/0.4
	Plan 6,3x	Neofluar 6,3x/0.2

2.2.3 Electron microscopy

2.2.3.1 Transmission electron microscopy (TEM)

Tissue samples from greenhouse plants were taken from shoots, cotyledons, roots and hypocotyl at Rhodes University.

Tissues were cut into pieces (no larger than 1x1x2mm and containing the respective structures of interest) in a wax-filled petri-dish containing a fixative solution (5% glutaraldehyde (GA) in 0,05M cacodylate buffer pH 7) and then fixed in a 5%GA solution for 6 hours at room temperature.

The sections were then rinsed in cacodylate buffer 6 x 10 minutes and then post-fixed in 2% osmium tetroxide solution at 6°C overnight.

Tissues were then washed with cacodylate buffer 6 x 12 minutes:

The tissue was then processed through a dehydration series of 30, 50, 70% ethanol (2 x 30min each), 90% ethanol (overnight), 95%, 100%, 100% dried ethanol and dried propylene oxide (2 x 30min each).
Tissues were embedded using ERL-SPURR epoxy resin (Spurr 1969).
Ultrathin sections were cut using a diamond knife mounted on a RMC MT-7 ultramicrotome (Research & Manufacturing Co. Inc., Tucson, Arizona).
Sections were collected on Formvar©-coated single-slot copper grids and stained in uranyl acetate (2% in H_2O) and Reynolds lead citrate (Reynolds 1963).
Sections were viewed and photographed using a Joel JSM 1210 transmission electron microscope (Tokyo, Japan).

2.2.3.2 Scanning Electron Microscopy (SEM)

Specimens were fixed and dehydrated as described in 2.2.3.1. Instead of resin embedding, specimens were critical point dried using CO_2 and sputtered with gold particles (as described in Rosenbauer & Kegel 1978) at the Rhodes University Electron Microscopy Unit.
Specimens were viewed and digitally photographed using a Philips XL20 scanning electron microscope at the Strahlenzentrum of the Justus-Liebig-University, Giessen.

2.3 Ecophysiology

2.3.1 Gas exchange measurements

2.3.1.1 Plant surface area calculation

The surface area of measured shoot sections was calculated as follows:
The length (l) of the stem section between two spines was determined and the stem diameter (d) was measured with a calliper in the middle of the section. The formula for calculating the surface area $A = l * d * \pi$ was used. For the spines, length and diameter were measured accordingly. (Spines were treated as cylinders for calculation as results differed minimal from results from surface calculation for cones). The calculated surface areas for each stem section and each spine were added and multiplied with 0.5 (assuming that photosynthetically active surface of the stem is 50% of the total surface: see discussion 4.3)

2.3.1.2 Gas exchange measurements in the laboratory

Gas exchange measurements of cotyledons/seedlings at the University of Giessen were conducted using a calibrated portable LCA-4 infra-red gas analyser (IRGA) with a PLC4 broad-type leaf chamber (ADC Ltd., Hoddesdon, England) for cotyledons and a broad-leaf chamber modified for stems was used for measuring shoots.
Gas exchange measurements for light, CO_2 and temperature response curves of greenhouse plants in the laboratory at Rhodes University were conducted using two sets of one CO_2 and one H_2O IRGAs (ADC 225 MK-3) (Figure 9) each, set and calibrated in differential and absolute mode, respectively.
Water-cooled glass cuvettes with known boundary layer resistance (see 2.3.1.2.1) were used. Water temperature of the cuvette circuit was controlled via a Lauda RC-8 recirculation chiller (Figure 9).

2.3.1.2.1 Boundary layer resistance

For exact calculation of CO_2 assimilation and transpiration (for details and equations see Field *et al.* 1989), the boundary layer resistance has to be known for any combination of used cuvettes and measured leaf/shoot form. Boundary layer resistance for *A. horridus* shoots in the glass cuvettes was determined as described by Parkinson (1985). A double layer of filter paper of known area and

approximately average stem shape and size, moistened with distilled water and supported by a wire frame, was placed inside the cuvette.

Air dried using Dri-Rite© was blown through the cuvette and the humidity of the air leaving the cuvette was measured with an ADC 225 MK3 water vapour IRGA. The temperature was monitored with an iron-constantan thermocouple placed between the filter paper inside the cuvette and a Fluke 51 digital thermometer (John Fluke MFG. Co. Inc., Everett, Washington, USA).

The flow rate was kept constant at 400ml/min and the measurements were taken at 21.5^{o} C. The boundary layer resistance was then calculated using the following equation:

$$r_b = [(x_f - x_o) / (x_o - x_i)] / S/W$$

where, r_b = boundary layer resistance

x_i = humidity of air entering the cuvette

x_o = humidity of air leaving the cuvette

x_f = saturation humidity at the filter paper temperature

S = projected area of filter paper

W = mass flow rate of air

Boundary layer resistance for the ADC cylindrical portable light chamber PLC was determined analogous following the procedure described in the manual.

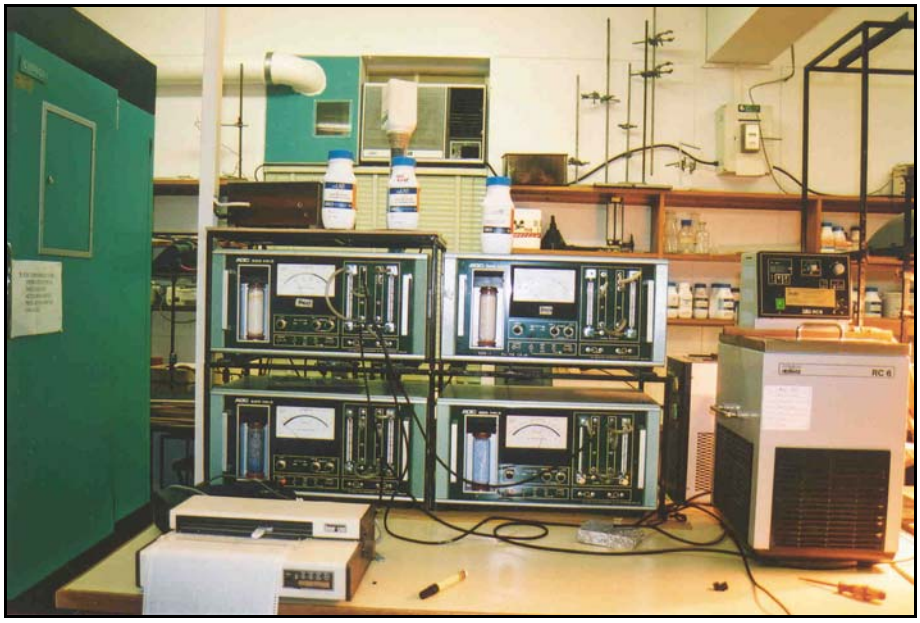

Figure 9: The four ADC 225 MK-3 infra-red gas analysers (IRGA) used for gas exchange measurements in the laboratory. On the right the Lauda RC-6 recirculation chiller used to control the cuvette temperature can be seen.

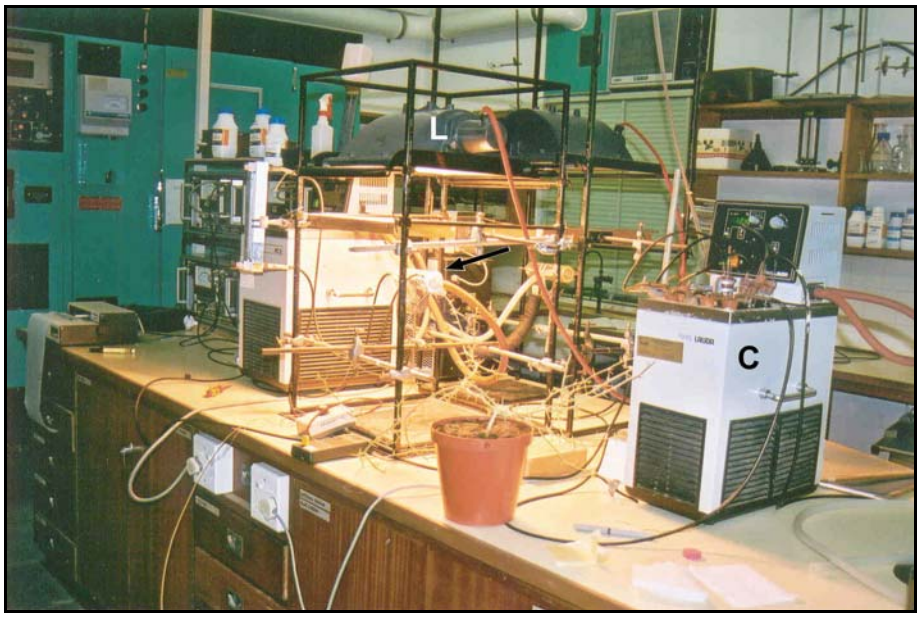

Figure 10: Experimental set up for the laboratory gas exchange measurements. The Lauda RC-6 recirculation chiller (C) on the right was used to control the water content of the ambient air that was passed through the cuvette. A shoot of the !nara plant in front is fixed and sealed in the cuvette (arrow) that can be seen underneath the Osram high pressure sodium lamp (L) in the middle.

2.3.1.2.2 Light, vapour pressure and temperature response experiments

For light intensity, vapour pressure deficit and temperature experiments, air was supplied from an outside source pumped by an ADC WA 197B-9 exhaust pump into a 25 litre buffer drum.

To set up and maintain a constant and known water vapour pressure in the supplied reference air, the air from the buffer unit was then passed through two glass “U”-pipes filled halfway with water and an empty test tube in a water bath (Lauda RMS-6 recirculation chiller, Optolabor, JHB, RSA) to saturate air at a known temperature with water vapour and prevent water bubbles from getting into the system, respectively (Figure 10).

Part of the air was passed through a adjustable precision flow meter (Fischer & Porter, Mod. 10A 3237N B10, F&P, Workington, England) and into the leaf cuvette. The air coming out of the cuvette was passed through the analysis tube of an ADC 225 MK3 CO_2 IRGA set in differential mode and on into a MK3 H_2O IRGA set in absolute mode. Reference air directly from the water bath was supplied to the reference tube of the CO_2 IRGA set in differential mode and passed on to a second MK3 H_2O IRGA in absolute mode.

Thus, CO_2 concentration was measured in differential mode, and H_2O vapour concentration of reference and analysis air was measured in absolute mode.

Leaf temperature was monitored with a iron-constantan thermocouple inside the cuvette attached to the shoot and a Fluka 51 digital thermometer.

Leaf temperature was controlled through water-cooling of the cuvette temperature using a Lauda RC-6 recirculation chiller.

Light was provided by a Vialox NAV-T400W high pressure sodium lamp (Osram, Johannesburg, RSA).

Light intensity was varied by placing shade cloth netting of different thickness and net size between the cuvette and the lamp. Light intensity ranged from 0 to 2000 µmol m^{-2} s^{-1}, as measured with an ELE SKP 200 photometer using a SKP 215 sensor.

Leaf, resp. cuvette temperature was regulated by adjusting the water temperature in the cuvette cooling circuit.

Water vapour pressure deficit was regulated by changing the cuvette temperature and by changing the temperature of the bath that saturated the supplied air with water vapour.

2.3.1.2.3 CO_2 response measurements

For CO_2 response experiments, air supplied from a gas cylinder (certified gas, Fedgas, Port Elisabeth, RSA) was diluted using an ADC GD-600 gas diluter and passed through the set-up as described in 2.3.1.2.2 instead of outside air.
The CO_2 concentration of the supplied air was monitored with an additional ADC 225 MK-3 CO_2 IRGA.
Plants were exposed to air containing 700ppm CO_2. The CO_2 concentration was lowered to zero ppm in steps of ~80ppm and then raised again to 700ppm. Plants were left to acclimate in 700ppm for 30-60 min and in 100ppm after being exposed to zero CO_2 for 30min.
Readings were taken when stable about 15min after the CO_2 concentration was changed.

2.3.1.3 Gas exchange measurements in the field

Gas exchange measurements in the field were conducted using a portable LCA-2 IRGA (ADC) with a portable PLC leaf cuvette of the large cylindrical type.
Air was drawn from a probe 5 meter above ground using a ADC-ASU mass flow meter. (Figure 11).
For the diurnal photosynthetic course under field conditions, gas exchange was measured on four different plants (Three at the Kuiseb river near the Gobabeb research station, one in the Khommabes valley).
Two 24h and two 14h measurements were conducted:
8 shoots were selected on each plant, tagged and the position of the leaf chamber was marked with a felt-tip pen. Photosynthesis and transpiration (resp. CO_2 and humidity difference between cuvette and ambient air) were measured hourly between sunrise and sunset, and three times at night during 24h measurements.
467 data sets (CO_2 difference, humidity, PAR and temperature) were recorded altogether.

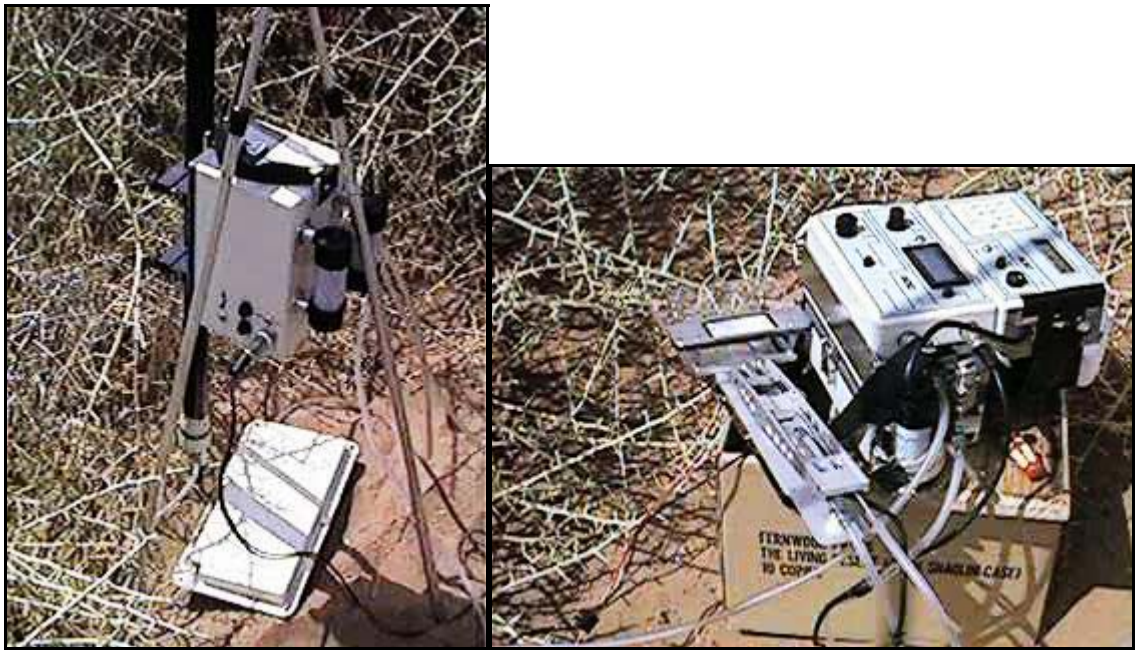

Figure 11: The portable LCA2 IRGA with the cylindrical leaf chamber PLC on the right and the ASU pump/flowmeter on the probe tripod with the buffer volume underneath.

2.3.1.3.1 Parameters recorded in the field

Apart from the data recorded with the LCA-2 (photosynthetic active radiation PAR, cuvette temperature T_c, calculated leaf temperature T_{leaf} , relative cuvette humidity RH_c, ambient and cuvette CO_2 concentration C_e, C_o) a number of parameters was recorded manually:

Ambient air temperature T_a, using a standard thermometer,

ambient relative humidity RH_a, using a sling psychrometer and a hygrometer,

soil temperature in 10cm depth T_s, using a wood-covered soil thermometer.

Parameters were recorded after each set of gas exchange measurements with the LCA-2, usually hourly.

2.3.2 Water potential measurements with the pressure-bomb

All water potential measurements were conducted with a Scholander pressure bomb (Scholander *et al.* 1965), using compressed air (AFROX Namibia) from cylinders.

2.3.2.1 Diurnal Course of Plant Water Potential

As most members of the Cucurbitaceae family, *Acanthosicyos horridus* exudes 'bleeding sap' of phloem origin (Richardson *et al.* 1982) when cut, forming a droplet on the cut surface. These droplets were collected for phloem sap analysis (sugars and amino acids, see 2.4.1) but interfered with water potential measurements by the Scholander bomb, as described later in this paragraph.
The sap is exuded in quantities of 10 to 50 µl - depending on size and function of the shoot and time of the day - and gels within two minutes, sealing the cut. To avoid sealing of the cut and water loss due to evaporation, which might falsify the actual pressure reading, shoots were placed into the pressure chamber within 90s. Since shortening the shoot or cutting off spines in order to fit the shoots into the pressure chamber resulted in unreliable readings, only shoots with the length of the lowest internode (distance form next higher order branch to first node) being at least 6cm and the overall length of the shoot being no more than 20cm were used.

When placed in the pressure bomb, the cut stumps exuded sap at low pressure at about –0,2 MPa making it difficult to distinguish between exuded sap and xylem water.
Additionally, due to the anatomy of the !nara, air entering through the stomata in the pressure chamber was forced along the continuous substomatal cavities and emerged at the cut, causing heavy bubbles that made it impossible to monitor the xylem.
This phenomenon was observed during daytime at about 2000kpa but at night started at 100kpa.
To keep the cut surface clear, an additional cut was made around the stem about 0,5mm deep and 3mm below the cut surface. Air from the cavities could then exit through this cut while the central xylem vessels where unaffected.
It is however possible that the plant water potential values recorded in this way where somewhat lower than the actual pressure of the xylem vessels.

Measurements were made both at the Gobabeb study site as well as on plants growing in the Khommabes valley.
All diurnal courses of water potential were plotted from measurements made in the morning, at midday and in the evening, in some cases with additional measurements made at night.

2.3.2.2 Pressure-Volume Curve (pV Curve)

For pressure-volume curves (pV curves), shoots from plants near Gobabeb station were cut in the evening, immediately re-cut under water, and taken to the laboratory in a sealed container. Shoots were kept in a sealed container with water overnight, to allow full rehydration.
Shoots were then put through rubber bungs, re-cut and immediately weighted on a laboratory precision scale (4 decimals). Xylem water pressure was then measured with the pressure bomb and shoots were again immediately weighted. The procedure was repeated until weight-, respectively water-loss became linear.
Dry weight of the measured shoots was determined afterwards (oven dried at 80°C until no further weight loss was observed).
A pressure-volume curve was plotted and evaluated as described in Beadle *et al.* (1993) (see 3.2.2.2)

2.3.3 Growth rate measurements

Young plants in the glasshouses were marked at an appropriate spot beneath the growing tip (3-5cm) with a felt-tip pen and the distance to the apex was measured with a ruler and noted.
Distances were measured twice daily, in the morning and in the afternoon for one month at Rhodes University.

For plants in the field selected tips and fruits were tagged. Shoots were marked as above and measurements taken every other or every third day. Fruit-growth was measured as increase in diameter, measurements taken with a vernier calliper, every second or third day.
New tips and fruits were selected for those eaten by donkeys, goats, jackals or insects during the observed time.

More specific methods as described in Beadle (1993) could not be used because they were either destructive, not appropriate to measure stem growth or growth of fruits that are difficult to reach or too time intensive.

2.3.4 Water content measurements

For the determination of water content, shoots of approximately the same length and size were cut, placed in a pre-weight (tara) vial and sealed. In the lab, the vial was weighted again, the brutto weight noted and shoots were oven-dried at 80°C until no further weight loss was recorded, usually after 7-10 days. The dried tissue was weighted again, the difference giving the total plant water.

Samples were collected on two consecutive days at 19.00h and on one day at 8.30, 13.30, 18.30 and 23.30h with 4 samples per plant per time, adding to 24 samples altogether.

2.4 Physiology

2.4.1 Transport sugar exudates and starch extracts

Samples of phloem exudate and bleeding sap were taken to analyse abundant transport sugars and starch content of the tissue as well as variation in the concentration during the day. Five vials with 10µl of sap droplets, three vials with exudate and three tissue samples for starch analysis were collected morning, midday and evening, two sets were also collected at night.

A variety of sampling methods are described in the literature (Richardson *et al*. 1982, van Bel *et al*. 1993) and were modified as follows:

2.4.1.1 Sampling in the field

For exudates, shoots of approx. 15cm length were cut, placed in 1ml Aqua dest in an 1,5ml Eppendorf vial sealed with Parafilm. Shoots were left to exude for one hour at ambient temperature. Vials were immediately put on ice and stored at –18°C to inactivate invertase until further processing. Shoots were dried at 80°C to determine dry weight.

Parallel, shoots and flowering buds were cut and the droplet of sap forming on the cut surface was collected with a 20µl Eppendorf micro-pipette. The droplets were transferred into 0,5ml cooled Aqua dest, placed on ice and stored at -18°C to prevent autoinverting of sugars until further processing.

For analysis of starch content, whole shoots were collected, placed on ice and boiled in double plastic bags for 10 minutes upon arrival at the research station or, where possible, directly in the field.

Inactivation of enzymes in exudate and sap samples through boiling proved to be unsuccessful due to high protein content in the samples, which was denatured by the boiling and agglutinated the samples.

2.4.1.2 Sampling of greenhouse plants

Exudates of shoots and cotyledons of young plants were collected at the JLU Giessen. Shoots and cotyledons were cut, put in vials filled with Aqua dest or Aqua dest and EDTA and left to exude, with samples taken after 2, 4.5, 7 and 23 hours. Shoot and Cotyledon tissue was also collected for analysis of starch and soluble sugar content. Tissue was immediately deep frozen after collection until further procession (see 2.4.1.3).

2.4.1.3 Preparation and analysis of samples

Droplet and Exudate samples were tested for concentration of sucrose, raffinoseoligosaccharides and other know transport carbohydrate with high-pressure-liquid-chromatography (HPLC) (Dionex ED 40 detector with GP40 gradient pump, Dionex Corp, USA)

Samples were diluted 1:10 for analysis in the HPLC and tested for myo-inositol, sorbit, galactinol, glucose, fructose, sucrose, raffinose, stachyose, and verbascose.

Tissue samples for the analysis of starch and soluble sugar content were freeze-dried with liquid nitrogen, homogenised in a cooled mortar-and-pestle, boiled with insoluble polyvinylpyrrolidone (Polyclar AT, Serva Chemicals) for 10min, and centrifuged twice. The resulting pellet was analysed for starch content using a Boehringerkit (Boehringer, Mannheim, Germany) and a photospectrometer (EIA Reader), the solution was analysed for soluble sugars using a HPLC.

2.5 Data Manipulation

Images taken with the Olympus DP-10 digital camera, taken with the Joel TEM digital camera, and images taken on film and later scanned in were manipulated using Photoshop 5.0 (Adobe Systems, USA) and Photopaint 8.0 (Corel 8.0, Corel, USA). Graphic programmes were used to add sizebars, to brighten up or enhance contrast in images, where necessary, to cut out /enlarge selected areas of interest and to retouch images in order to enhance quality (e.g. cover up areas where dirt from the camera lenses showed) without altering structures that were interpreted.

Gas exchange rates measured wit the LCA 4 were calculated immediately by the IRGA, stored and later on transferred via an RS232 to a personal computer and imported into Microsoft Excel 97 for further manipulation.

Gas exchange measurements carried out using the ADC LDC-2 and the 225 MK-3 types were transformed and calculated using Microsoft Excel 97/2000.

3 RESULTS

3.1 Anatomy

3.1.1 The Stem

While the stem of *Acanthosicyos horridus* shows all the essential Cucurbitaceae features (Metcalfe & Chalk 1972, Figure 12), it has a very distinct anatomy and differs from “standard” types of cucurbits in a number of details.

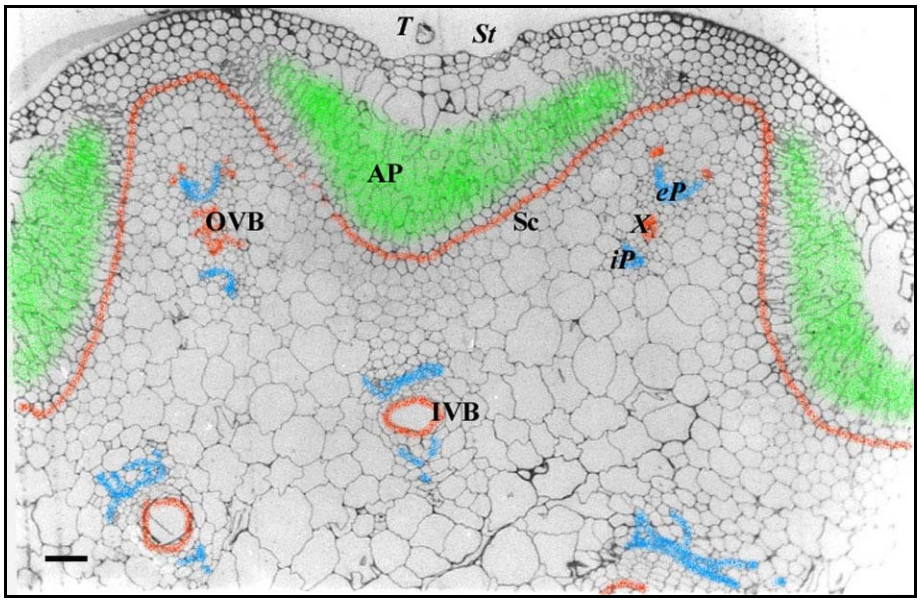

Figure 12: Semi-thin cross-section of a young stem of a greenhouse *A. horridus* plant. The sclerenchyma sheath (Sc) separates the ground parenchyma with the outer (OVB) and inner (IVB) vascular bundles from the assimilating parenchyma (AP). Stomata (St) are restricted to grooves above the AP. Trichomes (T) are abundant in the grooves. Sclerenchymatised cells and xylem (X) are colorized in red, chlorophyllous cells green, phloem tissue blue. eP: external phloem, iP: internal phloem. Extrafascicular phloem not visible. Bar: 50µm. Semi-thin section of resin embedded specimen (SPURRs). Stain: crystal violet, colorized.

3.1.1.1 The Outer Layer of the Stem – Cuticle and Epidermis

The !nara’s interface with the desert air consist of a single layer of small epidermis cells (2µm in diameter, 5-10µm long) with a thick cuticle (up to 5µm) and additional wax layers of up to 5µm thickness (Figure 14). In between the bows of assimilating parenchyma, there are 4-5 rows of subepidermal cells that are interconnected by abundant plasmodesmata arranged in fields. A sclerenchyma sheath separates the epidermal layers from the ground parenchyma (Figure 13).

Wax deposits are abundant especially in the stomatal grooves (see 3.1.1.2) and occur in various forms of scales, rods and pseudo-crystals.

Around the stomata, wax layers can be over 5µm thick.

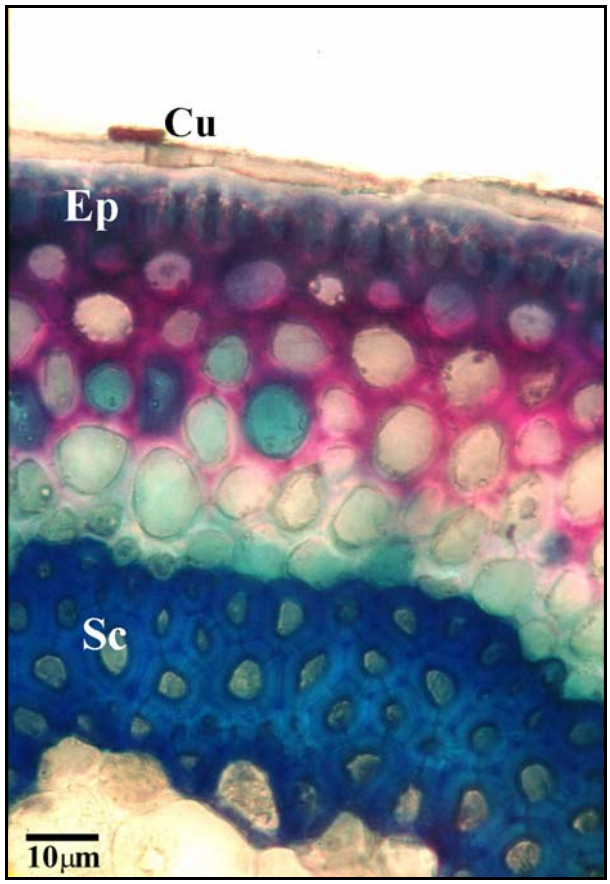

Figure 13: Outer layer of the !nara stem. Narrow epidermal cells (Ep) are covered by a thick cuticle and a wax layer (Cu). Underneath the epidermis 5 layers of subepidermal cells are bordered by thick-walled cells of the sclerenchyma sheath (Sc) that separate the epidermal layers from the ground parenchyma. Free hand section. Stain: toluidine blue.

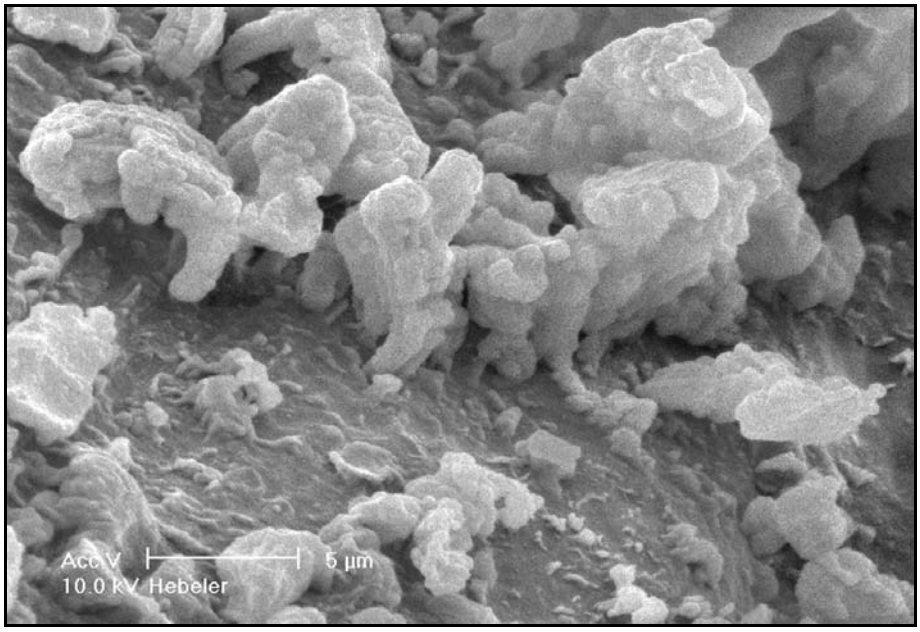

Figure 14: Scanning electron microscopy (SEM) image of wax structures found on the stem surface on the flanks of the stomatal grooves. Wax protrusions are more than 5µm thick.

3.1.1.2 The Photoassimilating Unit – Assimilating Parenchyma and Stomata

The assimilation parenchyma (AP) is separated from the ground parenchyma by a sclerenchyma sheath (see 3.1.1.3) that restricts the AP into flat, U-shaped ledges, which are continuous and orientated parallel to the stem. The AP consists mainly of narrow, elongated palisade parenchyma cells arranged in 4-6 rows. There is practically no spongy parenchyma; Cells at the border to the sclerenchyma are less elongated and more densely packed.

The palisade parenchyma cells are orientated in a slight angle towards each other, following the bow form that is given by the sclerenchyma sheath (Figure 15).

Cells have minimal contact to neighbouring cells, thus generating a high overall mesophyll surface area and these intercellular spaces extend to large substomatal cavities towards the epidermis.

The APs “folded-in” or U-shape appearance, is comparable in anatomy and function to the xeromorph roll- or folding leaves of some *Stipa* grasses, such as *Stipa pennata* or *S. capillata.* The AP bows are continuous through the length of the stem, resulting in longitudinal grooves, that give the stem it’s striped look (Figure 17).

Stomata are restricted to these grooves and are sunken within the tissue matrix (Figure 19) on the interior surface of the groove, resulting in minimal contact of the guard cells with the dry outside air. The stomata consist of two guard cells. The facing walls of the guard cells are thickened and end in narrow ledge rims, thus forming an additional seal (Figure 18). In top-view, the guard cells are surrounded by concentric circles of small epidermal cells that form a “funnel” from the level of the epidermis to the sunken guard cells and partly obscure the guard cell (peristomatal rim, Wilkinson 1979).

Trichomes are found inside these grooves in the proximity of the stomata (Figure 20).

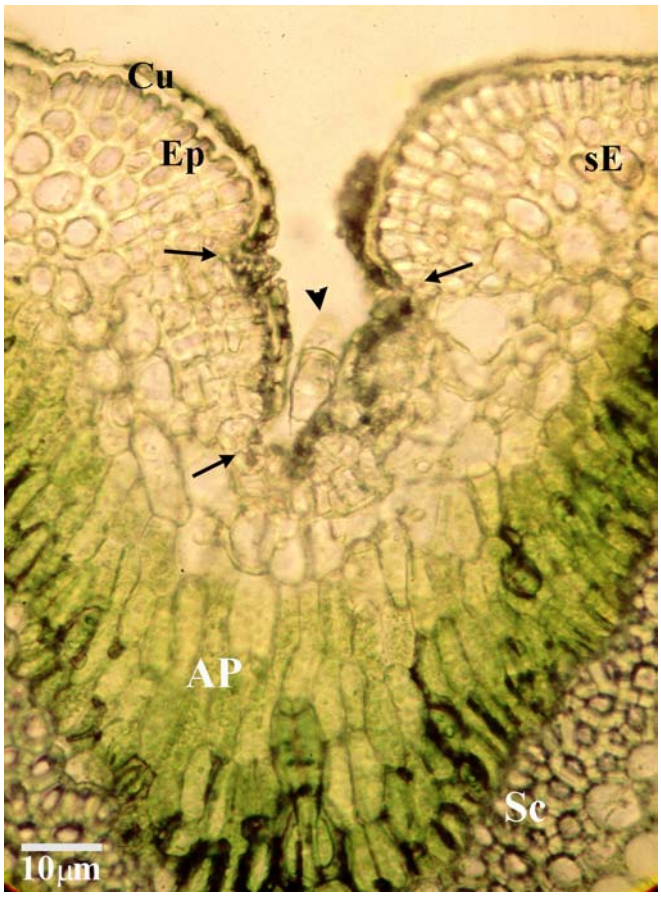

Figure 15: Cross section through an assimilation parenchyma bow (AP). The palisade parenchyma cells on both sides are orientated in an angle of nearly 90° towards each other, this way some cells are always orientated towards the sun. Stomata (dark arrows) are sunken within the tissue matrix inside the narrow groove. Cu: cuticle, Ep: epidermal cells, sE: subepidermal layer. Sc: sclerenchyma sheath, dark arrowhead: trichome. Free hand section, light microscopy. unstained.

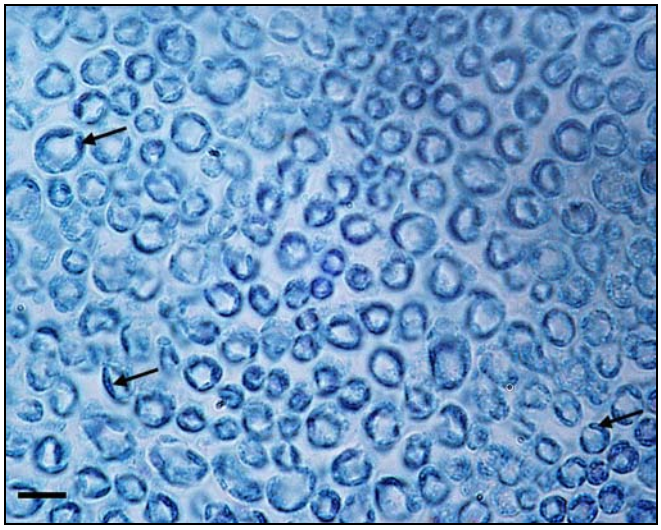

Figure 16: Top view of palisade parenchyma cells. Chloroplast (arrows) are situated along the side-walls of the cells. Note the intercellular spaces and the minimal contact of neighbouring palisade cells. Bar: 5µm. Tangential section, Paraplast wax embedding, light microscopy. Stain: safranin, fast-green.

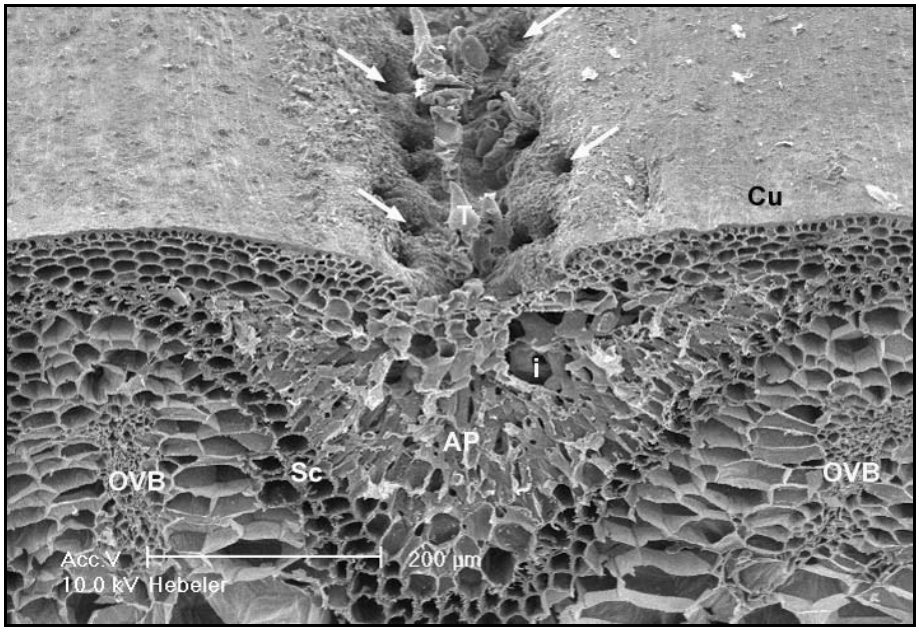

Figure 17: SEM image of a cross section through the assimilating parenchyma (AP). The AP is continuous along the stem and lined by the undulating sclerenchyma sheath (Sc). Stomata (arrows) are restricted to grooves running along above the AP. Note the large intercellular/substomatal spaces (i). Ep: epidermal cells, Cu: cuticle, OVB: outer vascular bundles, T: trichomes.

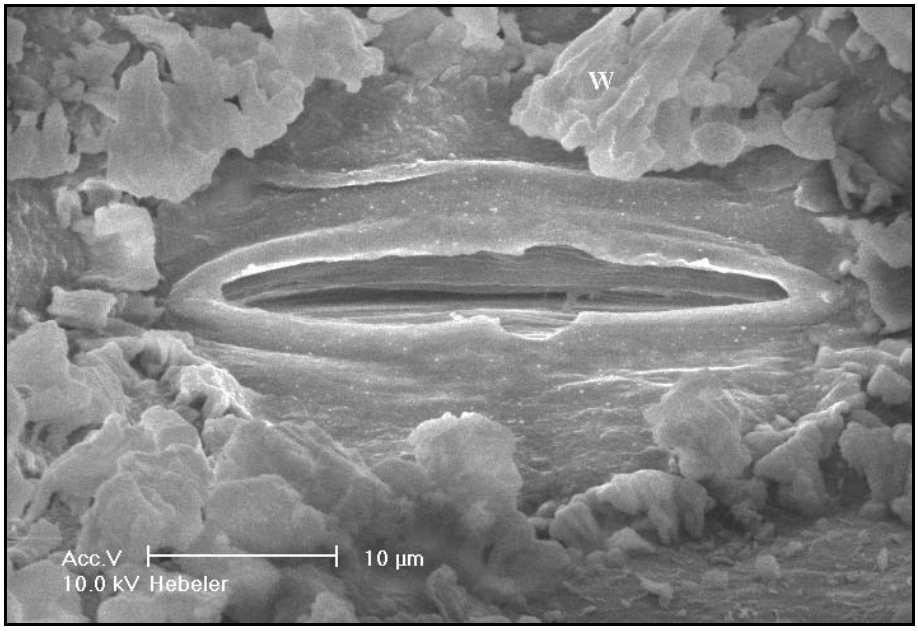

Figure 18: SEM image of a stoma. Note the peristomatal rim and the wax structures (W) around the opening.

Figure 19: Stoma sunken within the tissue matrix through a "funnel" of small epidermal cells. Note the thick cuticle (C).Epidermal cells (Ep), intercellular/substomatal space (i). Bar: 10µm. Paraplast wax embedding, light microscopy. Stain: safranin, fast-green.

The trichomes (Figure 21) belong to the uniseriate type according to Esau (1965). When examined under the phase contrast microscope, most of them appear to be alive with normal nuclei and cell structure according to Louw *et al.* (1986).

Due to the anatomy described above, the stems are peristomatic, and photosynthetic tissue is only found underneath approx. 50% of the epidermal layer (see discussion 4.3). Stomata are restricted to about 1/4 of the surface area, but stomatal density in the grooves is high (area of stomata is 30-40% of total epidermal surface area in the grooves).

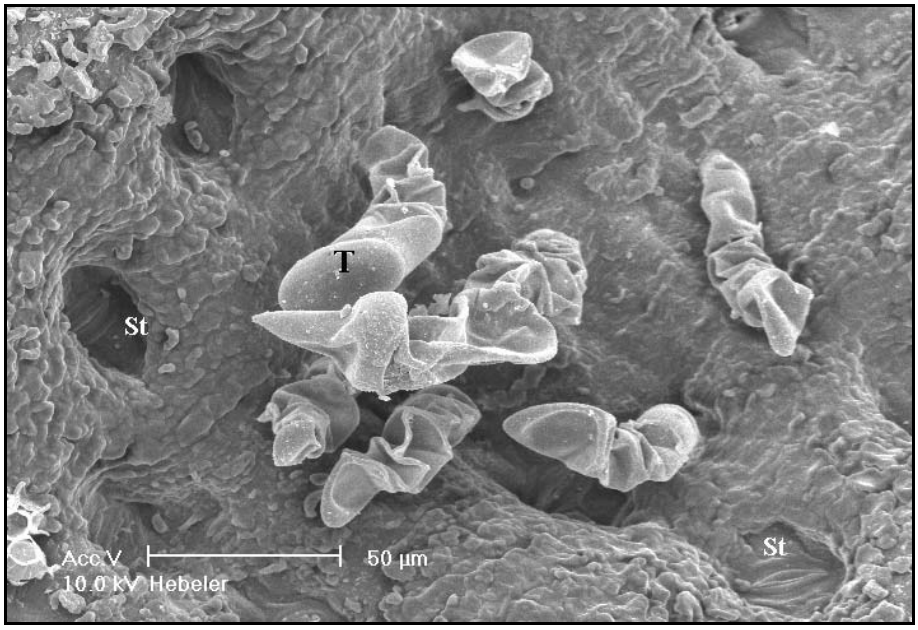

Figure 20: Top view of a stomatal groove. Stomata (St) are lowered within the tissue matrix and surrounded by thick layers of wax. Trichomes (T) fill the groove. Note that specimen was collected from young greenhouse plant. Grooves are wider and show less wax due to none-arid growing conditions. SEM image.

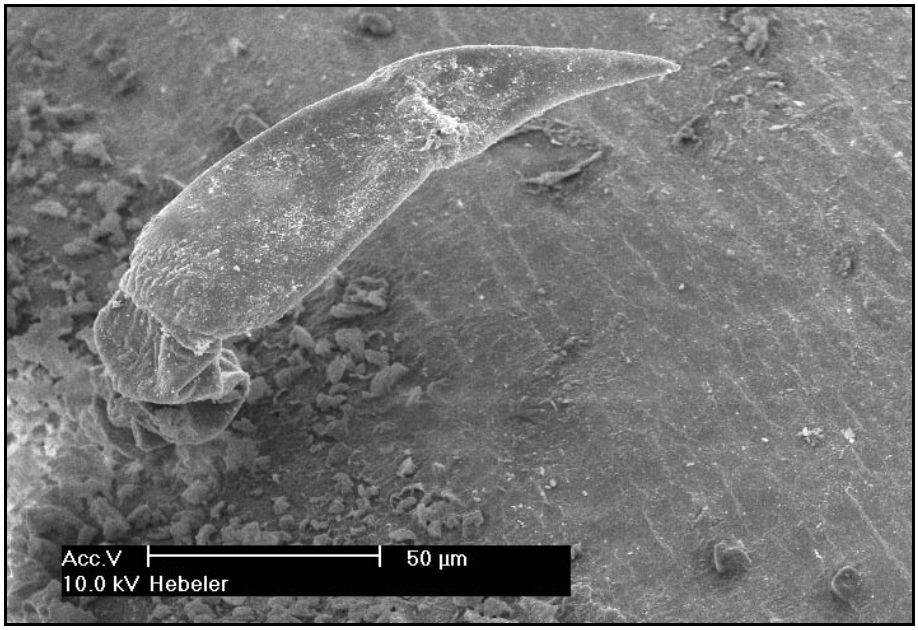

Figure 21: Trichome on the edge of a stomatal groove. Trichomes are not fully turgescent, possibly due to preparation/fixation and/or conditions shortly before fixation. SEM image.

3.1.1.3 The Sclerenchyma Sheath

A layer of sclerenchymatised cells that separate an inner from an outer parenchyma is characteristic for Cucurbitaceae.

In *A. horridus,* this sclerenchyma sheath has a number of distinct features.

It is continuous through the diameter of the stem but varies in thickness. While in young plants there are often only one or two sclerenchymatised cells between palisade parenchyma cells and the ground parenchyma in the proximity of the OVB, in mature plants the sheath can be up to 10 cells thick at it's innermost edge, closest to the inner vascular bundles.

The secondary cell walls of the sclerenchyma sheath cells can be extend and account for up to 50% of the cell diameter. Cell-cell contacts are abundant in the SS. Around the plasmodesmata fields the secondary cell walls are much thinner, creating pits in the cell walls, which can be easily observed with light microscopy (e.g. in sections stained with crystal violet, compare Figure 22).

Plasmodesmata in these pits can be branched towards either side or H-shaped.

There are also numerous PDs at the interfaces on both sides of the SS towards the palisade parenchyma and the ground parenchyma.

In between the AP bows, the SS extends to a layer of small subepidermal cells with abundant cell-cell contacts, followed by the epidermis and a thick cuticle (Figure 13 in 3.1.1.1)

A peculiarity of the sclerenchyma sheath can be found in almost every other section viewed: Amongst the longitudinal sclerenchyma fibres there appear to be patches/beams of cells that have thinner secondary walls, a higher plasmodesmal density, larger cell diameters and that are less elongated.

These cells seem to cross the sclerenchyma sheath from the assimilation parenchyma to the ground parenchyma in the vicinity of the xylem/ internal phloem of the outer vascular bundles in the manner of "Durchlasszellen" (gating cells) in the endodermis of roots (Figure 22). Alternatively, they could be secondary sclerenchymatous cells, that connect the original ring of sclerenchyma, which might have been interrupted by secondary growth.

Additionally, unlike in *Cucurbita maxima*, no vascular bundles or strands of extrafascicular phloem can be found outside the sclerenchyma sheath.

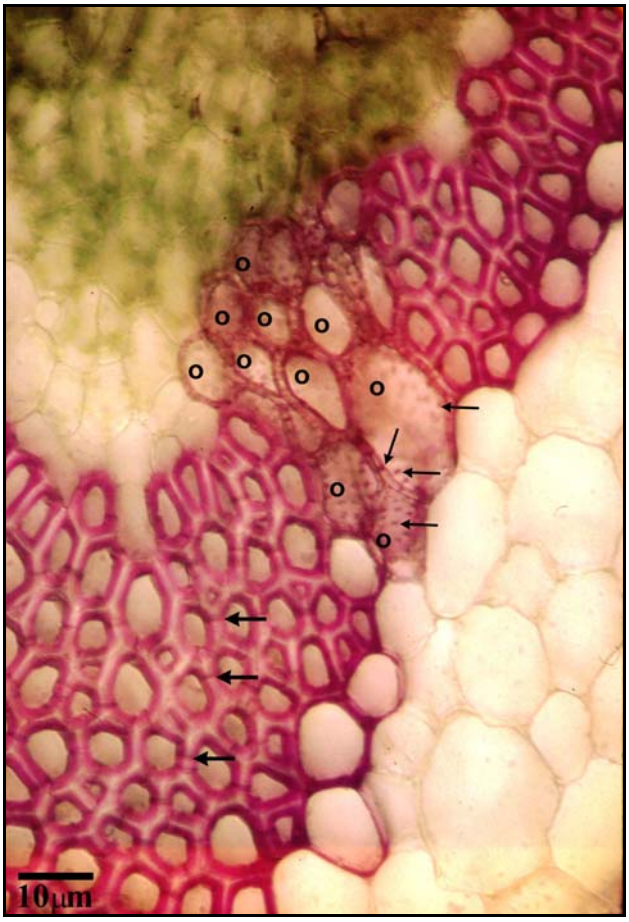

Figure 22: The sclerenchyma sheath in mature plants can be up to 12 cells thick. Secondary cell walls are stained red. Plasmodesmata fields are visible as red beams (large arrows) indicating abundant cell-cell connections. In nearly every cross section, patches of cells (o) that are less elongated, with thinner secondary walls and more frequent cell-cell connections (small arrows) can be found crossing the sclerenchyma sheath from the AP to the ground parenchyma. Free hand section. Stain: crystal violet.

3.1.1.4 The Inner Parenchyma of the Stem

The ground parenchyma makes up for most of the stem tissue. The diameter of ground parenchyma cells increases from the epidermis to the centre of the stem. Cells are thin-walled with large vacuoles. Considering the average water content of whole stems (75%, see 3.2.4) it can be assumed that the parenchyma functions as water storage and /or even has an influence on transpiration through passive regulation of the “aperture” of the grooves via turgor pressure, resp. hydration status of the parenchyma cells.

No starch was found in the ground parenchyma (I_2 KI staining, starch analysis) at all, but Kutschera *et al.*(1997) report a high starch content in root and underground stem tissue.

These large, mostly “empty”, translucent parenchyma cells also facilitate the transmission of light through to chlorenchyma on the distal side of the stem.

A ring of sclerenchymatous cells (pericycle) in the centre of young shoots can sometimes be found, but it is absent in older stems (Metcalfe & Chalk 1972).

3.1.1.5 The Vascular Bundles of the Stem

Two major types of vascular bundles can be clearly distinguished in transverse sections of *A. horridus* stems.

The ring of the outer vascular bundles, situated between the ridges of assimilation parenchyma – here called outer vascular bundles (OVB) - and the larger inner vascular bundles (IVB), arranged in 1-4 concentric rows.

Both types are bicollateral, with a more distinct external (abaxial) phloem, and both types can be interconnected through extrafascicular phloem (connecting to both internal and external phloem), see 3.1.1.5.3

At every node, the vascular bundles of the stem are interconnected by rings of commissural phloem (compare Webb & Gorham 1964) and the vascular bundles from the thorns connect to their stem equivalent..

While in younger stems and shoots only 2 rings of vascular bundles occur (one ring of outer and inner vascular bundles each, compare Figure 12), older stems with diameters of 2cm or more can have 3, 4 or even 5 concentric rings of vascular bundles. These stems have lost most of their chlorenchyma and seem to have mostly transport functions.

3.1.1.5.1 The Outer Vascular Bundles

The OVB have relatively few (3-8), small and thin-walled xylem elements (5-10µm in cross-section). The external (abaxial) phloem is larger and more distinct than the internal (adaxial) phloem and more or less continuous with the xylem. The internal phloem consists of no more than 4 or 5 companion cell/ sieve element complexes (CC/SE) and often is separated from the xylem by two or three ground parenchyma cells. It is sometimes lost completely, thus giving rise to collateral bundles amongst the otherwise bicollateral bundles.

In cross-sections, the external phloem often appears V-shaped (pointing towards the xylem, compare Figure 24.

Phloem fibres (sclerenchymatised metaphloem, PF in Figure 24) can always be found at both ends facing the sclerenchyma sheath, sometimes extending on both sides towards the xylem. The companion cell/ sieve element complexes are often clearly distinguishable under a light microscope (using crystal violet or toluidine

blue staining, Figure 23); they are replaced by parenchyma cells in the centre of the external phloem, giving it a V or U shape.

While in leaf minor veins the vascular bundles are surrounded by a bundle sheath, no bundle sheath is usually present in bundles of the stem.
In the OVB of *A. horridus* stems, the external phloem is bordered by single rows of (vascular) parenchyma cells (o in Figure 23 and Figure 28), neighbouring the phloem fibres mentioned above. However, this row of parenchyma cells surrounding the phloem (Figure 23) is discontinuous, is only found around the external phloem and varies considerable in size and structure. Small chloroplasts can sometimes be found.

The companion cells in the OVBs are mostly of the intermediary cell type (IC; companion cells with dense cytoplasm, heavily fragmented vacuoles and frequent plasmodesmatal connections to the surrounding parenchyma cells, Gamalei 1989, Turgeon *et al.* 1975) and larger in diameter (5-8µm) than their corresponding sieve elements, which are 2-5µm. PPUs between IC and SE are highly branched resulting in fields of 50-100 plasmodesmata (PDs) on the IC side (Figure 27) facing a handful of pores on the SE side (Figure 30)
There are also abundant cell-cell connections (PDs) between adjoining ICs and between ICs and phloem parenchyma cells (PPs) (Figure 28).
IC-IC PDs are usually of the H-type or more intensely branched, PDs between PP and ICs are usually branched towards the IC side (Figure 29). PDs between PPs or between PP and normal parenchyma cells can be of the H-type, branched or simple. These findings correspond with the scheme published by Kempers *et al.* 1998.
The highest PD number appears to be at the IC-IC and the IC-PP interface, were cell-cell connections are very frequent and intense creating a symplasmic continuity around the sieve elements. (Figure 28)
The internal phloem appears to have less SE-CC complexes, the companion cells can be ordinary CCs or IC, the CC/SE ration appears to be smaller than that of the external phloem.

In sections, PPUs and sieve plates are occluded with P-protein and callose, presumably as a result of wound reactions and stain with aniline blue/ calcofluor (Figure 25)

Internal and external phloem can be interconnected via extrafascicular phloem strands. Extrafascicular phloem strands can be found running along the sclerenchymatised border of the assimilating parenchyma. (see 3.1.1.5.3)

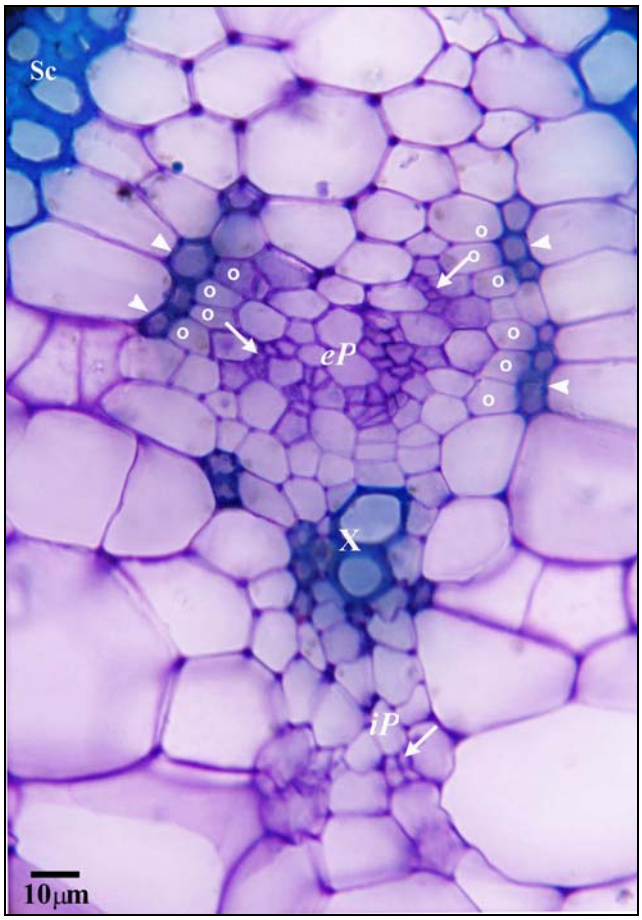

Figure 23: Bicollateral outer vascular bundle with small internal phloem (iP) and large external phloem (eP). The eP is enclosed on both sides by a number of thick-walled cells (white arrowheads), that stain red with safranin and could be phloem fibres. Each of these phloem fibre cells border with a single parenchyma cell (o) towards the phloem. Electron micrographs show these cells to share numerous plasmodesmata with the intermediary/companion cells of the eP se/cc complexes. The sieve elements (white arrows) are grouped and smaller than their corresponding companion cells. The cells (Sc) of the sclerenchyma sheath are situated between 3-6 cells away from the SE/CC complexes. Bar: 10µm. Hand section. Stain: toluidine blue.

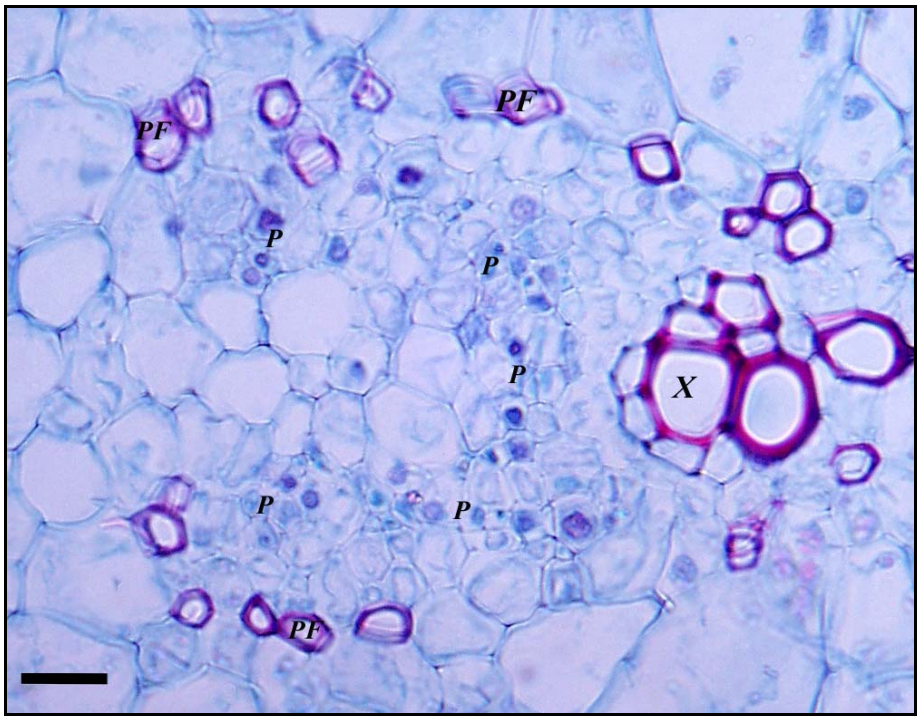

Figure 24: External phloem of an outer vascular bundle (OVB): The external phloem (P) is arranged in a U or horseshoe form with ground parenchyma cells in the centre and is surrounded by phloem fibres (PF) with strengthened secondary cell walls. X: large xylem vessel in the xylem. The internal phloem above the xylem is not shown. Bar: 10µm. Paraplast wax embedding. Stain: Safranin, Fast-Green

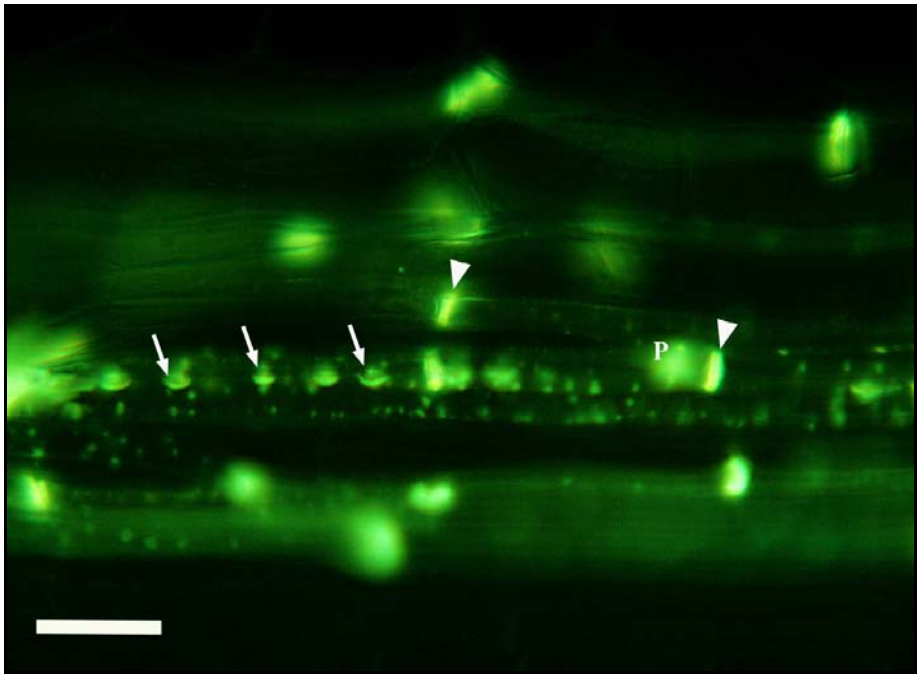

Figure 25: Sieve elements in the phloem of the outer vascular bundle. Callose stains bright yellow. The PPUs are clearly visible as small green dots, callose /P-protein caps occlude lateral sieve pores / PPUs on the SE side (arrows). Bright yellow bars are sieve plates (arrowheads) (partly out of focus), with P-protein (P, green autofluorescence), that accumulated due to the wound reaction. Bar: 5µm. Fluorescence image. Stain: Aniline blue, fluorescence brightener: Calcofluor.

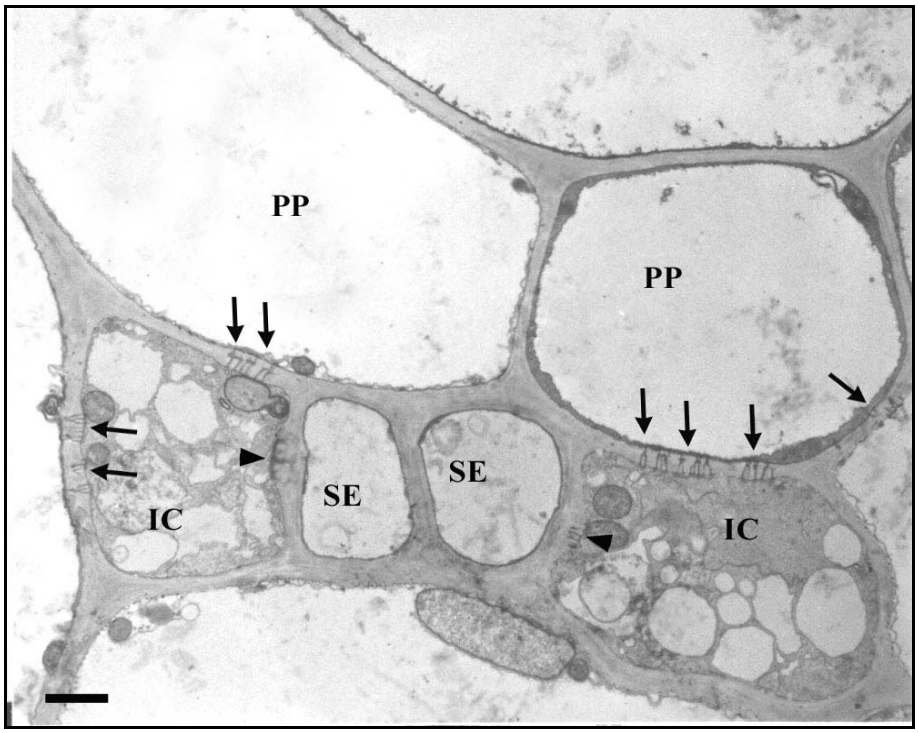

Figure 26: A CC/SE complex in the OVB. The companion cells are clearly of the intermediary cell type (IC), PPUs are visible (arrowheads). PDs (arrows) are frequent at the IC/PP interface and are branched on the IC side. This micrograph was used as a basis for the definition of cell types in other micrographs. PP: phloem parenchyma cell. SE: sieve element. Bar: 1µm. TEM picture, SPURRS embedded.

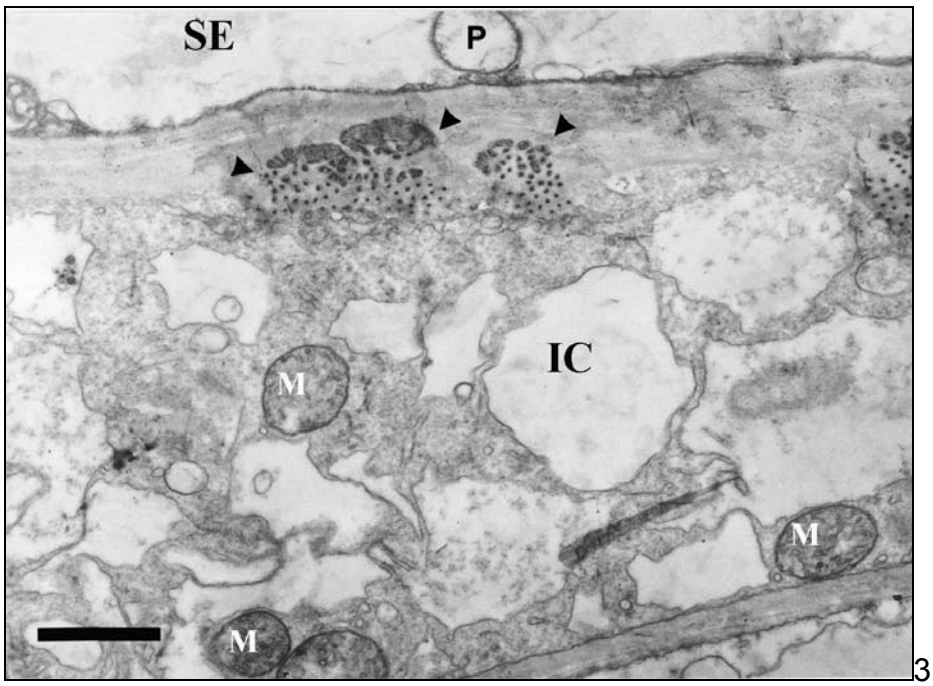

Figure 27: Cross section through an intermediary cell (IC) in the external phloem of an OVB. Plasmodesmatal fields (arrowheads) can be seen in the cell wall facing the corresponding sieve element (SE). The high grade of vacuolisation and a dense cytoplasm are key features of the intermediary cell type. M: mitochondria. P: P plastid (compare Ehlers *et al.* 2000) Bar: 1µm. TEM picture, SPURRS embedded.

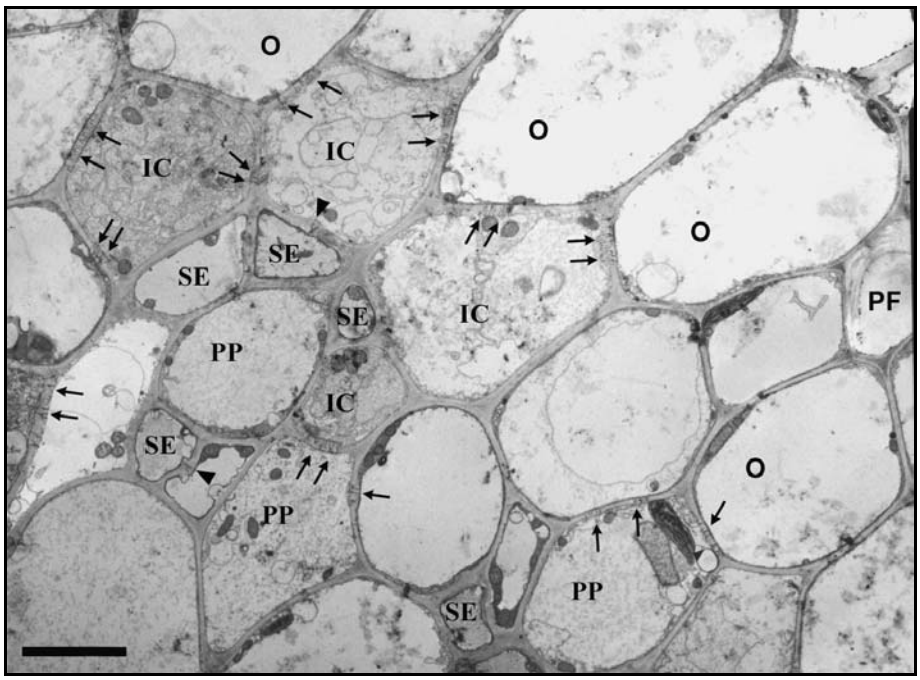

Figure 28: Sieve element/companion cell complexes of the outer vascular bundle. The companion cells are of the intermediary cell (IC) type and are much larger in size than their corresponding sieve elements (SE), a typical feature of loading phloem (see discussion, van Bel 1996a). *A. horridus* appears to be a "symplasmic loader" (ref. to text, Gamalei 1989, Turgeon *et al.* 1975) indicated by the IC structure of the companion cells and the high PD (arrows) frequency, especially at the IC/PP interface. The xylem is not visible, located on the bottom right side. The large parenchyma cells (o) visible in the top right corner are the parenchyma sheath like cells surrounding the external phloem. PF: phloem fibre, PP: phloem parenchyma, arrowheads: PPUs. Bar: 5µm. TEM picture, SPURRS embedded.

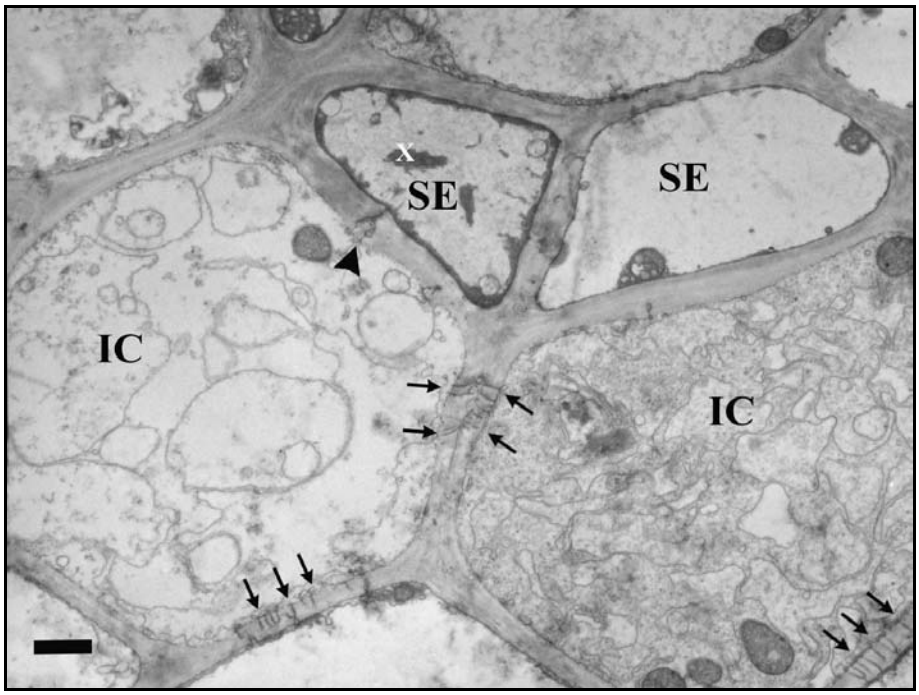

Figure 29: Detail of Figure 28. The companion cells are of the intermediary cell type (IC). Single branched PDs (arrows, lower right corner) connect to the adjacent phloem parenchyma cell (not shown), simple PDs interconnect the intermediary cells (IC). A PPU (dark arrowhead) connects the left IC to its sieve element (SE). P-protein is visible (white X), as a result of the wound reaction to the preparational cut. Bar: 1µm. TEM picture, SPURRS embedded.

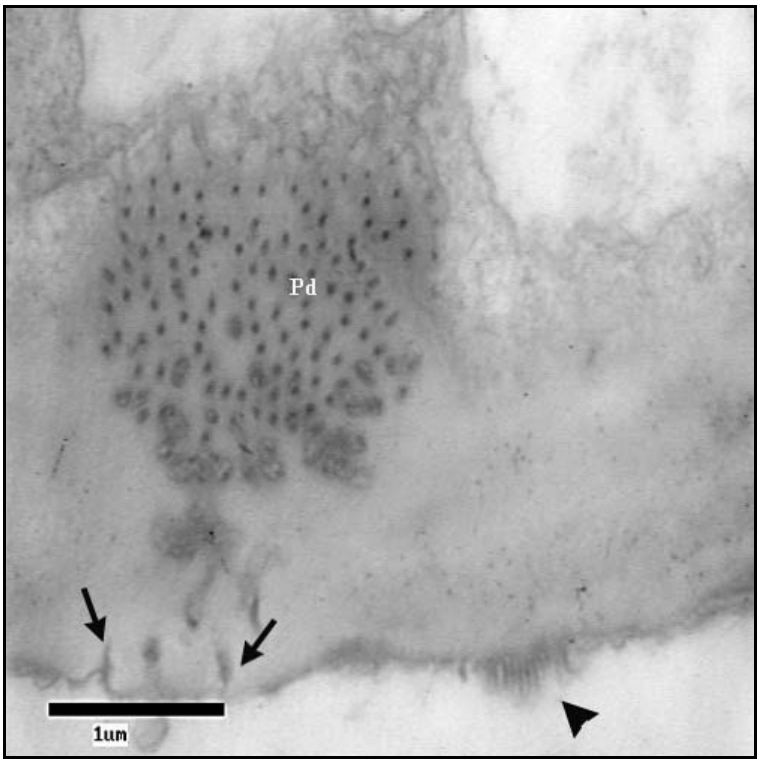

Figure 30: Detail of a pore-plasmodesmata unit PPU between an intermediary cell and its corresponding sieve element. Numerous, highly branched plasmodesmata (Pd) are arranged in fields on the IC side and open into few pores (arrows) on the SE side. Note the bands of stacked endoplasmatic reticulum (arrowhead) on the SE cell wall. Bar: 1µm. TEM picture, SPURRS embedded.

3.1.1.5.2 The Inner Vascular Bundles

Compared to the OVBs, the inner vascular bundles have a much larger xylem area. The xylem elements are more numerous and larger in diameter (80µm or more), surrounded by a collar of parenchyma cells, a feature characteristic for trees and shrubs.

Overall size of vascular bundles as well as numbers and diameters of xylem elements increase towards the centre of the stem.

The CC-SE size ratio in both external and internal phloem is lower than in the OVB, with cell diameters of 2-5µm for IC/CCs and 5-10µm for sieve elements.

Companion cells can be of the intermediary cell type, but ordinary companion cells that are less vacuolised and have less dense/granular cytoplasm are abundant.

Symplasmic connections of the companion cell with phloem parenchyma cells via PDs appear to be much less frequent than in the OVB phloem, although not enough sections were monitored to statistically support this observation. This observation corresponds with the ultrastructure found in transport phloem of *C. maxima* stems, as described by Kempers *et al.* 1998.

A large cambium consisting of several rows of cambial cells can be found between the xylem and the external phloem, a second strip of cambial tissue between the xylem and the internal phloem is distinct and clearly visible in most IVBs.

The external phloem is extend and “thins out” among numerous small parenchyma cells towards the sclerenchyma sheath (in bundles of the first row of IVB, Figure 31). No defined bundle sheath-like structure is detectable around the vascular bundles or the phloem area.

Numerous strands of extrafascicular phloem are interconnecting the IVBs, originating from both internal and external phloem, and the OVBs with the outer IVBs (Figure 31)

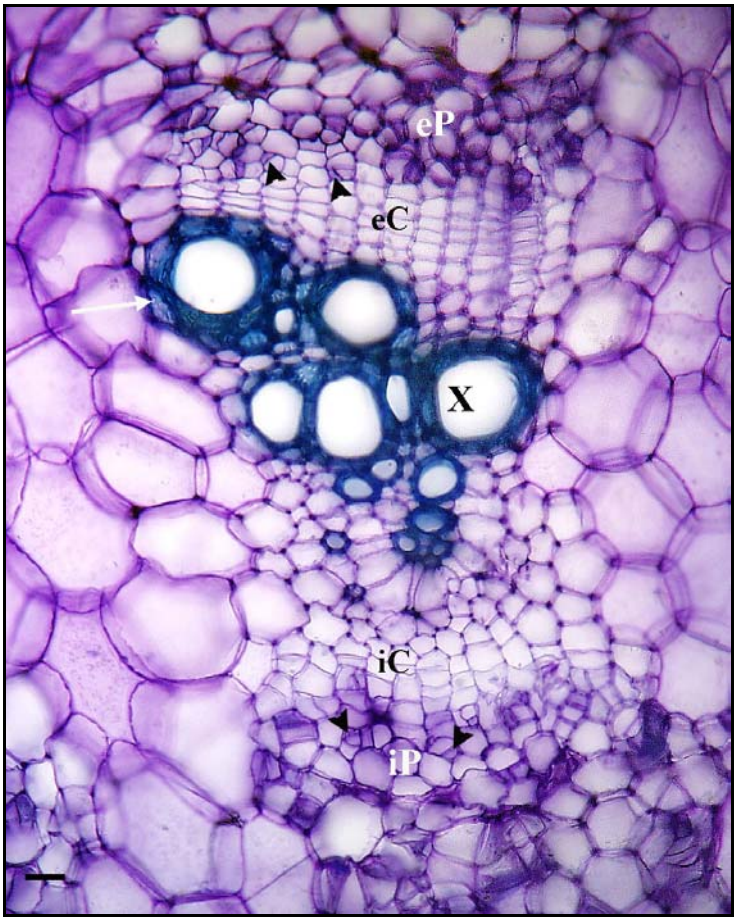

Figure 31: Freehand cross section through an inner vascular bundle (IVB). The xylem (X) consists of a number of large xylem elements surrounded by a rim of smaller sclerenchymatised cells, a feature of the primary xylem of woody species. In both external (eP) and internal phloem (iP) of the IVB, the companion cells (dark arrowheads) are smaller than their corresponding sieve elements. The inner phloem (iP), unlike in the outer vascular bundles, is well developed, both eP and iP are separated from the xylem by stripes of cambial tissue (eC and iC, respectively), although it is discussed among authors whether the stripe of small, undifferentiated cells between xylem and internal phloem (here: iC) is cambial. Bar: 5µm. Freehand section. Stain: toluidine blue.

3.1.1.5.3 The extrafascicular phloem

As found in other cucurbits, there are numerous strands of extrafascicular phloem (EFP) in the stem (Crafts 1932). Around the OVBs, EFP is running along the inner side of the sclerenchyma sheath, close to the AP. However, a loading function of the EP is unlikely (Schmitz *et al.* 1987).

EFP strands originate from both adaxial and abaxial phloem and often interconnect adaxial with abaxial phloem of the same vascular bundle. EFP also connects IVBs with other IVBs and OVBs. Extrafascicular phloem strands are less abundant towards the centre of the stem, no EFP is found outside the sclerenchyma sheath. EFP strands consist of single SE/CC complexes of approx. 50-100µm length.

In longitudinal as well as cross-sections, callose in both fascicular and extrafascicular sieve elements of *A. horridus* brightly stain with aniline blue/ calcofluor. (Figure 32 b, next page), although Kempers *et al.* (1993) reported hardly any callose deposits in extrafascicular phloem of *Cucurbita maxima*.

While until recently it was assumed that wound reaction dramatically increases callose formation in sieve plate pores, Ehlers *et al.* (2000) found hardly less callose in sieve plate pores of undamaged sieve elements than in pores of damaged ones.

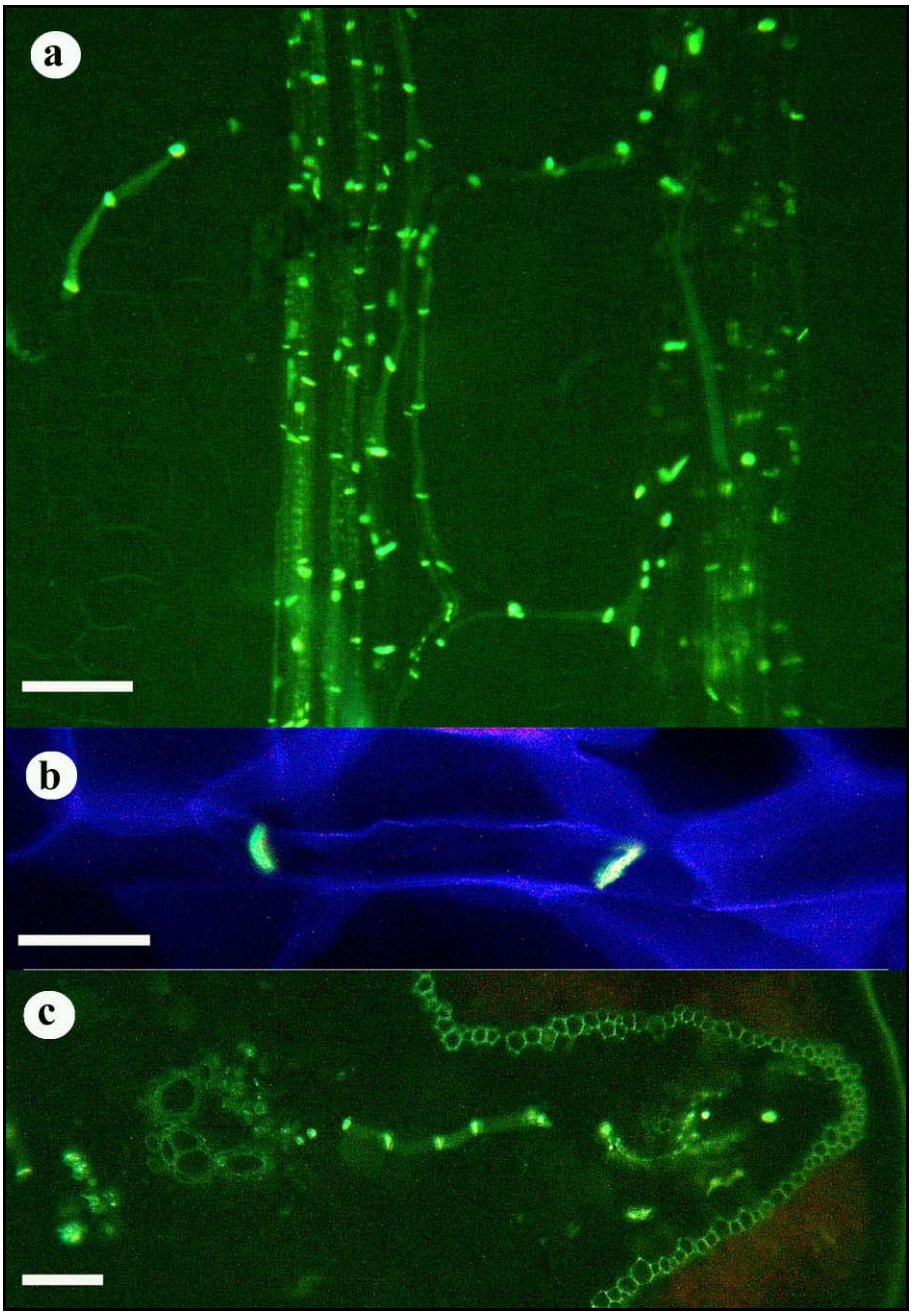

Figure 32: Fluorescence micrographs of extrafascicular/commissural phloem.
a Longitudinal freehand section of two neighbouring inner vascular bundles. Callose in occluded sieve plates is stained bright green. Note the two strands of commissural phloem connecting the two parallel vascular bundles. **b** Two sieve plates of sieve elements of the extrafascicular phloem. Sieve plates are stained bright yellow through the callose associated with the pores. **c** Extrafascicular phloem connecting the external phloem of the OVB on the right with the eP of the IVB on the left. Callose in sieve plates stains bright green, secondary walls in cells of the xylem and the sclerenchyma sheath autofluorescent green. Bars: **a**,**c** 40µm; **b** 5µm. Stain: Aniline blue + Calcofluor. Filter set: **a**,**c** Zeiss Standard Filter Set (DAPI); **b** Chroma Blue/Violet Filter Set.

3.1.1.5.4 Transport experiments with fluorescence dyes

Fluorescence probes (5,6-CF/5,6-CFDA) injected into the grooves or the substomatal cavities were not transported past the sclerenchyma sheath, neither via the apoplast (5,6 CF, apoplasmic marker) nor the symplast (5,6-CFDA).

5,6CF was hardly transported along the xylem during transpiration experiments, probably due to limited transpiration.

The only time 5,6CF was detected in the apoplast of the OVB phloem, was when the outer cortex was abraded beyond the sclerenchyma sheath (Figure 33)

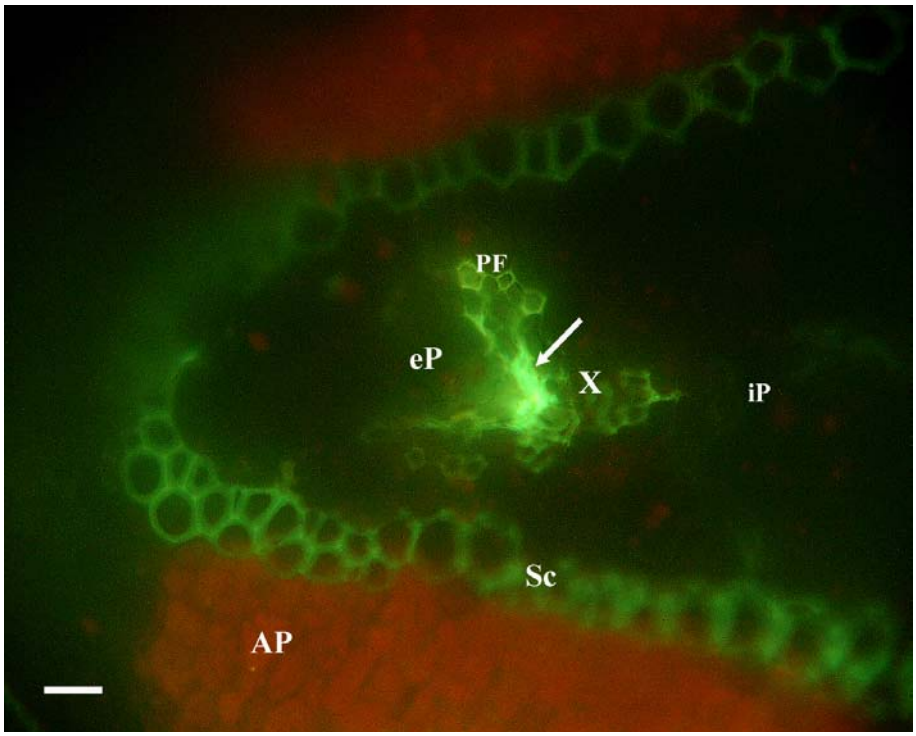

Figure 33: Fluorescence image of an OVB. 5,6 CF was applied to an abraded epidermis area. 5,6-CF (arrow: bright green fluorescence) is visible in the apoplast of the external phloem (eP). Sc: sclerenchyma sheath (green autofluorescence), AP: assimilating parenchyma (red autofluorescence), PF: phloem fibres, iP: internal phloem, X: xylem. Bar: 10µm. Free hand section. Stain: 5,6-carboxy-fluorescein. Filter: Zeiss Standard DAPI Filter.

3.1.1.6 The Hypocotyl

Transverse sections of hypocotyls from 2 month old plants show a lignified cortex, an endodermis and radial beams of xylem elements from the pith to the endodermis. The xylem is separated from a small phloem area by 3-4 layers of cambium cells.

The anatomy is according to that of common cultivated members of the cucurbit family.

3.1.2 Leaves: Leaflets and Cotyledons

3.1.2.1 Cotyledons

The cotyledons of *A. horridus* are epigaeic (epigäisch) and under normal condition fully extend to around 4 x 3 cm (l x w) about 10cm above ground 5-8 days after germination. When fully extend, they can be up to 1cm thick and are very tough, dark green on top and slightly lighter underneath. The single succeeding shoot that grows from the apical meristem is about 0,5cm in diameter and of the characteristic morphology of adult plants.

Apart from their slightly xeromorphic appearance, the cotyledons of the !nara are similar to these of other epigaeic cucurbits. There is an complex vascular system with large phloem areas extending throughout the cotyledons, the xylem area consists of a number of smaller vessels (Figure 34).

3.1.2.2 Leaflets of the first nodes of seedlings

On young plants, small leaflets are present on each of the first 5 or so nodes, covering the axillary meristems. The leaves are orientated parallel with the stem. The chlorenchyma is arranged in stripes on both sides of the leaflet. The centre of the leaflet consists of ground parenchyma and the vascular bundles – towards the tip of the leaflet, the ground parenchyma is replaced by assimilation parenchyma so that the vascular bundles are directly surrounded by chlorenchyma (Figure 35). Trichomes can be found on the upper side of the leaf, facing the stem. No sclerenchyma sheath is present.

Vascular bundles are bicollateral. In contrast to the stem, in *A. horridus* leaflets the internal phloem of the vascular bundles is distinct, while the external phloem (facing towards the upper side of the leaf = facing the stem) is only detectable in the major veins and arranged in three columns.

This anatomy corresponds with the fact that the internal (lower) phloem of the leaflet vascular bundles is continuous with the external phloem of the stem OVB. (Webb & Gorham 1964, compare 3.1.1.5.1)

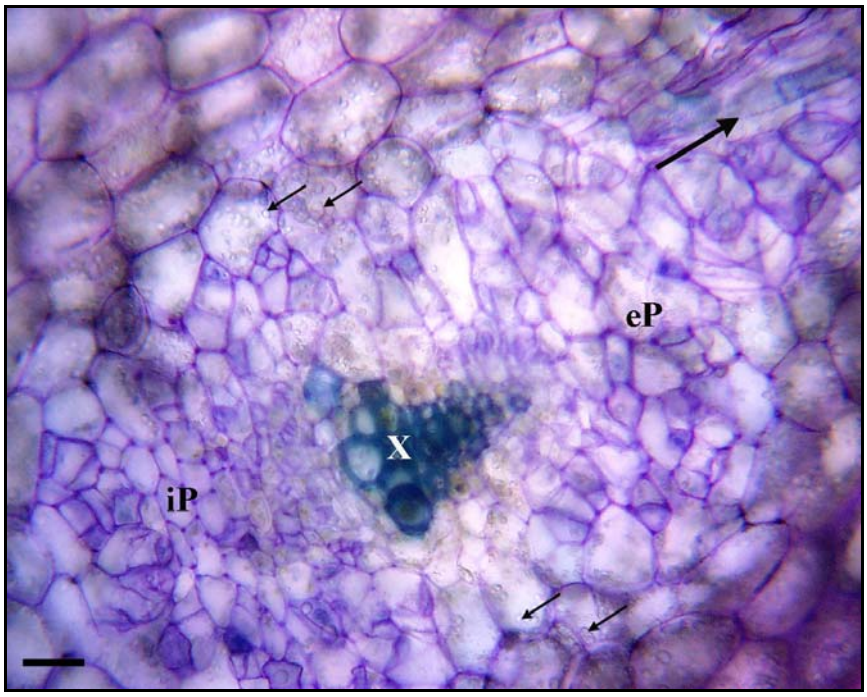

Figure 34: Cross section through a central vascular bundle of a !nara cotyledon. The internal phloem (iP) is large and distinct, the external phloem (eP) scattered and less distinct. Numerous small xylem elements are stained dark blue (X). A longitudinal orientated, commissural vascular bundle is visible in the upper right hand corner (large arrow). Starch grains are visible in the storage / parenchymatous tissue (small arrows). Bar: 40µm. Freehand section. Stain: toluidine blue.

Figure 35: Freehand section through a leaflet of the third internode. Vascular bundles (dark arrows) are surrounded by ground parenchyma, towards the tip and edges of the leaf the vascular bundles are in direct contact with the assimilating parenchyma (AP). Trichomes (arrowhead) can be found on the upper side of the leaf, facing the stem. Bar: 50µm. Freehand section. Stain: toluidine blue.

3.1.3 The Roots

Root sections reveal the tetrarch anatomy typical for cucurbit roots, featuring a rhizodermis and endodermis, 4 beams of xylem alternating with patches of phloem (Metcalfe & Chalk 1972, Esau 1960).

The xylem elements of the mature roots are amongst the largest known, Kutschera et al. (1997) describe xylem elements of nearly 1000µm diameter in major roots of a 60 year old *Acanthosicyos horridus* plant.

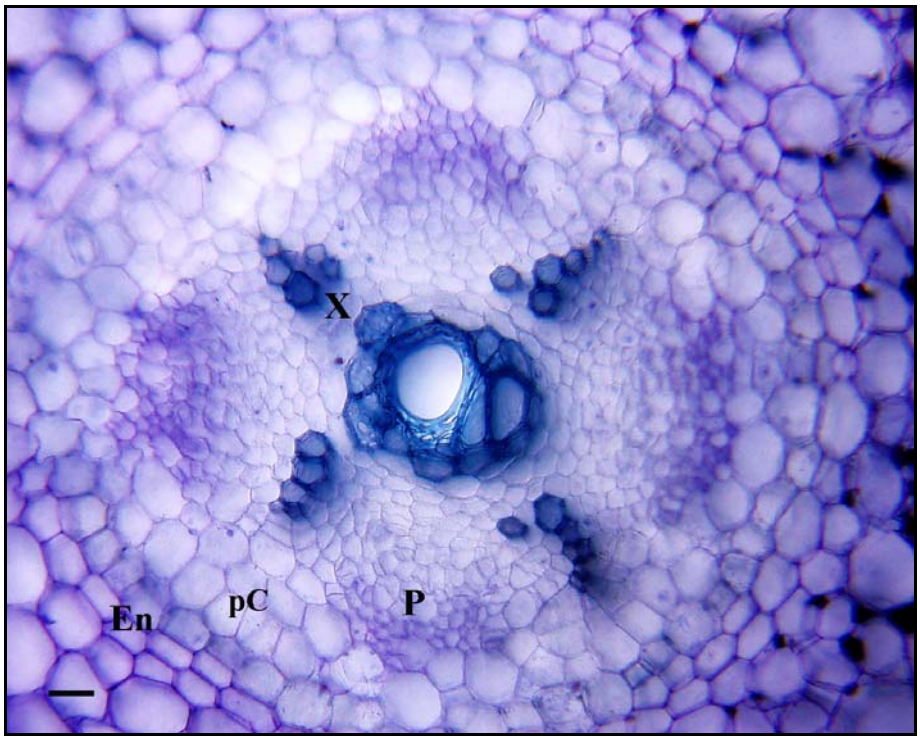

Figure 36: Cross section through the central cylinder of the root of a 6 week old *A. horridus* seedling. The roots shows the tetrarch anatomy, characteristic for most of the dicotyledonous families. The four-pole xylem (X) with four beams of xylem elements radiating from a centre (old stems of mature plants have a pith) towards the endodermis (En). The phloem (P) is situated in four patches between the xylem. pC: pericambium. Bar: 40µm. Freehand section. Stain: crystal violet

3.2 Ecophysiology

3.2.1 Gas Exchange

3.2.1.1 The diurnal photosynthetic course

During measurements in the field, it became clear that gas exchange was not uniform throughout all parts of one plant but varied on different shoots that showed different diurnal photosynthetic pattern.

Age, damage, height above ground, exposure to sunlight and wind (resp. temperature and light intensity) and shoot water potential did influence the maximal photosynthetic rate and the diurnal photosynthetic pattern within a frame set by overall stress level of the whole plant (water stress).

Maximum net assimilation (A) rate varied up to 300% or more on different shoots of the same plant. Unless the plant appeared to be heavily stressed, in which case the PS pattern was a simple one-maximum curve with a low maximum and a low slope (Figure 37, shoot 6), three general patterns of photosynthesis (PS) were apparent.

a) A steep slope, shortly after sunrise rising to a maximum at around 11h, dropping sharply until noon and than slowly decreasing until sunset (Figure 37, shoot 1).
b) A two-maximum-curve with a midday depression around 16h and the two maxima at around 11h and 17h (Figure 37, shoot 8)
c) A single maximum curve with the highest net PS at around 13-14h (Figure 37, shoot 2).
d) Constant low PS rate without distinct maximum (Figure 37, shoot 6)

8 shoots were measured on each plant, and each of the above patterns was recorded for at least one shoot on each plant. Naturally, a number of intermediate patterns were observed, e.g. curves with morning maxima and midday depressions.

Because of the high variability of maximum assimilation rate among shoots on one plant – resulting from the low overall photosynthesis, averaged photosynthesis curves show a relatively high error (compare Figure 38), which makes a reliable interpretation difficult (see discussion 4.3)

At the same time, these very low maximum PS rates (Figure 37,Figure 38) were the most intriguing observation made during this and all consecutive measurements.

Shoots on stressed plants did show an average net PS of 1,5 µmol/m^2 s during a 12h period, barely compensating dark respiration.

The highest net PS rate in the field ever measured was 8,4 µmol/m^2 s. This measurement was taken at around 11h on a plant after the groundwater reservoir was replenished by riverflow.

The measured transpiration rates of 1-2 mmol/m^2s (Figure 38) seem high when viewed in the context of low assimilation rates and result in relatively low WUE values (water use efficiency: µmol of CO_2 assimilated per mmol of H_2O transpired, compare Figure 39) between 1 and 2. However, the calculated daily transpiration rates range from 86 mol/m^2d on water stressed plants to 238 mol/m^2d on watered plants and lie well within the range of daily transpiration of desert plants compiled by Larcher 1994b.

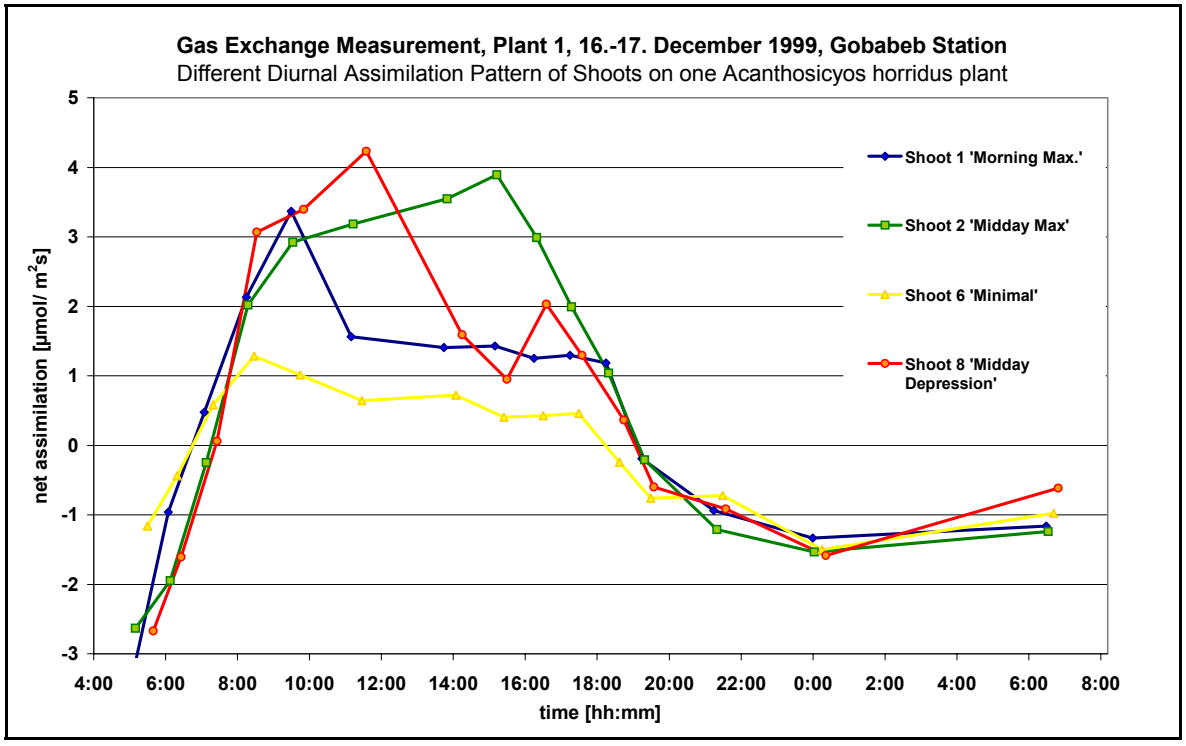

Figure 37: Diurnal courses of net assimilation of different shoots on the same *A. horridus* plant. Measurements were made on a plant near the Kuiseb riverbed close to Gobabeb station. Shoots of approx. the same length and age, but on different branches were selected. Maximum assimilation rate varies for up to 500% between different shoots (compare shoot 8 with shoot 6 at 12:00h), while the absolute difference is only 4µmol/m^2s, due to the low average net assimilation rate.

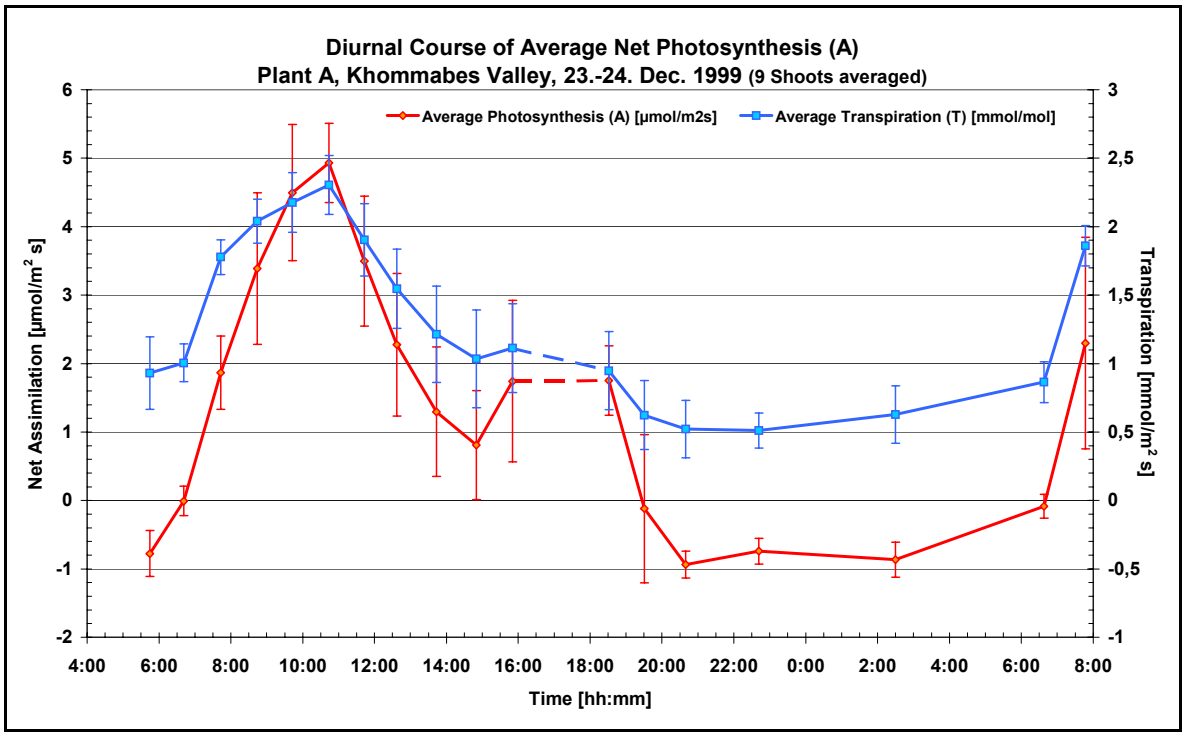

Figure 38: Diurnal course of absolute net assimilation and transpiration with standard deviation error bars. Measurements conducted on plant A in the Khommabes valley from December 23rd to 24th 1999. Note that transpiration at night is still ~25% of maximum daytime transpiration.

Apart from the overall very low net PS and high transpiration rates, the diurnal patterns of plants under different conditions followed the expected patterns of C3 xerophytes in hot, arid environments.

With temperatures and therefore vapour pressure deficit (VPD, difference in water vapour pressure between dry outside air and intercellular air) increasing until 15.00h (Figure 39), stomatal resistance r_b also increases to reduce transpiration and resulting in a midday depression of assimilation (Figure 38).

With temperature and VPD decreasing after 15.00h, stomatal resistance is reduced, resulting in a secondary maximum of assimilation around 17h.

At sundown r_b raises again with closing stomata, but transpiration during the night (1mmol/m^{2}s) is still about 25% of the daytime maximum.

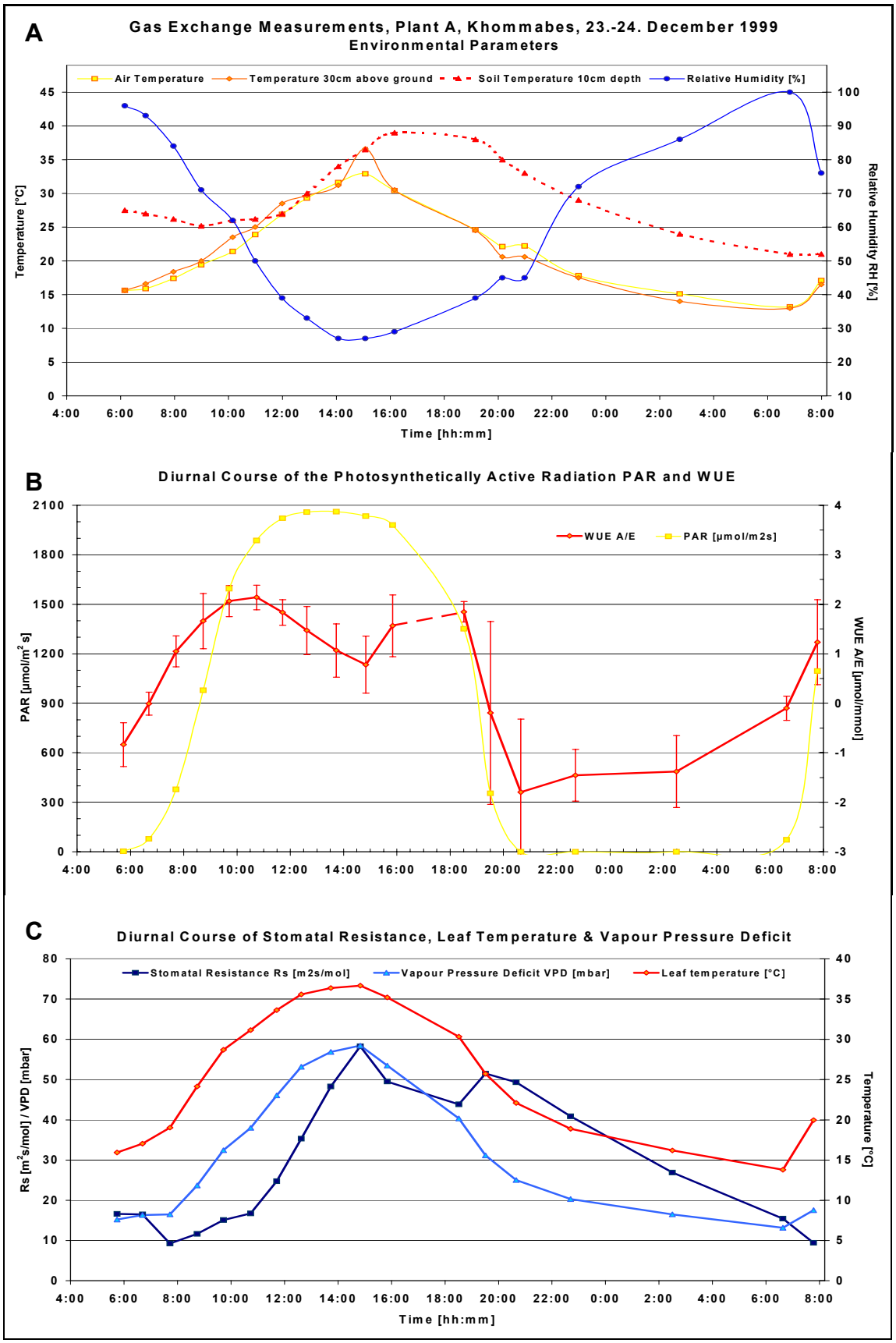

Figure 39: Diurnal course of environmental parameters (A; air temperature, temp. 30cm above ground, soil temp. in 10cm depth and relative humidity), PAR and WUE (B) and stomatal resistance, leaf temperature and VPD (C) of Plant A in the Khommabes Valley on December 23rd-24th 1999. (B,C: 9 data sets averaged)

Groundwater was replenished after a Kuiseb river flood that came off after rains in the highlands for about a week on December 18th 1999.

Net PS and transpiration of a plant near the riverbed after this flood both were substantially higher than recordings of plants before the flood (Figure 40).

With a higher groundwater availability, both curves also showed a more distinct pattern and WUE was higher after the river flow.

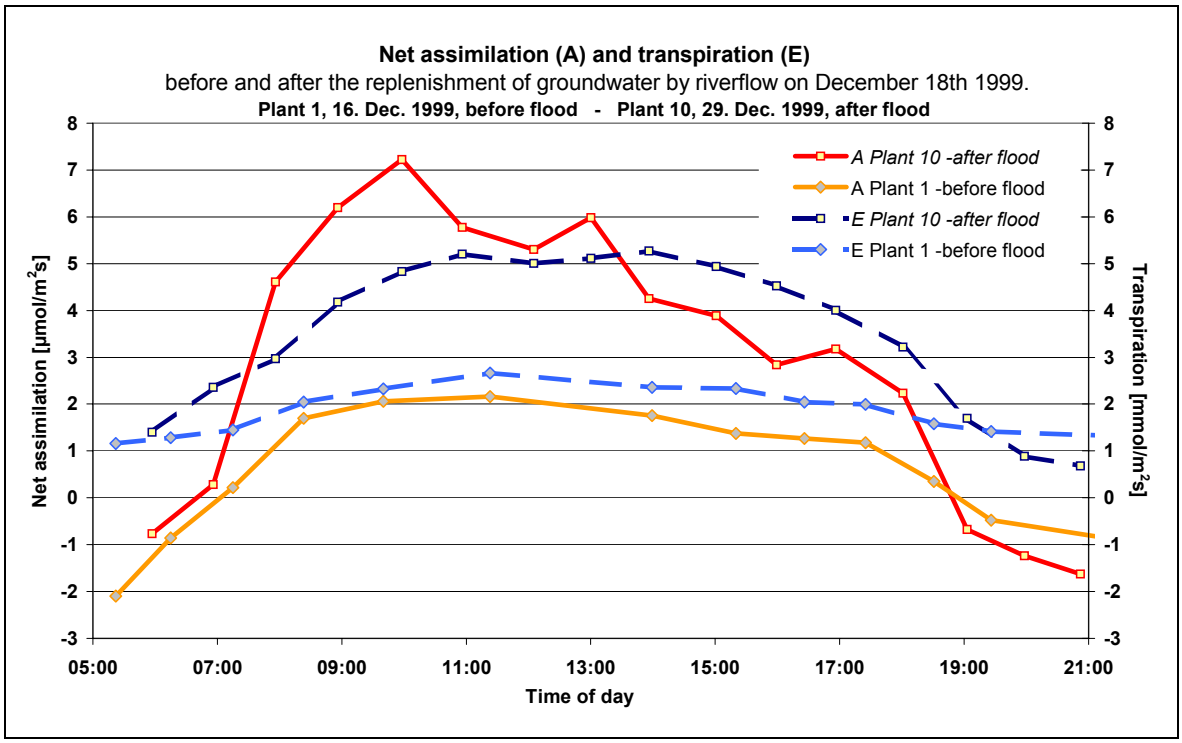

Figure 40: Diurnal course of net assimilation (A) and transpiration (B) of two plants near the riverbed before and after the replenishment of groundwater by a flood in the ephemeral Kuiseb river. Note the 3fold increase in max assimilation rate, accompanied by doubling of transpiration (curve averaged from 8 data sets).

3.2.1.2 Photosynthetic response to changing environmental parameters

3.2.1.2.1 Light-Response Curve:

Step by step increases of the incident photosynthetical active radiation PAR plotted against the corresponding net PS rate results in hyperbolic curves that saturate at around 700µmol/m^2 s PAR when light that passes the stem is reflected back to the stem from the bottom of the cuvette (e.g. when the lower half of the cuvette is covered with tin foil) (curves A in Figure 41).

If light is not reflected (exits the cuvette after passing the stem), the resulting PAR/A curve shows a linear slope and saturates at higher PAR of around 1000 – 1200 µmol/m^2 s or above (curves B in Figure 41).

This can be explained with the arrangement of the chlorenchyma. Due to self-shading of the stem, AP bows on the light-facing side of the stem saturate at 700µmol/m^2 s PAR. As PAR increases, light is transmitted through the stem to AP bows at the far side of the stem until net PS is saturated in all the AP bows.

PAR/A curves of cotyledons show the same behaviour.

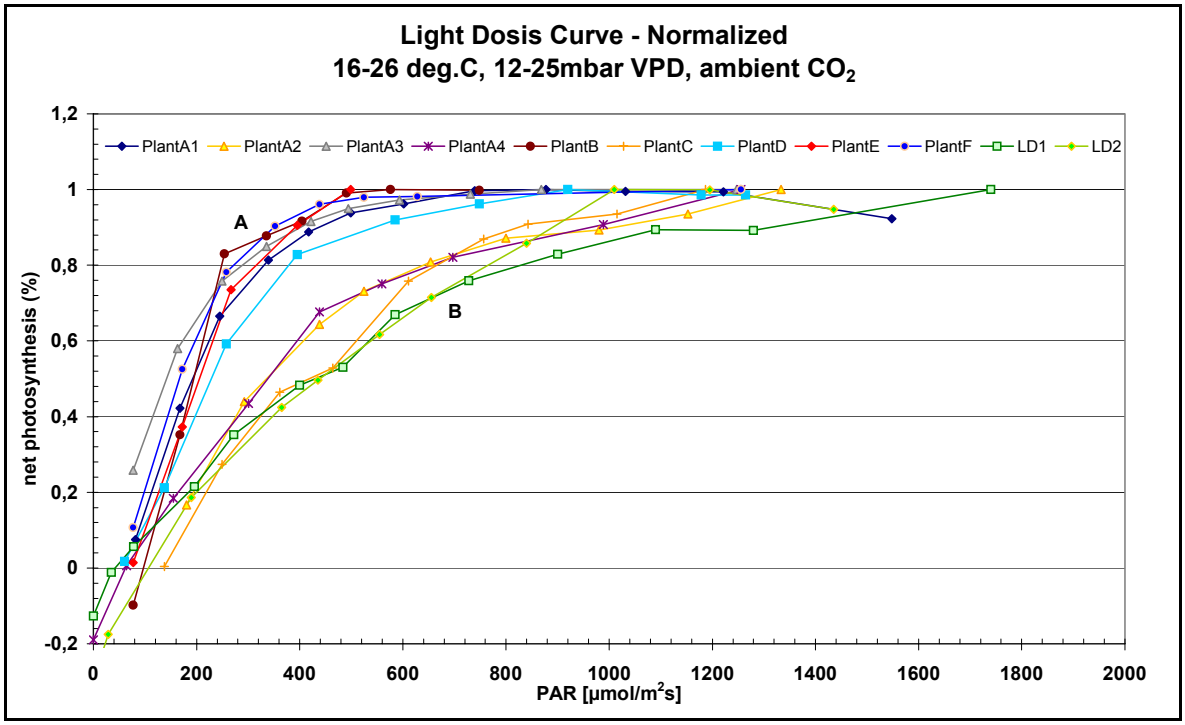

Figure 41: Normalized light response curve of 12 week old cultivated *A. horridus* plants. While most of the curves saturate at around 600 µmol/m^{2}s, some response curves show a near linear course and only saturate at PAR of 1200µmol/m^{2}s or above.

Dark respiration is compensated at around 70µmol/m^2 s – this should give the plant an average 13 hours of positive net PS. However, in the field dark respiration was compensated at around 70µmol/m^2 s in the morning but net PS became negative again from 6 pm or about 200µmol/m^2 s on.

3.2.1.2.2 CO_2 Response Curve:

The normalised CO_2 response curves revealed the CO_2 compensation point to be at around 45ppm, a value typical for C_3 plants. The value for the stomatal limitation derived from this chart is about 8%. It is the difference in percentage between the net assimilation at ambient= 360ppm internal (leaf) CO_2 concentration and the assimilation at 360ppm external (supplied air) CO_2 concentration (not plotted).
The value gives and estimation on to what extend the stomatal aperture influences (limits) the internal CO_2 concentration (and therefore the net PS): by a maximum of 8%.
However, at ambient air CO_2 concentration (360ppm) the CO_2 response curve is nearly saturated (Figure 42), which is rather a characteristic of C_4 plants (Taiz & Zeiger 1998).

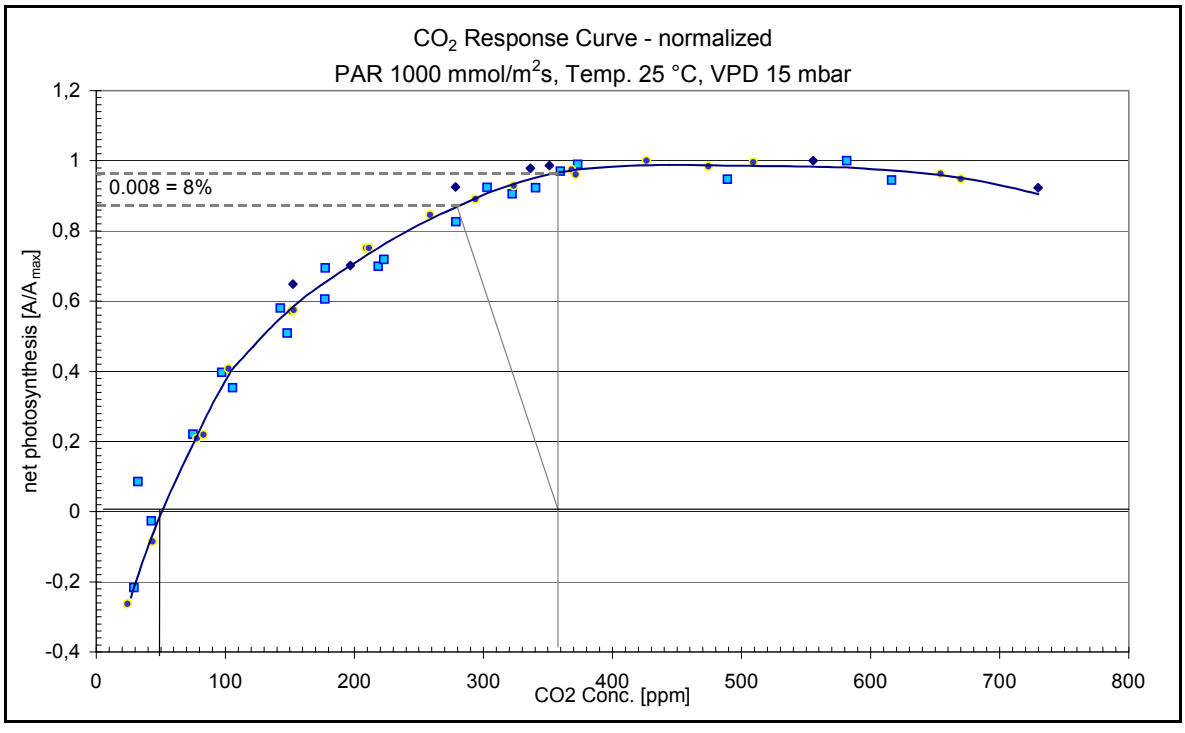

Figure 42: CO_2 response curve of greenhouse *A. horridus* plants. The curve saturates just above ambient CO_2 concentration. The difference of net assimilation at 360ppm internal CO_2 concentration (C_i, A intercepts curve) to net assimilation at 360ppm external CO_2 concentration (C_e, B intercepts curve) gives the stomatal limitation. The value derived from the chart is 8%. CO_2 compensation point is 45ppm. The saturation point is 440ppm.

3.2.1.2.3 VPD and temperature response curves:

The temperature optimum plants displayed mirrored the average temperature of the environment they were grown in (the growth chamber programme) ranging from 24 to 28°C and are consistent with the result of Seemann *et al.* (1984).

Measurements in the fields could not be taken with the LCA2.

Water vapour pressure deficit (VPD – the vapour pressure deficit between the ambient outside air and air in the substomatal cavities) measurements in the lab showed the optimal VPD to be around 10-15 mbar (net assimilation at constant temperature and CO_2 was maximal at VPDs around 10-15mbar).

Assimilation rates of *A. horridus* decreased at VPDs below 10mbar, while Dai *et al.*(1992) showed for *Ricinus communis* that net photosynthesis is maximal at 0 VPD and decreases with increasing VPD.

Maximum PS rates in the field were measured during midmorning when VPD values ranged between 35 and 40 mbar.

In diurnal curves with secondary maxima around 15h, VPD were 65 mbar and above. In some shoots, net CO_2 uptake was still measured at calculated VPD of 85 mbar.

VPD response curves were not very distinct and against expectations did not seem to have a great influence on net assimilation in the range between 5 and 35 mbar.

In the field, the course of assimilation seemed to be closer correlated to ambient air temperature and leaf temperature (compare results of Dai *et al.* 1992).

3.2.2 Water Potential

3.2.2.1 Diurnal Course of Plant Water Potential

Water potential values were difficult to obtain and varied a lot on different shoots. Water potential varied between –0,4 MPa to –2,5 MPa on single plants and during the daily course. These values are exceptionally high (positive) for a desert plant. This again points to a readily available source of water. 8-12 measurements per plant per time of day were necessary to plot a daily course. Plant water potential of water stressed plants at around 9 am were –1,2 MPa and sank to just below –1,6 MPa until 2pm. Plant water potential only slightly recovered to –1,5 MPa until 7 p.m. but rose to –0,9 MPa and above until midnight.

Values for plants after the river flow, and therefore with less water stress even lay 0,2 – 0,4 MPa above this (Figure 43).

Together with this, the bleeding of cut shoots, typical for cucurbits was observed, indicating a high phloem pressure and exuding sap in quantities of 50µl and more in the morning and before sunset.

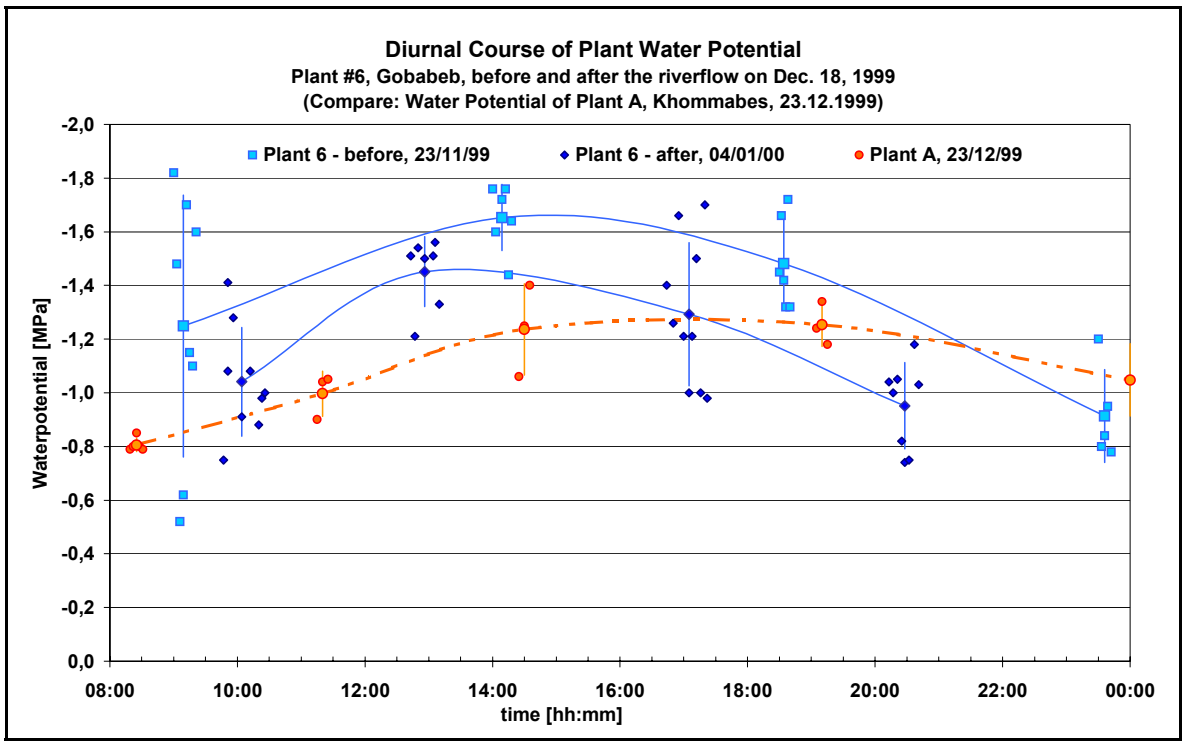

Figure 43: Diurnal course of plant water potential of plant 1, Gobabeb station, near the Kuiseb river bed, before and after the flow of the ephemeral river after heavy rainfall in the Namibian highlands on December 18th 1999. As a comparision, the plant water potential course of plant A in the Khommabes valley during the measurements on December 23rd 1999 are also plotted. The Khommabes valley aquifer is supposed to be continuous with the Kuiseb river groundwater.

3.2.2.2 *Pressure-Volume Curves*

Because of the problems described in 2.3.2 and because many shoots did not fully rehydrate, only one out of every 5-6 measurements was accurate enough for analysis. The presented pressure-volume curve was averaged from 6 data sets.
The average error (standard deviation over value) of the linear section is 12%, the average error of the exponential section is 20%. Due to the resulting relatively high absolute deviation of the exponential section, no bulk elasticity modulus was calculated (compare Boyer 1995)

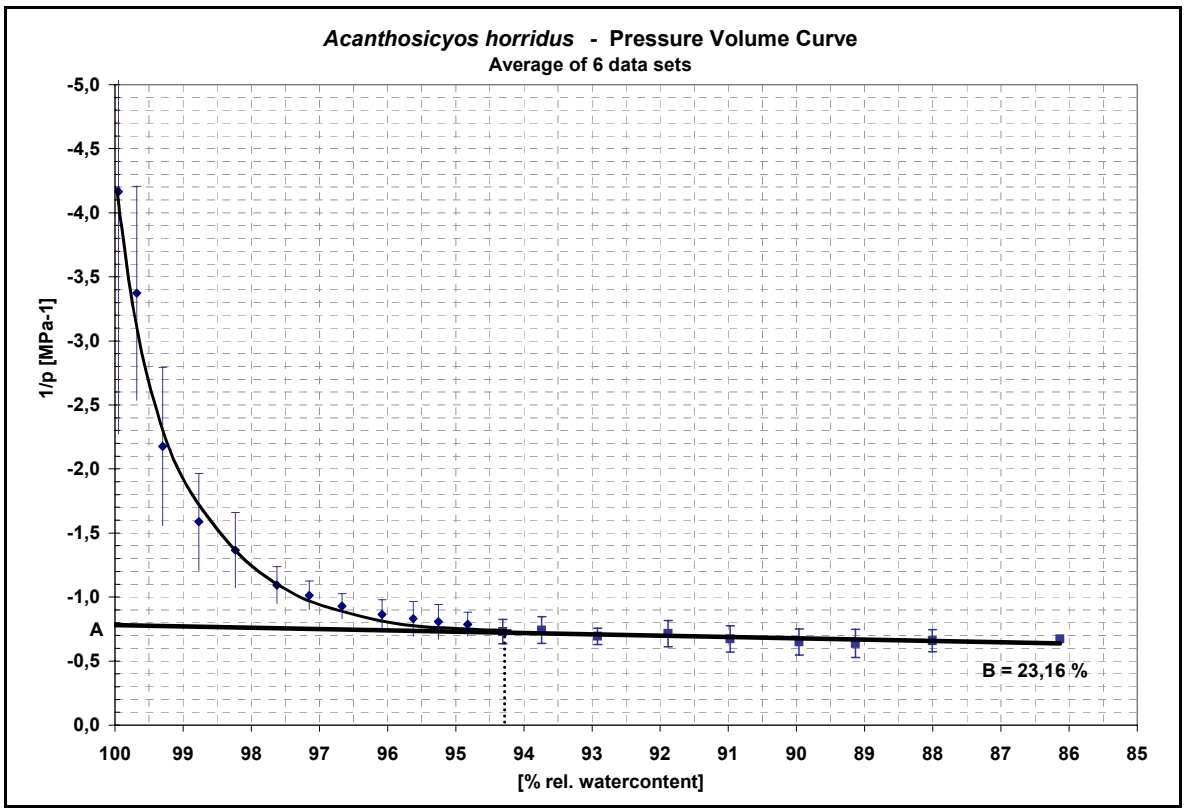

Figure 44: Pressure volume curve: Plant water pressure plotted against percent of relative plant water content (of fully hydrated shoot). For detailed evaluation see text.

Nevertheless, a number of parameters can be derived from the plotted curve.
When fully hydrated, the water potential ψ is highest (C= leaf water potential at full turgor, $1/\psi$ = -4,4 MPa^{-1}) at –0,23 MPa, but decreases rapidly with decreasing turgor when dehydrated. This is represented by the exponential slope of the curve. Turgor is fully lost when the slope of the curve becomes linear – then the water potential decreases with increasing osmotic potential (see Larcher 1994b, p. 181). For *A. horridus*, turgor is fully lost at about D=94,3% relative water content (RWC). The interception of the fitted line of the linear section with the y-axis predicts the

average osmotic potential π at full turgor to be A= –1,28 MPa. (–0,78 MPa^{-1}) (Figure 44)

The intercept of the fitted line with the x-axis B (slope of the linear section is y = -0,0102x + 0,2362, giving x=0,2316 for y=0) gives the ratio of apoplastic water content (23,16%).

The steep slope of the exponential section indicates a high elasticity module ε, characteristic for rigid cells (Larcher 1994b)

3.2.3 Growth Rates

Because of the difficulties of growing !nara plants in the green house, measured growth rates were very low.

Assuming that in it's natural habitat the !nara is dependent on ground water one would expect seedlings to grow very fast after good rains to develop sufficient biomass and reach the groundwater before rainwater is no longer available.

Growth rates in the growth chamber varied between 0,05 and 0,15 cm/h. Pumpkin (*Cucurbita maxima*) sprouts as a comparison can grow up to 0,3 cm/h ().

Growth measurements in the field showed that especially plants that were stressed by lack of water or grazing did not have any growing shoots while they bore fruit.

After the river flow, however, on single shoots or branches growth rates of 0,5cm/h and more were observed. Again, maximum growth rates of *C. maxima*, a typical representative of the fast growing Cucurbitaceae, are 0,3 cm/h.

The measurement of fruit growth did not yield any reliable data, because more than 80% of the tagged !nara melons were damaged or removed by herbivores (mostly goats and donkeys of the nearby settlement) within two or three days.

3.2.4 Water content

The average absolute water content of 24 samples is 71,83 +/- 2,02% (error: 2,8%). Young, less sclerenchymatised shoots and shoots with floral buds have a significant higher water content (Table 2). Within the limited number of samples, no daily pattern of water content was eminent.

Table 2: Determination of average dry-weight.

No.	Date / Time	Fresh Weight	Dry Weight	% H_2O	Comment
1	20.11.99/19.30h	1,0903	0,3069	71,85	
2	20.11.99/19.30h	1,1289	0,3018	73,27	
3	20.11.99/19.30h	0,9951	0,2562	74,25	
4	20.11.99/19.30h	1,2190	0,3101	74,56	
5	21.11.99/19.00h	1,1206	0,2788	75,12	
6	21.11.99/19.00h	1,0662	0,3058	71,32	
7	21.11.99/19.00h	1,2126	0,3643	69,96	
8	21.11.99/19.00h	1,7555	0,4962	71,73	
9	23.11.99/8.30h	0,9496	0,2620	72,41	
10	23.11.99/8.30h	0,7773	0,1324	82,97	young shoot
11	23.11.99/8.30h	0,6044	0,1706	71,77	
12	23.11.99/8.30h	0,7572	0,2322	69,33	
13	23.11.99/13.30h	0,8292	0,2311	72,13	
14	23.11.99/13.30h	1,0067	0,2963	70,57	
15	23.11.99/13.30h	0,6977	0,2121	69,60	
16	23.11.99/13.30h	1,1048	0,3123	71,73	
17	23.11.99/18.30h	1,4148	0,3192	77,44	w/ floral buds
18	23.11.99/18.30h	1,0235	0,2757	73,06	
19	23.11.99/18.30h	1,0417	0,2757	73,53	
20	23.11.99/18.30h	1,0922	0,3054	72,04	
21	23.11.99/23.30h	0,6827	0,1153	83,11	young shoot
22	23.11.99/23.30h	1,3286	0,3902	70,63	
23	23.11.99/23.30h	0,9179	0,2696	70,63	
24	23.11.99/23.30h	1,0662	0,3324	68,82	
					Std.Dev.
			Average:	**71,83**	+/- 2,02

3.2.5 Physiology - Transport Sugars and Starch

HPLC analysis of exudates and collected phloem sap droplets showed that raffinoseoligosaccharides (ROS) account for more than 80% of the detected transport sugars. In some samples of collected sap droplets, myo-inositol and galactinol was detected, as well as in some exudates. Also, fructose and glucose concentration was higher. However, because of the relative long time from sampling to analysis, some auto-protolysis and auto-inverting might have occurred. Also, because only relatively young shoots were feasible for droplet collection, the sap might contain catabolism products of ROS breakdown, such as myo-inositol, galactinol, etc. (Madore 1995)

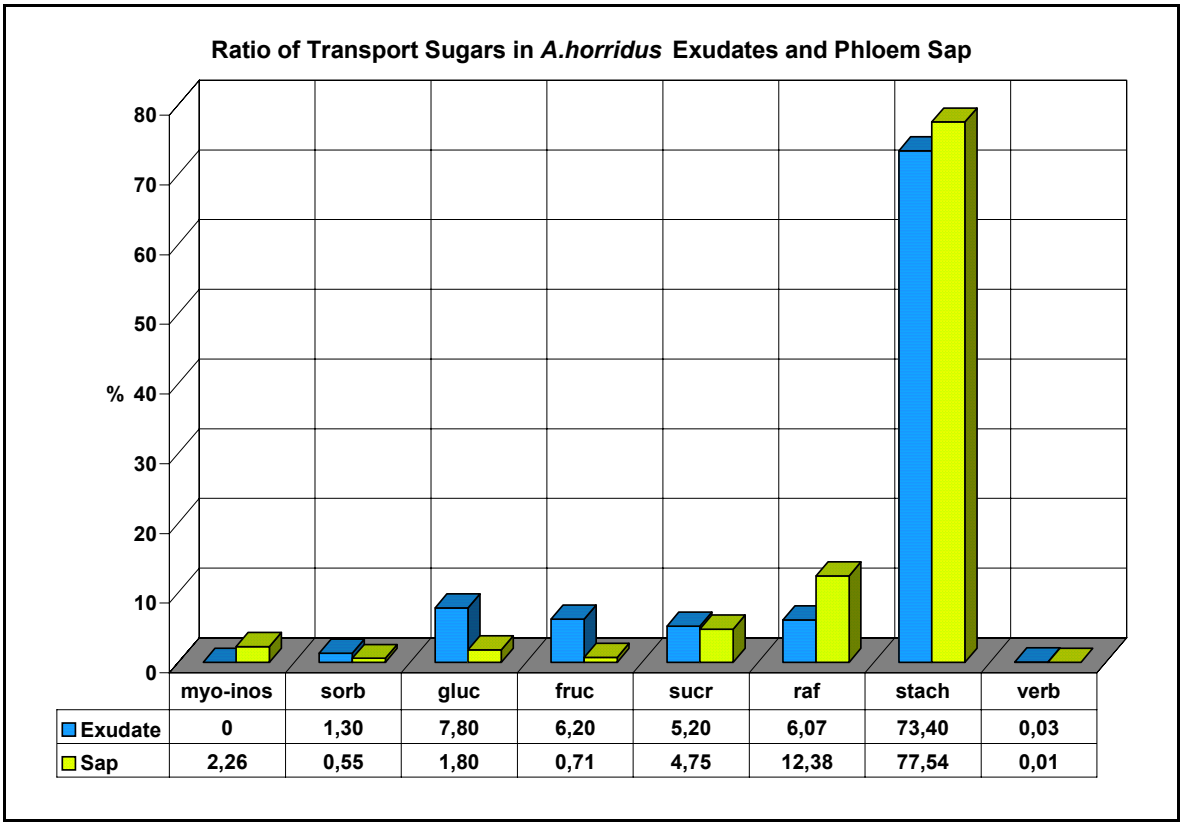

	myo-inos	sorb	gluc	fruc	sucr	raf	stach	verb
Exudate	0	1,30	7,80	6,20	5,20	6,07	73,40	0,03
Sap	2,26	0,55	1,80	0,71	4,75	12,38	77,54	0,01

Figure 45: Ratio of transport sugars in exudates and collected phloem sap droplets in percentage. Absolute sugar content varied between 16 and 45 µg/ml in exudates (µg sugar exudet in 1ml water in 1hour) and between 1,8 and 5mg/ml in droplets (absolute concentration in collected sap). myo-inos: myo-inositol, sorb: sorbit/sugaralcohols, gluc: glucose, fruc: fructose, sucr: sucrose, raf: raffinose, stach: stachyose, verb: verbascose.

The starch analysis of green-house plants revealed starch contents in stem sections of less than 0,05 mg per g fresh weight, a finding that corresponds with the fact that staining experiments for starch in sections were negative (KI/I_2) for all

parts of the stem from plants growing in the field as well as from green-house plants. Starch was however found in cotyledons and roots of seedlings from the green-house.

Kutschera *et al* (1997) found high starch concentrations and large starch grains in the roots of plants excavated near the Gobabeb research station.

Because excavation of the roots does severely damage the protected plants, no permission was granted for this project and samples could not been taken from plants in the field.

4 DISCUSSION

Plants that grow in areas of stable climatic and environmental conditions (speaking in evolutionary relevant terms), especially if they are slow growing or reach great ages (or organisms in steady environments with long generation spans in general), presumably are subject to a relatively small evolutionary pressure and therefore often are more archaic than members of the same family or genus that, for example, had to migrate during the iceages, and these “old” plants often have features that are closer to that of their common ancestors.

However, species growing under extreme conditions also develop special adaptations to their environment, again differentiating from their relatives.

A. horridus is a plant that is growing in an area were arid conditions have prevailed for at least 80 million years. Plants can grow for more than 100 years old and the generation span is estimated to be between 30-50 years.

Simultaneously, the !nara is growing in an extreme environment and has several xeromorphic adaptations.

Whichever is the dominating factor, *A. horridus* differs in a number of morphological and physiological factors from its cultivated relatives, of which the most obvious difference is the absence of leaves.

Also green, ergo photosynthesising stems are common in cucurbits, most of the photoassimilation normally is executed by the leaves.

Stem photosynthesis is common among desert species and can contribute 20% of the total CO_2 assimilation in species like *Sparteum junceum* (Nilsen & Bao 1990), were the stem photosynthesis alone maintains a positive total carbon balance when the leaves are lost during drought.

According to the “leak and load” model (Minchin & Thorpe 1987, van Bel 1993b), some assimilates in the transport phloem are always lost from the sieve tubes along the way and are pumped back by the companion cells.

Obviously, the companion cells in transport phloem must have some loading capacity. Whether the capacities of the transport phloem are sufficient for assimilate loading in species like *S. junceum* is not clear.

In permanently aphyllous species, were stem photosynthesis accounts for almost 100% of the gained carbon, like *A. horridus* (photosynthesis also takes place in the green petals and fruits), there must be an anatomical and/or physiological way to

unify the functions of loading and long-distance transport of assimilates in the vascular bundles of the stem.

4.1 Stem Anatomy and Functional Relationships to Assimilate Loading and Transportation

4.1.1 Vascular bundles and extrafascicular phloem

As described in section 3.1.1.5, the vascular bundles of the outer ring vary considerably from the vascular bundles towards the centre of the stem.

In these OVB, the external phloem (homologue to the abaxial phloem in leaves) is dominant - the internal phloem sometimes is missing completely.

Companion cells of the external phloem are mostly of the intermediary cell type (Figure 28-28), a feature found in the phloem of loading zones of symplastic loaders (Gamalei 1989, van Bel 1993a, van Bel & Gamalei 1992,), and the cc/se volume ratio is high (~3:1), meaning that companion cells are larger than their corresponding sieve elements - another characteristic of loading phloem (van Bel 1996a).

In the inner vascular bundles, in both external and internal phloem, companion cells are of the “ordinary” type and smaller than their corresponding sieve elements (se/cc ratio ~4:1), a reason to believe they are translocation channels.

The xylem is extend in the IVB and xylem elements are numerous, thick walled and much larger in diameter than in the OVB, which further supports this hypothesis.

This clearly indicates the external (abaxial) phloem of the outer vascular bundles to be the site of assimilate loading, additionally supported by it’s proximity to the assimilating parenchyma.

Considering this, the external phloem of the inner vascular bundles, located closest to the large centre of the bow of assimilating parenchyma, would be another possible site of phloem loading.

However, the large number of small parenchyma and sclerenchyma cells between the phloem and the chlorenchyma would be energetically uneconomic, assuming that at least the transport across the sclerenchyma sheath is symplastic (see 4.1.2)

HPLC analysis (see 3.2.5) showed raffinoseoligosaccharides (ROS), as in all cucurbits, to be the main transport sugars. Together with the anatomy of the OVB external phloem being similar to the type 1 (Gamalei 1989, see Figure 28) of leaf minor veins, it can be assumed that sieve element loading in the OVB of *A. horridus* is symplastic (for definition see van Bel 1993a).

The concentration of ROS against their concentration gradients in IC during phloem loading according to the polymer trapping theory (Haritatos & Turgeon 1995), requires narrowed plasmodesmata to function as a symplasmic size exclusion barrier: ROS are synthesised in the IC from sucrose and monosaccharide metabolites delivered from the bundle sheath (Turgeon 1995, Turgeon *et al.* 1993, Beebe & Turgeon 1992, Holthaus & Schmitz 1991). While the narrowed PDs of the IC permit transfer of smaller metabolites, the ROS are trapped because of their size.

This size exclusion barrier is usually at the intermediary cell/bundle sheath interface (Turgeon 1991).

In source tissue of *Cucurbita pepo* leaves, the abaxial phloem of minor veins features large intermediary cells with frequent plasmodesmatal contact to the surrounding bundle sheath cells (Turgeon *et al.* 1975) and smaller companion cells. However, even in higher order veins of *Cucurbita* petioles or stems, a bundle sheath cannot always be found, and is always absent around transport phloem in vascular bundles of the stem.

This means that for symplastic phloem loading in stems:

i) the ROS concentration/loading mechanism differs from the one described above,

ii) the size excluding function of the plasmodesmata is structurally limited to the IC side only and thus independent of the cells neighbouring the IC, or

iii). Other cells, possibly vascular or ground parenchyma cells, are executing bundle sheath

Taking into consideration that symplastic loading is supposed to be the evolutionary older form (Gamalei 1989), and assuming that *A. horridus* is a relative "archaic" representative of the Cucurbitaceae (see the beginning of this chapter), i) seems less likely, as well as ii) (compare Lucas *et al.* 1996, Beebe & Russin 1999, Botha & Cross 1999 and literature cited therein).

This brings attention to the clusters or rows of vascular parenchyma cells surrounding the external phloem between the se/cc complexes and the phloem fibres (3.1.1.5.1, “o” in Figure 23) in *A.horridus*.
Electron micrographs (Figure 28,Figure 29) show abundant plasmodesmata between these cells and the intermediary cells. PDs are always branched towards the intermediary cell side, a feature of bundle sheath/ IC interface (Flora & Madore 1996).
Also apart from their orientation and their plasmodesmatal frequency, these cells could not be differentiated from ordinary parenchyma cells, it is assumed that they form a discontinuous bundle sheath or parenchymatous sheath around the external phloem.
The distance assimilates would have to be transported from any sclerenchyma sheath cell in contact with the assimilating parenchyma to the nearest “parenchyma sheath” cell is almost always 5 or 6 cells.

The function of the internal phloem is unclear. While it is poorly developed in the OVBs and sometimes is missing completely, it is distinct in the IVB and also frequently connected by extrafascicular/ commissural phloem.
A possible explanation would be that the internal phloem exclusively functions as transport phloem and hence is only poorly developed in the OVB.
Botha & Evert (1978) showed that aphids preferably fed on abaxial (here: external) phloem of *Cucurbita maxima* leaves which led to the assumption that the adaxial (internal) phloem might be non-functional in mature cucurbit leaves.
It was shown that the adaxial phloem develops in cucurbit leaves before the onset of assimilate export (Turgeon & Webb 1976, Turgeon 1989) so a possible function of the internal phloem could be to supply source leaves with assimilates, a function that ceases with the maturation of the leaves.
However, autoradiographic experiments with developing *Cucumis* leaves (Schmitz *et al.* 1987) suggest the abaxial phloem to be the primary transport pathway.
And Bonnemain (1968, 1970) showed for tomato (*Solanum lycopersicum*) that the internal phloem was engaged in the nutrition of fruits while the external phloem supplied assimilates to vegetative sink organs.
For *A. horridus*, the role of the internal phloem remains obscure.

Extrafascicular phloem is abundant in *A.horridus*. Sieve elements are found running along the inside of the sclerenchyma sheath, close to the assimilating parenchyma, connecting to both external and internal phloem of the OVBs. EFP is also connecting external with internal phloem in both IVB and OVB. Additionally, EFP is functioning as commissural phloem in the internodes, interconnecting vascular bundles.
EFP strands are connecting OVBs with IVBs and different IVBs with each other approximately every 200µm (compare plate **a**, Figure 32).

In cross sections of cucurbit stems, vascular bundles are usually arranged in two concentric rings (Metcalfe & Chalk 1972). While this is true for young shoots of *A. horridus*, older stems often have three or more rings of vascular bundles. These stems are usually of larger diameter (up to 2 cm or more), woody and with little or no chlorenchyma. Their function is the transportation of water and assimilates to and from the roots or other, distant part of the plant.
In an environment of shifting sand, large parts of the plant body can be covered with sand and patches of above ground plant matter of the same plant can be scattered in an area of up to 300m^2. Often, parts of the plant emerge from the sand hummock a substantial distance away from the original site of germination, and thus the root system. Older parts of the stem that are covered with sand lose their chlorenchyma but still increase in diameter. When a plant is excavated by wind or human activity, it is difficult to tell whether one is looking at parts of the root system, the hypocotyl or parts of the main axis, especially because adventive roots can form along sand covered stems. While only the roots seem to store starch and draw groundwater (Kutschera *et al.* 1997), the extend transport system of the plant includes large parts of old, sand covered shoots that can have up to 5 rows of vascular bundles with more than 30 bundles altogether.
During secondary growth, OVBs apparently emerge from dividing existing bundles, while new assimilation parenchyma and a stomatal groove forms in the outer cortex above. However, its is still unclear how IVBs, which form these additional rings of vascular bundles, emerge.

4.1.2 The sclerenchyma sheath

A sclerenchymatous sheath in the outer cortex is characteristic for the Cucurbitaceae. In herbaceous members without secondary growth it is often continuous throughout the diameter of the stem. It is remarkable for a woody species with considerable secondary growth like *A.horridus* that the sclerenchyma sheath (SS) is continuous despite the growth pressure that tears apart the rows of sclerenchyma cells in other species.

This could explain the rows of larger cells found in almost every section crossing the sclerenchyma sheath (Figure 22) to be secondary sclerenchyma cells that develop closing the gaps torn by secondary growth.

Easily detectable even under a light microscope, there are abundant cell-cell connections between cells of the sclerenchyma sheath SS as well as towards the assimilation parenchyma and the ground parenchyma.

Assuming that most of the SS PDs are functional, the SS would not hinder symplasmic transport of assimilates from the AP to the ground parenchyma or the vascular bundles.

However, the SS could function as an apoplasmic barrier against water loss and help maintain the high phloem pressure/ osmotic pressure recorded in *A. horridus*.

From the sclerenchyma sheath, assimilates could either be unloaded into the apoplast and retrieved from cells of the above described parenchyma sheath cells or the assimilates could follow a completely symplasmic transport pathway to the phloem (van Bel 1996b, compare Richardson *et al* 1984; see Figure 46, after Botha & van Bel 1992).

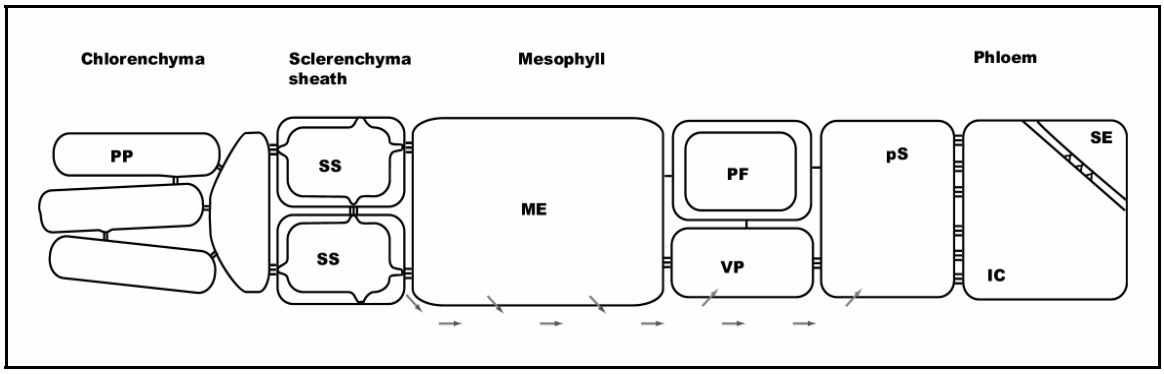

Figure 46: Symplasmic connections and possible transport pathways of assimilates from the chlorenchyma to the phloem of the OVB. Solid lines show plasmodesmatal connections. Plasmodesmatal frequencies are estimated from TEM sections. Assimilates can be transported symplastically via plasmodesmata from the chlorenchyma to the phloem. Arrows indicated a possible apoplasmic step in assimilate transportation from the sclerenchyma sheath (SS) to the parenchyma sheath (pS) surrounding the external phloem. PPUs connect intermediary cell (IC) with sieve elements (SE). PP: palisade parenchyma cells, PF : phloem fibre, VP : vascular parenchyma cell.

Unlike in other cucurbits (Kempers *et al.* 1993, Crafts 1932), no extrafascicular phloem can be found outside the sclerenchyma sheath. This is consistent with the concept of a possible role as a barrier: extrafascicular phloem outside the SS would have to connect to vascular bundles within, disturbing the continuity of the otherwise continuous sheath.

In addition, there is little ground parenchyma outside the SS, as it borders either the cells of the assimilation parenchyma, or the subepidermal layer, leaving little space for vascular tissue.

A high degree of sclerenchymatisation is often found in xerophytes, especially in Mediterranean species (Gibson 1983) to counter effects of wilting, but the !nara appears to have a high water potential throughout the drought season (see 3.2.2.1 and 4.3). Nevertheless, the undulating form of the sclerenchyma, in combination with the thick cuticle/epidermis similar to that of corrugated board, gives the shoots a high degree of stability and torsion resistance. This enables the plant to reach heights of 150cm and more, which is favourable not only because air temperature is lower at greater height over the hot sand, but because the higher a plant growths, the more shade it casts, minimizing temperature of the ground directly underneath the plant and of shoots within the bush, creating a cooler and more humid atmosphere.

4.2 Structure of the Photoassimilating Unit and Ecophysiological Implications

Looking at the anatomical characteristics of the !nara, the first remarkable detail is the size of its epidermis cells covered by a very thick cuticle. Unlike the flat, large cells of for example *Cucumis* species (Esau 1965), the epidermal cells of *A. horridus* are small and cylindrical and arranged like palisades.

Two possible explanations for this extraordinary appearance are that for one, only a small fraction of each cell's wall area is exposed to the dry outside air, thus reducing the risk of dehydration for each cell.

Second, a densely packed layer of cells covered by a thick cuticle could give the stem additional support and elasticity against torsional strain, thus forming a kind of exoskeleton, complemented by the sclerenchyma sheath inside the stem ("corrugated board" structure, see 4.1.2).

Apart from these structural functions, a thick cuticle obviously is designed to minimize cuticular conductance for water vapour (g_{cut}) and thus uncontrolled transpirational water-loss. Additionally, the UV-absorbing phenolics of the cuticle might protect the chlorenchyma against radiation and photoinhibatory damage (Gibson 1998, Björkmann & Demmig-Adams 1994).

Inside the stomatal grooves, the epidermal surface was found to be covered with wax protrusions of up to 5µm thickness (Figure 14, Figure 18).

Their function could be multiple. The most probable one is to reflect radiation and thus keep surface temperature low (Taiz & Zeiger 1998), maintaining a higher relative humidity around the stomata. Even though waxes are hydrophobic, their rough structure might render the surface more wettable and together with the trichomes might retain fog precipitation on the plant surface (personal observation, discussed later).

Also, the wax layers around the stomatal openings enhances the effect of sunken stomata and increases the diffusion pathway.

The wax structures also increase the boundary layer resistance of the stem, but Gibson (1983) estimated that even a thick layer of trichomes would not have a significant effect on the boundary layer of cylindrical stems (Nobel 1974) under desert conditions.

Ehleringer & Mooney (1978) came to the same result for xeromorphic leaves of *Encelia farinose*, but showed that trichomes reflect infra-red radiation much more than PAR. The same might be true for the trichomes found in *A. horridus*.
However, in *A. horridus*, trichomes and epicutan waxes are restricted to the stomatal grooves. While trichomes and glandular hairs are characteristic for the Cucurbitaceae (Metcalfe & Chalk 1972), in tropical species they generally function as a repellent against herbivores, fungi etc.
Their arrangement in *A. horridus* suggests their role to be mainly to influence gas exchange. Furrows or grooves in photosynthetic stems increase the boundary layer resistance and trichomes and waxes inside these grooves might have a greater effect on boundary layer resistance than Gibson (1983) calculated for round stems.
Another function could be the retention or absorbance of fog water, even though first tests of water uptake experiments as described by Grammatikopoulos & Manetas (1994) for *Phlomis fruticosa* did not yield clear results for *A. horridus*, personal observation)

A typical xeromorphic feature (Gibson 1998) found in *A. horridus* are the sunken stomata. The stomata of common cucurbits are often raised above the epidermal level, especially in the stem, In *A. horridus,* the stomata are not only arranged in grooves along the stem, but also are additionally sunken into the tissue matrix.
Together with the increased boundary layer resistance achieved by stomatal grooves, trichomes and wax protrusions, the sunken stomata would result in a higher humidity around the guard cells and along the stomatal grooves and thus in a smaller water vapour gradient between the air in the grooves and air in the substomatal cavities. This would reduce H_2O diffusion respectively transpirational water loss but not CO_2 diffusion and thus increase the water use efficiency (WUE).
Sunken stomata also increase the general diffusion pathway and decrease the stomatal conductance (g_{st}) (Gibson 1983) which again slightly favours CO_2 diffusion (Larcher 1994b).
However, Gibson (1998, 1983) showed that a large resistance of superstomatal chambers (R^{sstc}) could limit the maximum rate of net assimilation and would be most “efficient” in fully hydrated plants that keep their stomata open.

However, assuming the main strategy of desert plants to be the maximization of photosynthetic efficiency rather than simple minimization of transpiration, the explanation could be that this adaptation *de facto* increase transpiration and therefore photosynthesis, because the superstomatal chambers shelter the guard cells from the dry desert air and in this way enable the plant to keep stomata open despite large VPDs (Schulze *et al.* 1972, Gibson 1998, compare Cowan 1994).
This would enable desert plants to photosynthesise under less favourable conditions. The gas exchange rates of *A. horridus* support this theory.

An xeromorphic adaptation often found in leaves of desert plants, but rare in stem (Gibson 1983) is the anatomy of the assimilating parenchyma:
The palisade parenchyma consists of 4-6 rows of narrow and densely packed cells with minimal contact to each other, exposing most of the cell wall to an extend system of intercellular air space.
This creates a large mesophyll surface area A_{mes} and a high A_{mes}/A (A: total stem surface area) ratio. The diffusion of CO_2 from the intercellular air into the photosynthetic cells is facilitated (Nobel 1991) because CO_2 diffusion is more rapid in the gas than in the liquid (cell wall) phase.
This results in a higher WUE and maximizes photosynthesis. For the same reason, the stomatal density in the grooves is high (stomata account for 30-40% of the surface area in the stomatal grooves): CO_2 can diffuse faster from the outside air into the substomatal cavities, when conditions are favourable and stomata are open.
The densely packed palisade parenchyma cells also result in a high chloroplast per unit area ratio. Assuming that light is not a limiting factor in the desert environment of the !nara, this means the photosynthetic output of this tightly packed chlorenchyma would be equal to a larger, but thinner chlorenchyma area. At the same time, temperature control is easier, just as a thick, narrow leaf does not heat up as quickly as a thin, broad one, a factor assumed to be the evolutionary driving force behind the phenomenon of microphylly (Gibson 1998).
The bow form of the chlorenchyma and the resulting the fan-shaped arrangement of the palisade cells might hold additional benefits for *A. horridus*.

Incident light that penetrates the layers of palisade cells of one AP due to the "sieve effect" (Taiz & Zeiger 1998) can be radiated to neighbouring APs or APs on the far side of the stem through "light channelling" (Vogelmann 1993).
This lens effect of palisade parenchyma cells might be supported by the large, translucent cells of the inner stem parenchyma. The fact that net photosynthesis of !nara shoots saturated at PAR far above 700 µmol/m^2s when incident light was not reflected back to the stem during light-response experiments (3.2.1.2.1) support this theory.
The bow form of the chlorenchyma (or "furrowing" of the stem) also increases the photosynthetically active surface and thus increases maximum photosynthesis.
Some general advantages of (exclusively) having chlorenchyma in round stems for *A. horridus* might be "automatic sun-tracking", as some AP is always orientated perpendicular to the sunlight; maximizing PAR utilisation with minimum IR radiation (see "lens effect" above); possible recycling of respiratory CO_2; utilisation of indirect light that is reflected because of the high albedo of sand.

All of the adaptations (compare Table 3) designed to optimise light utilisation and/or to reduce heating through absorption or reflection improve the water use efficiency, because transpirational water loss is not only a function of stomatal aperture (and therefore internal CO_2 concentration), but also of leaf temperature, since a lower leaf temperature results in a smaller water vapour gradient (VPD) to the ambient air and consequently in a smaller driving force for transpirational water loss (Gibson 1998, Taiz & Zeiger 1998, Larcher 1994 and literature cited therein).

Table 3: Anatomical features of the stem and possible ecophysiological effects.

Feature	Effect
Thick cuticle	Reduction of cuticular transpiration
	Absorption of UV light and prevention of damage photosynthetic organs
Epicutan waxes and trichomes	Reduction of stem temperature through reflection and/or absorption of IR radiation
	(Higher boundary layer resistance)
Stomatal grooves, sunken stomata	Minimization of contact of guard cells with dry air to keep stomata open under unfavourable conditions;
	Increased diffusion pathway favours CO_2 against H_2O diffusion
	Higher boundary layer resistance.
High stomatal density in the grooves	Rapid CO_2 diffusion when stomata are open under favourable conditions
Small, narrow, densely packed palisade parenchyma cells with minimal contact	High A_{mes}/A ratio; High surface/volume ratio of cells, faster CO_2 diffusion through the gaseous phase
	High chloroplast density
Furrowing of stem	Increased photosynthetic area, maximizing net PS
Bow-form of chlorenchyma	Lens-effect: efficient usage of UV light through radiation to other APs in the stem
Chlorenchyma in round stem	Recycling of respiratory CO_2
	Harvesting of reflected light (high albedo of sand)
	Maximized light harvest in morning and evening (“automatic sun-tracking”)

4.3 Gas Exchange and Water Potential

Gas exchange measurements on *A. horridus* plants in the field confirmed the !nara to be a C_3 plant: Net assimilation at night is negative, excluding CAM mechanism and the CO_2 compensation (Figure 42) point of 45ppm is characteristic for C_3 plants (Taiz & Zeiger 1998)

The observed diurnal patterns of gas exchange are well described in the literature (Nilsen *et al.* 1993, Nilsen & Bao 1990, Larcher 1994b, Hennesey *et al* 1993 and literature cited therein).

The four patterns shown in Figure 37 basically represent diurnal courses of photosynthesis under increasing levels of stress (water, temperature), as described for example by Larcher (1994b) (Abb.2.50 and Abb.2.51, p.104/5):

- *A single maximum curve with the highest net PS at around 14h (Figure 37, shoot 2):*
  Maximum PS rate at highest temperature (Q_{10}), PS rate decreases with temperature and PAR. (Diurnal PS pattern: optimal temperature: shoot with mild to no water stress)
- *two-maximum-curve with two maxima in the morning and the afternoon and "midday depression" of the PS rate around 15h (Figure 37, shoot 8):*
  Morning maximum under favourable conditions, midday depression due to closing of stomata to reduce transpiration or due to direct temperature stress when stomata are kept open to cool the plant. Second maximum when temperature/water stress decreases. (Diurnal PS pattern: super-optimal temperature and moderate humidity: shoot with mild water stress)
- *One-maximum curve with max PS rate in the morning (Figure 37, shoot 1):*
  Favourable conditions with moderate temperatures and VPD and maximum PAR in the morning. With increasing temperature equalling transpiration the PS rate decreases due to water and temperature stress. No recovery with decreasing temperatures in the afternoon. (Diurnal PS pattern: super-optimal temperature with low humidity, shoot with moderate to high water stress)
- *Constant low PS rate without any distinct maxima (Figure 37, shoot 6):*
  Net PS rate is minimal during the complete diurnal course because of low plant water status and heavy water stress.

The fact that the patterns described above (Figure 37) were recorded on different shoots of the same plant on the same day indicates that the water status can vary considerably on different shoots of the same plant and is dependent on factors like distance from the main tap root, exposure to sun and wind, height over the hot sand, damage from herbivores etc.

The most striking detail of the plotted assimilation curves (Figure 37, Figure 38) is the low overall rate of photosynthesis (PS) between 2 and 5 µmol/m^2s.
These measurements were taken during drought, but even in diurnal courses measured after a riverflow replenished the groundwater at the plant site, maximum net assimilation did not exceed 9 µmol/m^2s (Figure 40).
However, the replenishment of the groundwater and as a consequence the improvement of the plant water status (Figure 43) resulted in a significant increase of net assimilation of 50% and more (average PS: 8.2 µmol/m^2s, absolute max PS 11.3 µmol/m^2s).
Table 4 presents the average assimilation rates recorded in the field and during laboratory experiments.

Table 4: Assimilation rates of *A. horridus* recorded in the field and in the laboratory. Values recorded during drought in brackets

		Field data after rain (during drought)	**Laboratory data** (abs. max)
Average assimilation rate	[µmol/m^2s]	3-8 (1-5)	
Maximum assimilation rate	[µmol/m^2s]	11,3	8,5 (16,2)[#]

[#]recorded under elevated CO_2 concentration of 460ppm

Assimilation rates of 2-4µmol/m^2s are among the lowest recorded for desert xerophytes (Table 5). A_{max} of stems of nonsucculent aphyllous shrubs and trees from the southern desert regions of the United States range between 8 (*Senna armata*) and 24 µmol/m^2s (*Porophyllum gracile*) (Ehleringer *et al.* 1987 and Nilsen *et al.* 1996, respectively in Gibson 1998).
In contrast, many desert plants are highly effective in carbon assimilation with high A_{max} rates exceeding 30 µmol/m^2s in the field (A_{max} of *Camisonia claviformis* (C_3) was 59 µmol/m^2s under optimal field conditions - Mooney *et al* 1976 in Gibson 1998).

Table 5: Average values of photosynthesis, transpiration, water use efficiency and water potential of *A. horridus*, xeromorphic desert shrubs, CAM plants and mesophytes / crop plants of the temperate zone. Data taken and/ or calculated from Larcher (1994b), Taiz & Zeiger (1998), Flach & Eller (1993), DeLuca *et al.* (1977). Maximum values in brackets.

	A. horridus	Xermorphic desert shrubs	CAM plants	Mesophytes
Net Assimilation [µmol/m^{2}s]	2-8 (11)	(3) 10-15 (30)	5-12 (20)	20-40 (60)
Transpiration [mmol/m^{2}s]	1,5-5 (6)	0,5-4 (8)	0,2	2-5
Daily Transpiration - dry season [mol/m^{2}d]	86-140	65-160	0,35	150-380
Daily Transpiration - rain season [mol/m^{2}d]	232	160-280	17	
WUE [mmol/mol]	0,5 –2,2 (4,2)	4-8 (14)	20 (30)	1-5
Water potential [-MPa]	0,2 – 1,8 (2,2)	5-8 (16)	0,8-2	1-3

However, assimilation rates in *A. horridus* are low during drought despite high water potential (plant water potential is high even for mesophytes and even lies slightly above values of CAM plants - Table 5, Larcher 1994b)

Controversially, the recorded transpiration rates are high compared to other desert plants: Before the flood, transpiration rates ranged between 1,5 and 2,5 mmol/m^{2}s during the day (0,5-1 mmol/m^{2}s at night). After the river flow transpiration doubled to 3-5 mmol/m^{2}s with increasing rates of assimilation.

These values lie well within the range of mesophytic crop plants of the temperate zone (Table 5).

The low rates of assimilation and the high transpirational water-loss result in extremely low values for water use efficiency (µmol of CO_2 fixed per mmol of H_2O transpired). Calculated values for WUE varied between 0,5 and 1,5 for all plants with a maximum WUE measured in the field of 2.2 µmol/mmol. During laboratory experiments the highest WUE recorded was 4.2 µmol CO_2 fixed per mmol H_2O transpired.

These values are low even for mesophytes of the temperate zones (Table 5), which usually have abundant water available and show much higher rates of photosynthesis.

One reason for the low WUE might be the fact that the !nara is a C_3 plant, but Ehleringer & Monson (1993) stated that C_4 plants have no significant advantage over C_3 plants in cold deserts.

However, there are other desert plants, notably woody species, that exhibit low rates of (leaf) photosynthesis. The creosote bush *Larrea tridentate*, a dominant evergreen shrub of the North American deserts, has photosynthetic values of 3-4 µmol/m^{2}s during drought, while A_{max} at optimal field conditions is 14-16 µmol/m^{2}s. Still, the maximum rate of assimilation under favourable conditions is higher and low photosynthesis during drought goes along with low transpiration rates (Rundel & Sharifi 1993 in Gibson 1998).

The ecophysiological strategy of *Larrea tridentate* might be the same as in *A. horridus*. An opportunistic strategy, e.g. minimizing assimilation and transpiration during drought and maximizing carbon gain for the cost of higher transpiration under favourable conditions, is common for plants of dry habitats with periodic (regular, e.g. annual) precipitation (Gibson 1998, Larcher 1994b).

Also this is not true for the Namib desert, where rainfall is unpredictable for distinct areas and might only occur every 5 or so years, (Hutchinson 1995) during the wet season of the highlands, water is transported to the desert by ephemeral rivers like the Kuiseb (see 1.2), where plants growing near the river can profit from the resulting replenishment of the groundwater.

In contrast, while many opportunistic desert plants lose a sometimes substantial part of their biomass to reduce transpirational surface during drought, for example by shedding their leaves (Gibson 1983), *A. horridus* might trade in the high transpirational water loss during drought for a steady carbon gain throughout the year that enables the plant to maintain all of its large biomass, which in turn allows a massive boost of carbon uptake with doubled to tripled net assimilation as soon as water is plentiful. This could explain how growth rates of up to 0.8 cm/h can be supported in single shoots.

Maintaining an extended stem and root system also creates large storage capabilities for starch, water and nutrients.

It appears as if *A. horridus* has traded in effective photosynthesis under favourable conditions for a steady carbon gain throughout the year and during drought.

The access to groundwater might enable *A. horridus* to follow this strategy.

While together with maintaining such a high water potential (Table 5,Table 6,3.2.2.1) this appears to be a “water-wasting strategy”, the high hydration status and the consequently open stomata also increase WUE (see discussion of “resistance of superstomatal chambers” on page 76)

Also, the measured photosynthetic rates of *A. horridus* in the field might be lower than the actual values due to some reasons:

Experiments were conducted during the flowering and fruiting season. Additionally, it was not possible to select shoots for gas exchange measurements that did not have any axillary meristems, of which some might have been active (a problem already encountered by Louw *et al.*). For these reasons, respiration might have been high, lowering net assimilation. If respiratory CO_2 from internal stem tissue was recycled in *A. horridus*, measurements would also be lower than the actual PS rate.

Also, due to the functional principle of the ADC LCA-2 IRGA, where dry air is passed through the leaf chamber, by the time readings are stable, stomata might have begun to close and measured assimilation is below the initial rate (a problem solved in the LCA-4 version of the gas analyser).

Also, because the VPD is higher when air of zero humidity is passed through the chamber, transpiration might increase.

During laboratory experiments, the !nara plants were often stressed because of the difficulties that arose growing them in pots and because of their high susceptibility to pests and diseases.

When viewed in the context of possible slightly higher assimilation rates and/or lower transpiration rates, resp. higher WUE, the gas exchange values of *A. horridus* are close to that of xeromorphic Mediterranean species like *Sparteum junceum*, as measured by Nilsen & Bao (1990) (Table 6).

Table 6: Comparison of net assimilation rates, transpiration, water use efficiency, conductance (G_s) and water potential of *A. horridus* and the Mediterranean *Sparteum junceum* (Spanish broom), a large, common shrub with small ephemeral leaves. Data from Nilsen & Bao 1990.

		A. horridus	*S. junceum*			
			well-watered		water stressed	
		Field (Lab)	Leaves	Stem	Leaves	Stem
A	[µmol/m^{2}s]	2-11	16	5	8	4
E	[mmol/m^{2}s]	2-5	3-7	2-6	0,8-2	1,5-2,5
WUE	[µmol/mmol]	0,5-2,2	2-4	1-2	5-8	1-2
G_s	[mol/m^{2}s]	0,04-0,1 (0,15)	0,15-0,35	0,05-0,15	0,15-0,36	0,05-0,16
Water potential	[-MPa]	0,2 - 1,8	0,5-1,5	0,3-0,9	0,5-1,6	0,3-0,10

Another factor that influences the values of photosynthesis and transpiration is the photosynthetically active area the rates (µmol and mmol per m^2 and second, resp.) relate to. In gas exchange measurements on leaves, this would be the simple (or double) leaf surface area. In furrowed or spiny stems this is either the projected area (of photosynthetically active surface) or total surface area (Ehleringer *et al.* 1987 and Nobel *et al.* 1996, resp. in Gibson 1998)

Due to the special anatomy of *A. horridus*, the surface area was calculated as described in 2.3.1.1 under the assumption that underneath 50% of the surface area light will directly be transmitted to chlorenchyma. Both the fact that under much of the stem surface no chlorenchyma is present and the fact that the furrowing of the stem increases the photosynthetically active surface (PAS) were taken into account. The recorded values were not related to the total stem surface because assimilation and transpiration rates would have been too small and would have made comparison with data from other authors difficult.

Obviously, a re-evaluation of PAS would influence both assimilation and transpiration rates – relating the data to the total surface area for example would halve the rate, assuming PAS was 30% of total stem area would increase values by 1.5.

Assimilation and transpiration rates need to be reconfirmed, possibly ascertained by other means of determination like fluorescence measurement or carbon isotope discrimination (see 5)

However, the calculated WUE (A/E) is independent of the estimation of the PAS as both assimilation rate and transpiration increase or decrease proportional with the surface area.

The low WUE value indicate the availability of a water source, most possibly ground water, to the plant.

Two other possibilities are

a) water storage in the extent root system, but it is doubtful whether the average yearly amount of rain of 100mm is sufficient to replenish these storage system

b) the utilisation of fog water. Although until now no usage or uptake of fog water was shown, the possibility should not be ruled out (see comment on water uptake experiments on page 76).

The CO_2 response curve (see 3.2.1.2.2) does not fully correspond with the above hypothesised functional relationships (4.2).
A CO_2 compensation point of 45ppm was expected for a C_3 plant (Taiz & Zeiger 1998).
The saturation point of 440ppm is close to ambient CO_2 concentration and together with the low stomatal limitation of 8% indicates that the low photosynthesis is not so much a result of limited CO_2 diffusion but is rather limited by physiological factors, such as ribulosebiphosphate RuBP regeneration (9,6µmol/m^2s) or carboxylation efficiency (51,1 mmol/m^2s) or RuBISCO levels (nitrogen might be a limiting factor for *A. horridus* in the nutrient deficient soils of its habitat, compare Abrams *et al.* 1997).
A low stomatal limitation is unexpected, considering the anatomy of the stomata (in grooves, sunken within the tissue matrix, surrounded by trichomes and wax).
CO_2 measurements in the laboratory might not representative due to possible stress of the plants as a result of the problematic cultivation.
The calculated values of stomatal limitation, RuBP regeneration (Table 7) etc. should therefore be treated as rough approximations. More experiments are necessary to verify these results, which is why they will not be discussed in great detail here.
Especially values like stomatal limitation are difficult to derive in the usual way designed for leaves and their physical and physiological properties, because the anatomy of *A. horridus* stems differs substantially from that of leaves.
If the photosynthesis was indeed limited by physiological factors, a multiplication of net assimilation rate after watering would be hard to explain, especially since water potential measurements show that shoots are sometimes nearly fully turgescent during drought:

The plant water potential derived from the pV curves was determined to be –0,23 MPa at full turgor (see 3.2.2.2).
Low values for plant water potential in the field varied between –0,25 and –0,4 MPa. This would mean that *A. horridus* plants would maintain some fully turgid stems and thorns in a hyperarid desert during the dry season!

If this is indeed so, then together with the observed increase of assimilation and transpiration after the replenishment of groundwater (Figure 40), the data confirms that *A. horridus* must have access to groundwater.

At the same time, a high percentage of the total free water (23%) is in the apoplast (Figure 44), supporting the hypothesis of an existing apoplasmic barrier to reduce water loss through the chlorenchyma.

Lowest measured plant water potential in the field was -1,8MPa (-0,56 MPa^{-1}) corresponding with a relative water content of 77,6% of maximum hydration, which is not critical even for most mesophytes:

According to Larcher (1994b) the average minimum relative water content mesophytes can endure for 12-48h without taking damage ranges between 90 and 50%, in extremes even 10%. For xerophytes the value ranges between 5 and 0%.

While anatomically *A. horridus* is a xerophyte, it's physiological characteristics are that of a mesophytes. The !nara melon appears to be a water waster, which found its niche in a xeric ecosystem and successfully faces the harsh conditions of the desert.

Table 7: Physiological parameters recorded / calculated for *A. horridus* from field and laboratory data

Parameter	UNIT	Field	abs. max	Lab	max.
Maximum photosynthetic rate (averaged)	[µmol/m^2s]	8,2	11.3	8,5	16,2*
Average transpiration rate	[µmol/m^2s]	2 - 5		5 - 8	
WUE	[µmol/mmol]	0.5 - 1.5	2,2	3,5	4,4
Light compensation point	[µmol/m^2s]	80	morning	65	
		210	evening		
CO_2 compensation point	[µmol/m^2s]			45	
RuBP regeneration limitation	[µmol/m^2s]			9,6	
Carboxylation efficiency	[mmol/m^2s]			51,1	
Stomatal limitation	[%]			8	
Quantum efficiency	[%]			2	
Optimum temperature	[°C]			24-28	
Optimum VPD	[%]	35		<20	
Grow rate	[cm/h]	0,25	0,8	0.06 - 0.14	0,25
Average water content	[%]	71,8	83,1		

* recorded under elevated CO_2 concentration of 460ppm.

5 PROSPECTS

Despite the difficulties encountered raising plants in the green-house and the problems encountered during planting experiments in the natural habitat (personal observation), the extremely high growth rates that can be observed under optimal field conditions suggest that agricultural use might be possible.

It should be taken into consideration that the natural generation span for *A. horridus* plants is +/-50 years. This means that cultivated !naras would have to be well watered during the first one or two years and afterwards depend on groundwater access. Watering as well as intense groundwater usage will pose problems in the Kuiseb environment.

Additionally it was experienced that young plants in the fields are extremely susceptible to herbivores and drought. Furthermore, !nara plants in the green-house were prone to pest like scales and to fungi infections. Because of the associated VA micorrhyza, fungal infections are difficult to treat.

Scientifically it would be interesting to further investigate the phloem loading in *A. horridus* regarding the localisation of the polymer trapping interface, resp. whether the parenchyma sheath found around the external phloem of OVBs is an incomplete (homologue or analogue) or rudimentary bundle sheath.

It is also necessary to reconfirm and standardise assimilation and transpiration rates, either by relating them to dry weight or chlorophyll content (fluorescence measurements, see Seeman *et al.* 1984, Bolhàr-Nordenkampf & Öquist 1993) or by determination through carbon isotope discrimination (Farquhar *et al.* 1989).

The whole carbon economy of *A. horridus* promises to be an interesting study object, as it is unclear whether the !nara could be storing ROS (Bachmann *et al.* 1995), whether assimilates are predominantely exported to roots or submerged parts of the shoot for storage, whether the site of unloading in sink tissue is the phloem of the OVB or IVB, etc.

I hope this thesis helped to contribute to the understanding of the complex physiology and ecology of the !nara melon *Acanthosicyos horridus* and to encourage further research.

References

Abrams, M.M., Jacobson, P.J., Jacobson, K.M., Seely, M.K. 1997: Survey of soil chemical properties across a landscape in the Namib Desert. *J. Arid Env*. 35: 29-38

Ammerlaan, A., Kempers, R., van Bel, A.J.E. 1996: Symplasmic isolation of sieve element-companion cell complex in stem is universal. *J. Exp. Bot*. 47: 1300

Arnold, T. H., De Wet, B. C. 1993: Plants of southern Africa: names and distribution. *Mem. Bot. Surv. S.Africa* No. 62

Arnold, T.H., Wells, M.J., Wehmeyer, A.S. 1985: Khoisan food plants: taxa with potential for future economic exploitation. Wickens, G.E., Goodin, J.R. and Field, D.V., (eds.) *Plants for Arid Lands*. Unwin Hyman, London, 69-86

Bachmann, M., Inan, C., and Keller, F. 1995: Raffinose oligosaccharide storage. In: Madore, M.A., Lucas, W.J. (eds.): *Carbon Partitioning and Source-Sink Interactions in Plants*, Am. Soc. Plant Physiol.: 215-225

Balachandran, S., Xiang, Y., Schobert, C. 1998: Phloem sap proteins from *Cucurbita maxima* and *Ricinus communis* have the capacity to traffic cell to cell through plasmodesmata. *Proc. Nat. Acad. Sci USA* 94 (25), 14150-14155

Beadle, C.L. 1993: Growth analysis. In: D.O. Hall, J.M.O. Scurlock, H.R. Bolhar-Nordenkampf, R.C. Leegood, S.P. Long (eds.): *Photosynthesis and Production in a Changing Environment.* Chapman & Hall, London, 37-46

Beadle, C.L., Ludlow, M.M., Honeysett, J.L. 1993: Water relations. In: Hall, D.O., Scurlock, J.M.O., Bolhar-Nordenkampf, H.R., Leegood, R.C., Long, S.P. (eds.): *Photosynthesis and Production in a Changing Environment.* Chapman & Hall, London, 113-130

Beebe, D.U., Russin, W.A. 1998: Plasmodesmata in the phloem-loading pathway. In: van Bel, A.J.E., von Kesteren, I. (eds.): Plasmodesmata. Springer Verlag. Heidelberg.

Beebe, D.U., Turgeon, R. 1992: Localisation of galactinol, raffinose, and stachyose synthesis in *Cucurbita pepo* leaves. *Planta* 188: 354-361

Beer, A. 1954: *Acanthosycios horridus*, Erfahrungen in Europa. GBB 7/1954: 67-68

Björkmann, O., Demmig-Adams, B. 1994: Regulation of photosynthetic light energy capture, conversion, and dissipation in leaves of higher plants. In: Schulze E.-D., Caldwell, M.M. (eds.): *Ecophysiology of Photosynthesis.* Ecological Studies 100, Springer, Berlin, 17-47

Bolhàr-Nordenkampf, H.R., Draxler, G. 1993: Functional leaf anatomy. In: D.O. Hall, J.M.O. Scurlock, H.R. Bolhàr-Nordenkampf, R.C. Leegood, S.P. Long (eds.): *Photosynthesis and Production in a Changing Environment*. Chapman & Hall, London, 91-111

Bolhàr-Nordenkampf, H.R., Öquist, G. 1993: Chlorophyll fluorescence as a tool in photosynthesis research. In: D.O. Hall, J.M.O. Scurlock, H.R. Bolhàr-Nordenkampf, R.C. Leegood, S.P. Long (eds.): *Photosynthesis and Production in a Changing Environment*. Chapman & Hall, London, 193-206

Bonnemain, J.L. 1970: Histogenèse du phloèm interne et du phloèm inclus des Solanacèes. *Rev. Gén. Bot.* 77: 5-51

Bonnemain, J.L. 1968: Transport du 14C assimilé chez les Solanacées. *Rev. Gén. Bot.* 75: 579-610

Botha, C.E.J., Cross, R.H.M. 1999: Plasmodesmal Imaging - towards understanding structure. In: van Bel, A.J.E., von Kesteren, I. (eds.): Plasmodesmata. Springer Verlag. Heidelberg.

Botha, C.E.J., van Bel, A.J.E. 1992: Quantification of symplastic continuity as visualised by plasmodesmagrams: diagnostic value for phloem-loading pathways. *Planta* 187: 359-366

Botha, C.E.J., Evert, R.F. 1978: Observations of preferential feeding by the aphid, *Rhopalosiphum maidis* on abaxial phloem of *Cucurbita maxima*. *Protoplasma* 96: 75-80

Boyer, J.S. 1995: Measuring the Water Status of Plants and Soils. Academic Press, ISBN 0-12-122260-8

Cowen, I.R. 1994: As to the Mode of Action of the Guard Cells in Dry Air. In: Schulze E.-D., Caldwell, M.M. (eds.): *Ecophysiology of Photosynthesis*, Ecological Studies 100, Springer Berlin, 216-218

Crafts, A. 1932: Phloem anatomy, exudation and transport of organic nutrients in cucurbits. *Plant Physiol*. 7:183-225

Craven, P., Marais, C. 1986: Namib Flora. Gamsberg Macmillan Publ., Windhoek

Dai, Z., Edwards, G.E., Ku, M.S.B. 1992: Control of photosynthesis and stomatal conductance in *Ricinus communis* L. by leaf to air vapour pressure deficit. *Plant Physiol.* 99: 1426-1434

Dawson, W.R., Pinshow, B., Bartholomew, G.A., Seely, M.K., Shkolnik, A., Shoemaker, V.H., Teeri, J.A. 1989: What's so special about the physiological ecology of desert organisms? *J. Arid Env.* 17: 131-143

De Luca, P., Alfani, A., De Santo, A.V. 1977: CAM, transpiration, and adaptive mechanisms to xeric environments in the succulent cucurbitaceae. *Bot. Gaz.* 138: 474-478

Dentlinger, U. 1977: An ethnobotanical study of the !nara plant among the Topnaar hottentots of Namibia. *Munger Africana Library Notes* 38: 3-39

Ehleringer, J.R. 1994: Variation in gas exchange characteristics among desert plants. In: Schulze E.-D., Caldwell, M.M. (eds): *Ecophysiology of Photosynthesis*., Ecological Studies 100, Springer Berlin, 361-392

Ehleringer, J.R., Monson, R.K. 1993: Evolutionary and ecological aspects of photosynthetic pathway variation. *Annu. Rev. Ecol. Syst*. 24: 411-439

Ehleringer, J.R., Philips, S.L., Comstock, J.P. 1992: Seasonal variation in the carbon isotope composition of desert plants. *Funct. Ecol.* 6: 396-404

Ehleringer, J.R., Comstock, J.P., Cooper, T.A. 1987: Leaf-twig carbon isotope ratio differences in photosynthetic-twig desert shrubs. *Oecologia* 71: 318-320

Ehleringer, J.R., Mooney, H.A. 1978: Leaf hairs: effect on physiological activity and adaptive value to a desert shrub. *Oecologica* 37: 183-200

Ehlers, K., Knoblauch, M., van Bel, A.J.E. 2000: Ultrastructural features of well-preserved and injured sieve elements: minute clamps keep the phloem transport conduits free for mass flow. *Protoplasma* 214: 80-92

Esau, K. 1965: Plant Anatomy. John Wiley & Sons Inc., New York.

Evert, R.F. 1990: Dicotyledons. In: Behnke, H.D., Sjolund, R.S. (eds.): *Sieve Elements*. *Comparative Structure, Induction and Development*. Springer Verlag, Berlin, 103-137

Evert, R.F., Russin, W.A., Botha, C.E.J. 1996: Distribution and frequency of plasmodesmata in relation to photoassimilate pathways and phloem loading in the barley leaf. *Planta* 198: 572-579

Farquhar, G.D., O'Leary, M.H., Hubick, K.T. 1989: Carbon isotope discrimination and photosynthesis. *Annu. Rev. Plant Physiol.* 40: 503-537

Field, C.B., Ball, J.T., Berry, J.A. 1989: Photosynthesis: principles and field techniques. In: Pearcy, R.W., Ehleringer, J., Mooney, H.A., Rundel, P.W. (eds.): *Plant Physiological Ecology*. Chapman & Hall, London, 209-253

Flach, B.M.-T., Eller, B.M. 1993: Diurnal pattern of transpiration, water uptake and water budget of succulents with different CO_2 fixation pathways. *Bot. Acta* 107: 46-53

Flora, L.L., Madore, M.M. 1996: Significance of minor-vein anatomy to carbohydrate transport. *Planta* 198: 171-178

Gamalei, Y. 1991: Phloem loading and its development related to plant evolution from trees to herbs. *Trees* 5: 50-64

Gamalei, Y. 1989: Structure and function of leaf minor veins in trees and herbs. *Trees* 3: 96-110

Gibson, A.C. 1998: Photosynthetic organs of desert plants. *BioScience* 48: 911-920

Gibson, A.C. 1983: Anatomy of photosynthetic old stems of nonsucculent dicotyledons from North American deserts. *Bot. Gaz.* 144: 347-362

Goudie, A. 1993: The Nature of the Environment. Blackwell Publishers, Oxford.

Grammatikopoulos, G., Manetas, Y. 1994: Direct absorption of water by hairy leaves of *Phlomis fruticosa* and its contribution to drought avoidance. *Can. J. Bot.* 72: 1805-1811

Grusak, M.A., Beebe, D.U., Turgeon, R. 1996: Phloem loading. In: Zamksi, E., Schaffer, A.A. (eds.): *Photoassimilate Distribution in Plants and Crops. Source-Sink Relationships*, Marcel Dekker, Inc., New York, 209-227

Gut, S. 1988: Untersuchungen zum Feuchtehaushalt in den Dünen der zentralen Namib. Dipl. Arbeit, Geogr. Inst. Uni. Zürich

Haritatos, E., Turgeon, R. 1995: Symplastic phloem loading by polymer trapping. In: Pontis, H.G., Salerno, G.L., Echeverria, E.J,: *Sucrose Metabolism, Biochemistry, Physiology and Molecular Biology Vol.14*. Am. Soc. Plant Physiol., 216-224

Hennesey, T., Fredern, A., Field, C.B. 1993: Environmental effects on circadian rhythms in photosynthesis and stomatal opening. *Planta* 189: 369-376

Holthaus, U., Schmitz, K. 1991: Distribution and immunolocalization of stachyose synthase in *Cucumis melo* L. *Planta* 185: 479-486

Hutchinson, P. 1995: The climatology of Namibia and its relevance to the drought situation. In: Moorsom, R., Franz, J., Mupotola, M. (eds.) 1995: *Coping with Aridity. Drought Impact and Preparedness in Namibia.* Brandes & Apsel/NEPRU, Frankfurt/Windhoek, 17-37

Hylands, P.J., Magot, M.S. 1986: Cucurbitacins from *Acanthosicyos horridus*. *Phytochemistry* 25: 1681-1684.

Jarvis, A.J., Davies, W.J. 1998: The coupled response of stomatal conductance to photosynthesis and transpiration. *J. Exp. Bot*. 49: 339-406

Joubert, F.J., Cooper, D.R. 1953: Naras seed protein (*Acanthosicyos horrida*). *Nature* 172: 1190.

Kempers, R., Ammerlaan, A., van Bel, A.J.E. 1998: Symplasmic constriction and ultrastructural features of the sieve element/companion cell complex in the transport phloem of apoplasmically and symplasmically phloem-loading species. *Plant Physiol.* 116: 271-278

Kempers, R., Prior, D.A.M., van Bel, A.J.E., Oparka, K.J. 1993: Plasmodesmata between sieve elements and companion cells of extrafascicular stem phloem of *Cucurbita maxima* permit passage of 3kDA fluorescent probes. *Plant J.* 4: 567-575

Klopatek, J.M., Stock, W.D. 1994: Partitioning of nutrients in *Acanthosicyos horridus*, a keystone endemic species in the Namib Desert. *J. Arid Environm*. 26: 233-240

Klopatek, C.K., Morton, J.B., Klopatek, J.M. 1992: The occurrence of VA mycorrhiza in the hyperarid Namib desert. *Bull. Ecol. Soc. Namibia* 73: 233

Knapp, R. 1973: The Vegetation of Africa (with references to Environment, Development, Economy, Agriculture and Forestry Geography). Gustav Fischer Verlag, Stuttgart.

Knoblauch, M., van Bel, A.J.E. 1998: Sieve tubes in action. *Plant Cell* 10: 35-50

Köppen, W. 1992: Klimate der Erde, bearbeitet von R. Geiger. In: *Dierke Weltatlas*. 1996, Westermann Verlag, Braunschweig, 222-223

Kutschera, L., Lichtenegger, E., Sobotik, M., Haas, D. 1997: Die Wurzel, das neue Organ. Eigenverlag, Pflanzensoziologisches Institut, Klagenfurt

Lange, O.L., Schulze, E.-D., Kappen, L., Evenari, M., Buschbom, U. 1975: CO_2 exchange patterns under natural conditions of *Caralluma negevensis* a CAM plant of the Negev desert. *Photosynthetica* 9 (3): 318-326

Larcher, W. 1994a: Photosynthesis as a tool for indicating temperature stress events. In: Schulze E.-D., Caldwell, M.M. (eds.): *Ecophysiology of Photosynthesis.* Ecological Studies 100, Springer, Berlin, 261-277

Larcher, W. 1994b: Ökophysiologie der Pflanzen. Eugen Ulmer Verlag, Stuttgart.

Louw, G.N., Seely, M.K. 1982: The Ecology of Desert Organisms. Longmans, New York

Louw, G.N., Seely, M.K., Gernecke, D. 1984: Photosynthesis, transpiration and stomatal morphology in the leafless, desert cucurbit, *Acanthosicyos horridus. unpublished data*

Lucas, W.J., Balachandran, S., Park, J., Wolf, S. 1996: Plasmodesmatal companion cell-mesophyll communication in the control over carbon metabolism and phloem transport: insight gained from viral movement proteins. *J. Exp. Bot*. 47: 1119-1128

Madore, M.,A. 1995: Catabolism of raffinose family oligosaccharides by vegetative sink tissues. In: Madore, M.A., Lucas, W.J. (eds.): *Carbon Partitioning and Source-Sink Interactions in Plants.* Am. Soc. Plant Physiol.: 204-214

Metcalfe, C.R., Chalk, L. 1972: Cucurbitaceae. In: *Anatomy of the Dicotyledons*:. Oxford University Press, Oxford, 684-691

Minchin, P.E.H., Thorpe, M.R. 1987: Measurement of unloading and reloading of photo-assimilate within the stem of bean. *J. Exp. Bot.* 38:221-220

Mitchell, D., Seely, M.K., Roberts, C.S., Pietruszka, R.D., McClain, E., Griffin, M. , Yeaton, R.I. 1987: On the biology of the lizard *Anglosaurus skoogi* in the Namib Desert. *Madoqua* 15: 201-216

Mooney, H.A., Ehleringer, J.R., Berry, J.A. 1976: High photosynthetic capacity of a winter desert annual in Death Valley. *Science* 194: 322-324

Moritz, W. 1992: Die Nara, das Brot der Wüste. In: *Aus alten Tagen in Südwest*. Heft II, Eigenverlag, Windhoek

Nilsen, E.T., Rundel, P.W., Sharifi, M.R. 1996: Diurnal gas exchange characteristics of two stem photosynthesising legumes in relation to the climate at two contrasting sites in the Californian desert. *Flora* 191:105-116

Nilsen, E.T. 1995: Stem photosynthesis: extent, patterns, and role in plant carbon economy. In: Gartner, B.L. (ed): *Plant Stems - Physiology and Functional Morphology*. Academic Press, 223-240

Nilsen, E.T., Sharifi, M.R. 1994: Seasonal acclimation of stem photosynthesis in woody legume species from the Mojave and Sonoran Deserts of California. *Plant Physiol* 105: 1385-1391

Nilsen, E.T., Karpa, D., Mooney, H.A., Field, C.B. 1993: Patterns of stem photosynthesis in two invasive legumes species of coastal California. *Am. J. Bot*. 80:1126-1136

Nilsen, E.T., Bao, Y. 1990: The influence of water stress on stem and leaf photosynthesis in *Glycine max* and *Spatium junceum* (Leguminosae). *Am. J. Bot*. 77: 1007-1015

Nobel, P.S. 1991: Physiochemical and Environmental Plant Physiology. Academic Press, San Diego

Nobel, P.S. 1983: Spine influences on PAR interception, stem temperature, and nocturnal acid accumulation by cacti. *Plant, Cell and Environ.* 6: 153-159

Nobel, P.S. 1974: Boundary layers of air adjacent to cylinders. *Plant Physiol*. 54: 171-181

Oparka, K.J., Turgeon, R. 1999: Sieve elements and companion cells - traffic control centers of the Phloem. *Plant Cell* 11: 739-750

Parkinson, K.J. 1985: A simple method for determining the boundary layer resistance in leaf cuvettes. *Plant, Cell and Environ.* 8: 223 – 226

Pereira, J.S. 1994: Gas exchange and growth. In: Schulze E.-D., Caldwell, M.M. (eds.): *Ecophysiology of Photosynthesis*. Ecological Studies 100, Springer, Berlin, 147-181

Pfeifer, E.H. 1979: !Nara & Topnaar hottentots. *South West African Annual* 19: 158-159

Pharr, D.M., Huber, S.C., Sox, H.N. 1985: Leaf carbohydrates status and enzymes of translocate synthesis in fruiting and vegetative plants of *Cucumis sativus* L. *Plant Physiol*. 77: 104-108

Prior, D.A.M., Oparka, K.J., Roberts, I.M. 1998: En bloc optical sectioning of resin-embedded specimens using a confocal laser scanning microscope. *J. Microscopy* 193: 20-27

Reynolds, E.S. 1963: The use of lead citrate at high pH as an electron-opaque stain in electron microscopy. *J. Cell Biol.* 17:208-212

Richardson, P.T., Baker, D.A., Ho, L.C. 1984: Assimilate transport in cucurbits. *J. Exp. Bot*. 35: 1575-1581

Richardson, P.T., Baker, D.A., Ho, L.C. 1982: The chemical composition of cucurbit vascular exudates. *J. Exp. Bot*. 33: 1239-1247

Robinson, M.D., Seely, M.K. 1980: Physical and biotic environments of the southern Namib dune ecosystem. *J. Arid Environm.* 3: 183-203.

Roer, H. 1975: The life cycle of the Namib Desert beetle *Onymacris plana* Peringuey (Coleoptera, Tenebrionidae, Adesmiini) with special regard to its migratory behaviour. *Bonn. Zool. Beitr.* 26: 239-256

Rosenbauer, K.A., Kegel, B.H. 1978: Rasterelektronenmikroskopische Technik. Präparationsverfahren in Medizin und Biologie. Thieme Verlag, Stuttgart.

Rundel, P.W., Sharifi, M.R. 1993: Carbon isotope discrimination and resource availability in the desert shrub *Larrea tridentate*. In: Ehleringer, J.R., Hall, A.E., Farquhar, G.D. (eds.): Stable Isotopes and Plant Carbon/Water Relations. Academic Press, San Diego, 173-185

Sandelowsky, B. H. 1990: *Acanthosicyos horridus*, a multipurpose plant of the Namib Desert in south-western Africa. In: Bates, D. M., Robinson R. W., Jeffrey, C. (eds.) 1990. *Biology and Utilization of the Cucurbitaceae*. Cornell Univ. Press, Ithaca, New York, 349-355

Sandelowsky, B.H. 1977: Mirabib: an archaeological study in the Namib. *Madoqua* 10: 221-284

Schaffer, A.A., Pharr, D.M., Madore, M.A. 1996: Cucurbits. In: Zamksi, E., Schaffer, A.A. (eds.): *Photoassimilate Distribution in Plants and Crops. Source-Sink Relationships*. Marcel Dekker Inc., New York, 157-183

Schmitz, K., Cuypers, B., Moll, M. 1987: Pathway of assimilate transfer between mesophyll cells and minor veins in leaves of *Cucumis melo* L. *Planta* 171: 19-29

Scholander, P.F., Hammel, H.T., Bradstreet, E.D., Hemmingsen, E.A. 1965: Sap pressure in vascular plants. *Science* 148: 339-346

Schulze, E.D., Lange, O.L., Buschbom, U., Kappen, L., Evenari, M. 1972: Stomatal responses to changes in humidity in plants growing in the desert. *Planta* 108: 259-270

Schwartz, H.M. and Burke, R.P. 1958: The chemistry of nara seed (*Acanthosicyos horrida*, Hook) III. The amino acid composition of the protein. *J. Sci. Food Agric.* 9: 159-162

Seely, M. K.1987: The Namib. Natural History of an Ancient Desert. Publ.: Shell Namibia Ltd., Windhoek, Namibia.

Seely, M.K., Henschel, J.R. 1998: The climatology of Namib fog. In: Schemenauer, R.S., Bridgeman, H. (eds.): *Proceedings of the 1st Conference on Fog and Fog Collection.* Vancouver, Canada; 353-356

Seely, M.K., Henschel, J.R., Robertson, M. 1998: The ecology of fog on Namib desert dunes. In: Schemenauer, R.S., Bridgeman, H. (eds.*): Proceedings of the 1st Conference on Fog and Fog Collection.* Vancouver, Canada; 183-186

Seeman, J.R., Berry, J.A., Downton, W.J.S. 1984: Photosynthetic response and adaptation to high temperature in desert plants. A comparison of gas exchange and fluorescence methods for studies of thermal tolerance. *Plant Physiol.* 75:364-368

Shilomboleni, A. 1998: The !nara and factors that lead to its decline in productivity. Report on the NARA project, Gobabeb Training and Research Center, Ref.No. 15427

Sinclair, R., Venables, W.N. 1983: An alternative method for analysing pressure-volume curves produced with the pressure chamber. *Plant, Cell and Environ*. 6: 211-217

Small, J.G.C. & Botha, F.C. 1986: Seed dormancy and possible ecological implications in some African cucurbits with special reference to *Citrullus lanatus*. *Env. Quality Ecosyst. Stabil*., Bar-Ilan University Press, Ramat-Gan, Israel 23-34

Spurr, A.R. 1969: A low-viscosity epoxy resin embedding medium for electron microscopy. *J. Ultrastruct. Res*. 26: 31-43

Storad, C.J. 1991: Fruit of the dunes. *ASU Research* 6: 2-8. Tempe, Arizona

Taiz, L., Zeiger, E. 1998: Plant Physiology. Benjamin/Cummings, Redwood City.

Teller, J.T., Lancaster, N. 1985: History of sediments at Khommabes, central Namib desert. *Madoqua* 14 (3): 267-278

Tibbitts, T.W., Langhans, R.W. 1993: Controlled-environment studies. In: D.O. Hall, J.M.O. Scurlock, H.R. Bolhar-Nordenkampf, R.C. Leegood, S.P. Long (eds.): *Photosynthesis and Production in a Changing Environment*. Chapman & Hall, London, 65-79

Turgeon, R. 1995: The selection of raffinose family oligosaccharides as translocates in higher plants. In: Madore, M.A., Lucas, W.J. (eds.): *Carbon Partitioning and Source-Sink Interactions in Plants*. Am. Soc. Plant Physiol.: 195-203

Turgeon, R. 1991: Symplastic phloem loading and the sink-source transition in leaves: a model. In: Bonnemain, J.-L., Delrot, S., Lucas, W.J., Dainty, J. (eds.): *Recent Advances in Phloem Transport and Assimilate Compartmentation*. Ouest Editions, Nantes, France, 18-22

Turgeon, R. 1989: The source-sink transition in leaves. *Annu. Rev. Plant Physiol. Plant Mol. Biol.* 40: 119-138

Turgeon, R., Beebe, D.U., Gowan, E. 1993: The intermediary cell: minor vein anatomy and raffinose oligosaccharide synthesis in the Scrophulariacaeae. *Planta* 191: 446-456

Turgeon, R., Hepler, P.K. 1989 Symplastic continuity between mesophyll and companion cells in minor veins of mature *Cucurbita pepo* L. leaves. *Planta* 179: 24-31

Turgeon, R., Webb, J.A. 1976: Leaf development and phloem transport in *Cucurbita pepo*: maturation of the minor veins. *Planta* 129: 265-269

Turgeon, R., Webb, J.A., Evert, R.F. 1975: Ultrastructure of minor veins in *Cucurbita pepo* leaves. *Protoplasma* 83: 217-232

U.S. Department of Agriculture 1922: *Acanthosicyos horrida* Welw., 55486. USDA Inventory Seeds and Plants Imported 1922. No. 71. U.S. Department of Agriculture. Washington, D.C, 49

van Bel, A.J.E. 1996a: Interaction between sieve element and companion cell and the consequences for photoassimilate distribution. Two structural hardware frames with associated physiological software packages in dicotyledons? *J. Exp. Bot.* 47: 1129-1140.

van Bel, A.J.E. 1996b: Carbohydrate processing in the mesophyll trajectory in symplasmic and apoplasmic phloem loading. *Progr. Bot.* 57: 140-167

van Bel, A.J.E. 1993a: Strategies of phloem loading. *Annu. Rev. Plant Physiol. Plant Mol. Biol.* 44: 253-281

van Bel, A.J.E 1993b: The transport phloem. Specifics of its function. *Progr. Bot.* 54: 134-150

van Bel, A.J.E., Ammerlaan, A., van Dijk, A.A. 1993: A three-step screening procedure to identify the mode of phloem loading in intact leaves: evidence for symplasmic and apoplasmic phloem loading associated with the type of companion cell. *Planta* 192: 31-39

van Bel, A.J.E., Gamalei, Y.V. 1992: Ecophysiology of phloem loading in source leaves. *Protoplasma* 83: 217-232

van Bel, A.J.E., Kempers, R. 1997: The pore/plasmodesm unit: key element in the interplay between sieve element and companion cell. *Progr. Bot.* 58, Springer Verlag, Berlin

van den Eynden, V., Vernemmen, P., van Damme, P. 1992: The Ethnobotany of the Topnaar. Universiteit Gent/ The Commission of the European Community: 34-37

van der Schoot, C., van Bel, A.J.E. 1989: Architecture of the internodal xylem of tomato (*Solanum lycopersicum*) with reference to longitudinal and lateral transfer. *Amer. J. Bot*. 76: 487-503

Vogelmann, T.C. 1993: Plant tissue optics. *Annu. Rev. Plant Physiol. Plant Mol. Biol.* 44: 231-251

Volk, G.M., Turgeon, R., Beebe, D.U. 1996: Secondary plasmodesmata formation in the minor-vein phloem of *Cucumis melo* L. and *Cucurbita pepo* L. *Planta* 199: 425-432

Walter, H., Breckle, S.W. 1986: Ecological Systems of the Geobiosphere. II. Tropical and Subtropical Zonobiomes. Berlin, Springer Verlag: 465 pp

Ward, J.D. 1984: Aspects of cenoyoic geology in the Kuiseb valley, central Namib desert. *Madoqua* 14 (3): 263 ff / PhD, Dept. Geology, Univ. Natal, Pietermaritzburg, SA

Webb, J.A., Gorham, P.R. 1964: Translocation of photosynthetically assimilated ^{14}C in straight-necked squash. *Plant Physiol.* 39: 663-672

Wilkinson, H.P. 1979: The plant surface (mainly leaf), Part 1, Stomata. In: Metcalfe C.R., Chalk, L. (eds): *Anatomy of the Dicotyledons*. 2nd Edition, Clarendon Press, Oxford, 97-117.

Ziegler-Jöns, A., Selinger, H. 1987: Calculation of leaf photosynthetic parameters from light-response curves for ecophysiological applications. *Planta* 171: 412-415

Internet Sources used:

http://www.rbgkew.org.uk/ceb/sepasal/acantho.htm

http://ostracon.biologie.uni-kl.de/b_online/d50/nara.htm

http://www.greatestplaces.org/book_pages/namib/narras/narra.html

http://www.hort.purdue.edu/newcrop/proceedings1999/v4-400.html

http://www.cucurbit.org/family/species/Acanthosicyos/acantx.html

Appendix A - Manufactures

ADC The Analytical Development Co., Ltd., Hoddesdon, England

Boehringer, Mannheim, Germany

Capital Enterprises, New Germany, RSA

Conviron Controlled Environments Ltd., Winnipeg, Manitoba, Canada

Chroma Technology Corp.

Dionex Corporation, Sunnyvale, California 94088, USA

Eppendorf, Eppendorf AG, Barkhausenweg 1, 22339 Hamburg, Germany (www.eppendorf.com)

Fedgas, Alrode, Port Elisabeth, RSA

Fischer & Porter, Workington, England

John Fluke MFG. Co. Inc., Everett, Washington, USA

Joel, Tokyo, Japan

Labcon (PTY) Ltd., Krugersdorp, RSA

Leitz Wetzlar, *now* Leica Microsystems AG, Ernst-Leitz-Str.17-37, 35578 Wetzlar, Germany (www.leica-microsystems.com)

Molecular Probes Europe BV, PoortGebouw, Rjinsburgerweg 10, 2333 AA Leiden, The Netherlands (www.probes.com)

Olympus, Olympus Optical Co. (Europa) GmbH, Wendenstr. 14-18, 20097 Hamburg, Germany (www.olympus.de)

Optolabor, JHB, RSA (Lauda)

Osram, Johannesburg, RSA

Philips Johannesburg, RSA

Research & Manufacturing Co. Inc., Tucson, Arizona

Sigma, PO Box 4853, Atlasville 1465, South Africa (www.sigma-aldrich.com)

Zeiss, Carl Zeiss AG Mikroskopie, Königsallee 9-21, 37081 Göttingen, Germany (www.carl-zeiss.de/micro)